

APPENDIX 3.D: VERTICAL HANDLING OF OVERPACK WITH HEAVIEST MPC

3.D.1 Introduction

There are two vertical lifting scenarios for the HI-STORM 100 during the normal operation procedures at the ISFSI pad. The first scenario considers the vertical lifting of a fully loaded HI-STORM 100 with four synchronized hydraulic jacks, each positioned at each of the four inlet vents located at the bottom end. This operation allows the installation of air pads under the HI-STORM 100 baseplate. The second scenario considers the lifting of a fully loaded HI-STORM 100 vertically through the four lifting lugs located at the top end. The lifting device assemblage is constructed such that the lift forces at each lug are parallel to the longitudinal axis of the HI-STORM 100 during the operation. The stress intensity induced on the cask components as a result of these operations is determined, analyzed, and the structural integrity evaluated. The finite element models for the analyses in this appendix have been color coded to differentiate cask components. The legends for the color codes are listed in Sections 3.D.3 and 3.D.4 below.

3.D.2 Assumptions

- a. Conservatively, the analysis takes no credit for the structural rigidity of the radial concrete shielding between the outer and the inner shells of the HI-STORM 100 and also no credit for the structural rigidity of the MPC pedestal shield. Hence, the weight of the radial concrete shielding, the MPC pedestal shield, and the MPC are respectively applied as surface pressure on the baseplate during the vertical lifting of HI-STORM 100 from the bottom end through the inlet vents and, as lumped mass during the vertical lifting of HI-STORM 100 at the top end through the lifting lugs. Property values used are approximately equal to the final values set in the Tables in Chapter 3. Drawings 1495, 1561 and associated Bills of Materials are used for dimensions.
- b. The acceleration of gravity of 1.15g is considered in order to account for a 15% dynamic load factor due to lifting. The 15% increase, according to Reference 2, is considered in crane standards as appropriate for low speed lifting operations.
- c. The shield shell, which was removed from the HI-STORM 100 design as of 6/01, is not explicitly modeled. The weight of the shield shell, however, is

conservatively added to the weight of the inner shell for top end lift and as a lumped mass for the bottom end lift. Added weights are obtained by direct calculation.

- d. The geometry of the HI-STORM 100 is considered for the analysis of the top lift in this appendix¹.

3.D.3 Analysis Methodology - Bottom Lift at the Inlet Vents

A 3-D, 1/4-symmetry, finite element model of the bottom segment of the HI-STORM 100 storage overpack is constructed using the ANSYS 3-D elastic shell element SHELL63. ANSYS is a general purpose finite element program. The Young's modulus, at 300 degree F, the Poisson's ratio, and material density for SA516-70 steel are respectively taken as 29.34E+06 psi, 0.29, and 0.288 pounds per-cubic-inch. The respective thickness of the HI-STORM 100 components are also appropriately considered, i.e., 1.25 inches for the inner shell, 0.75 inches for the outer shell, 2.0 inches for the baseplate, 0.5² inches for the radial ribs, 2 inches for the inlet vent horizontal plate, and 0.75 inches for the inlet vent vertical plates. The model is terminated approximately 20 inches above the base of the HI-STORM 100 storage overpack with the weight of the sections of the HI-STORM 100 storage overpack not modeled lumped at the top end of the finite element model. The contact surface between the inlet horizontal plate and hydraulic jack is fixed vertically.

An equivalent pressure load of 31.61 psi from the weights of the heaviest MPC and the pedestal shield is applied on the HI-STORM 100 baseplate over the surface area covered by the pedestal (the applied total load is 116,067 lb. based on a 68.375" outer diameter). The equivalent pressure load of 20.55 psi from the weight of the radial concrete shielding is applied on the baseplate as well as the inlet vent horizontal plates. The applied equivalent pressure loads include the 15% load increase above the dead load to account for inertia effects developed during a lift operation. Figure 3.D.1 shows the plot of the finite element model for the bottom lift scenario. Figure 3.D.1 is color-coded to differentiate cask components as follows:

¹It is recognized that the HI-STORM 100S overpack is lighter than the HI-STORM 100 overpack and the outlet air ducts are located in the lid in the 100S. Safety factors computed in this appendix are also reported in Subsection 3.4.3.5 of this FSAR. Similar calculations have been performed in Holtec calculation packages for the 100S overpack, where differences in configurations between the two overpack designs warrant. Safety factors for the HI-STORM 100S are also reported in Subsection 3.4.3.5.

² Analysis is conservative since final rib thickness is 0.75 inch.

Figure 3.D.1 Cask Component Color Codes

<u>Component</u>	<u>Color</u>
Baseplate	Blue-Purple-Red
Inner Shell	Green
Outer Shell	Magenta
Rib	Dark Blue
Inlet Vent Vertical Plate	Mustard
Inlet Vent Horizontal Plate	Color Grid

3.D.4 Analysis Methodology - Top End Lift

3.D.4.1 Model at Top near Lift Points

A 3-D, 1/8-symmetry, finite element model of the top segment of the HI-STORM 100 is constructed using ANSYS 3-D elastic shell element SHELL63, 3-D structural solid with rotation SOLID73, and 3-D structural mass element MASS21. The material properties used, i.e., Young's Modulus, the Poisson's ratio, and material density are identical to those listed in Section 3.D.3. The respective thickness of the HI-STORM 100 components (in addition to the inner shell, the outer shell, and the ribs) are also appropriately considered, i.e., 0.75 inches for the top plate, 1.25 inches for the exit vent horizontal plate, 0.5 inches for the exit vent vertical plate, 0.75 inches for the horizontal step plate and the vertical step plate. The model is terminated at about 43 inches from the top end of the HI-STORM 100. The mass of the sections of the HI-STORM 100 not modeled, with the exception of the overpack lid and the shield blocks, are lumped at the lower end of the finite element model. A bounding value for the mass of the overpack lid and the shield blocks are lumped at the top end of the vertical step plates. All lumped masses use the ANSYS MASS21 elements. The lifting lug is explicitly modeled with the ANSYS SOLID73 element. The SOLID73 element is selected for its compatible degrees-of-freedom with the ANSYS SHELL63. The top end of the lifting lug in the finite element model is restricted from vertical translation. Since the lifting lug itself is not part of the HI-STORM 100 system, the model of this component is performed only to a level necessary to properly simulate the location of the lift point. Figures 3.D.2a, 3.D.2b, and 3.D.2c show the detailed plots of the finite element model for the top lift scenario. Figures 3.D.2a, 3.D.2b, and 3.D.2c are color-coded to differentiate cask components as follows:

Figure 3.D.2 Cask Component Color Codes

<u>Component</u>	<u>Color</u>
Inner Shell	Cyan
Outer Shell	Red
Step Horizontal Plate	Purple
Step Vertical Plate	Purple
Exit Vent Horizontal Plate	Green
Exit Vent Vertical Plate	Magenta
Rib	Mustard
Top Plate	Blue
Anchor Block	Cyan
Lug	Cyan

We note that the analysis model used here included small “step” plates. The step plate has been eliminated in the storage overpack in Revision 5 (see drawings in Chapter 1) to simplify fabrication. The removal of the “step” plates also removes a potential area of stress concentration from the configuration. Therefore, the analysis reported here, which retains the step, produces conservative stress results and is bounding for the final configuration in this area of the structure.

3.D.4.2 Model Near Baseplate

The 2-inch thick, HI-STORM 100 baseplate is fabricated from SA-516-Grade 70 carbon steel material. The baseplate is continuously welded to the inner shell, the outer shell, the inlet vents, and the MPC pedestal shell. During a vertical lift using the top end lift lugs, the baseplate supports the MPC, the MPC pedestal, and the radial concrete shielding between the inner shell and the outer shell. The stress intensity and the associated distribution on the HI-STORM 100 baseplate as a result of the vertical lift through the lifting lug is evaluated using the same finite element model as that described in Section 3.D.3 above. For this analysis, the finite element model in Figure 3.D.1 is restrained against vertical translation at the top end of the model away from the baseplate. The weight of the pedestal, the MPC, and the radial concrete shield are applied as pressure loads as described in Section 3.D.1, and no hydraulic jacks are assumed in-place in the inlet vents.

3.D.5 Stress Evaluation

For all analyses, safety evaluation is based on the consideration of all components as Class 3 plate and shell support structures per the ASME Code Section III, Subsection NF. Stress intensity distributions are obtained for all sections of the model. Although the relevant Code section places limits on maximum stresses, the use of a stress intensity based safety factor is used here for convenience. The distribution of stress intensity on the HI-STORM 100 from the bottom end lifting through the inlet vents is shown in Figure 3.D.3. The maximum surface stress intensity, located on the inlet vent plate, is 13,893 psi based on the element distribution used. As seen from Figure 3.D.3, this surface stress intensity bounds the values at all other locations and therefore could be used to provide a bounding safety factor for all sections modeled in this simulation. The nature of the finite element model is such that the surface stress intensity results near discontinuities in loading or in the structure include secondary stress intensity components as well as primary membrane and primary bending. In particular, this stress intensity component includes secondary effects both from the abrupt change in the applied load and from the joint between the horizontal and vertical plates of the inlet vent. Away from this local region, we can estimate from the distributions plotted in Figure 3.D.3 that the maximum primary membrane plus primary bending stress intensity is approximately 8000 psi.

The distributions of stress intensity on the HI-STORM 100 from the top end lifting through the lifting lugs are shown in Figures 3.D.4a and 3.D.4b, and 3.D.4c. Figures 3.D.4a and 3.D.4b show a cut through the middle surface of the radial rib and rib bolt block. The maximum stress intensity consistent with the finite element discretization, located on the rib plate, is 16,612 psi (Figure 3.D.4b). This stress is localized and represents a mean stress intensity plus secondary membrane stress intensity components introduced from the abrupt geometry change where the rib bolt block is welded to the radial rib. If attention is focused on the radial rib away from the local discontinuity, then the mean stress intensity is approximately 10,000 psi (the iso-stress intensity boundary between yellow and yellow-green in Figure 3.D.4(b)). Figure 3.D.4c shows the "step" (no longer present in the structure) and identifies the local stress intensity amplification that no longer is present.

The stress intensity distribution on the baseplate due to the lifting of HI-STORM 100 through the top end lifting lugs are shown in Figures 3.D.5a, 3.D.5b, and 3.D.5c. These three figures show different views of the components and identify the locations of maximum stress intensity. The maximum stress intensity on the baseplate occurs, as expected, just inboard of the inner shell of the storage overpack and has a maximum value, consistent with the level of discretization, of 10,070 psi (Figure 3.D.5a). It is clear from the distribution that this includes

a significant secondary stress intensity component introduced by the inlet vent vertical plate. Away from this local region, the surface stress intensity reduces to approximately 7000 psi. At this location, we consider the result to represent the combined primary membrane plus primary bending stress intensity.

The results of these analyses are summarized as follows (neglecting secondary effects introduced by geometry and load changes):

For the top lift, maximum membrane stress intensity, excluding very localized secondary effects due to geometric discontinuities, is in the radial rib, and has the value 10,000 psi. Since this analysis is based on a 0.5" thickness rather than the actual final plate thickness 0.75", for the purpose of establishing a bounding safety factor, we further reduce this stress intensity by 2/3. Therefore, the appropriate safety factor (SF) is (see Table 3.1.10)

$$\text{SF}(\text{membrane stress intensity in radial rib}) = 17,500 \text{ psi} / (10,000 \text{ psi} \times 2/3) = 2.63$$

For the same top lift, the bounding safety factor for primary membrane plus primary bending (excluding local discontinuity effects) is computed for the baseplate as:

$$\text{SF}(\text{primary membrane plus primary bending stress intensity in baseplate}) = 26,250 \text{ psi} / 7000 \text{ psi} = 3.75$$

For the bottom lift,

$$\text{SF}(\text{primary membrane plus primary bending in inlet vent horizontal plate}) = 26,250 \text{ psi} / 8000 \text{ psi} = 3.28$$

The previous calculations have been based on an applied load of 115% of the lifted load with safety factors developed in accordance with ASME Section III, Subsection NF for Class 3 plate and shell support structures. To also demonstrate compliance with Regulatory Guide 3.61, safety factors based on 33.3% of the material yield strength are presented. These safety factors can be easily derived from the previous results by replacing the allowable stress by 33.3% of the material yield strength (1/3 x 33,150 psi from Table 3.3.2 for SA-516).

Therefore, the following bounding results are obtained:

$$\text{SF}(\text{membrane} - 3W) = 2.63 \times 33,150 \text{ psi} / (3 \times 17,500 \text{ psi}) = 1.66$$

$$\text{SF}(\text{membrane plus bending} - 3W) = 3.28 \times 33,150 \text{ psi} / (3 \times 26,250 \text{ psi}) = 1.38$$

3.D.6 Bolt and Anchor Block Thread Stress Analysis under Three Times Lifted Load

In this section, the threads of the bolt and the bolt anchor block are analyzed under three times the lifted load. The thread system is modeled as a cylindrical area of material under an axial load. The diameter of the cylinder area is the basic pitch diameter of the threads, and the length of the cylinder is the length of engagement of the threads. See Holtec HI-STORM 100 drawing numbers 1495 (sheets 2 and 3) and 1561 (sheet 2) for details.

3.D.6.1 Geometry

The basic pitch diameter of the threads is: $d_p = 3.0876"$

The thread engagement length is: $L = 3$ in.

The shear area of the cylinder that represents the threads: $A = 3.14159 \times L \times d_p$

The shear stress on this cylinder under three times the load is: $3W \times 1.15/nA = 10,670$ psi

where the total weight, W , and the number of lift points, n , are 360,000 pounds and 4, respectively, and the 1.15 represents the inertia amplification.

3.D.6.2 Stress Evaluation

The yield strength of the anchor block material at 350 degrees F is taken as 32,700 psi per Table 3.3.3. Assuming the yield strength in shear to be 60% of the yield strength in tension gives the thread shear stress safety factor under three times the lifted load as:

$$SF(\text{thread shear} - 3 \times \text{lifted load}) = .6 \times 32,700/10,670 = 1.84$$

The lifting stud material is SA564 630 (age hardened at 1075 degrees F). The yield strength of the stud material at 350 degrees F is 108,800 psi per Table 3.3.4.

The load per lift stud is $P = 3W/4 \times 1.15 = 310,500$ lb.

The stud tensile stress area is (see Machinery's Handbook, 23rd Edition, p. 1484)

$$A = 7.10 \text{ sq. inch.}$$

Therefore, the tensile stress in the stud under three times the lifted load is

$$\text{Stress} = P/A = 43,733 \text{ psi}$$

The factor of safety on tensile stress in the lifting stud, based on three times the lifted load, is:

$$\text{SF}(\text{stud tension} - 3 \times \text{lifted load}) = 108,800/43,733 = 2.49$$

It is concluded that thread shear in the anchor block governs the design.

3.D.7 Weld Evaluation

In this section, weld stress evaluations are performed for the weldments considered to be in the primary load path during lifting operations. The allowable stress for the welds is obtained from Reference [3].

3.D.7.1 Anchor Block-to-Radial Rib (Lift from Top)

There are double sided fillet welds that attach the anchor block to the radial ribs (see drawings 1495, sheet 3 and 1561 sheet 2). The following dimensions are used for analysis:

Total Length of weld = $L = 12" + 5"$ (Continuous weld along sides and bottom - see drawing 1561 sheet 2)

Weld leg size = $t = 0.75"$

Weld throat allowable shear stress = $S_a = 0.3S_u$ where S_u is the ultimate strength of the base metal (per [3]) = $.3 \times 65,650 \text{ psi}$ (Table 3.3.3 gives the ultimate strength of the anchor block base material).

$$S_a = 19,695 \text{ psi}$$

The following calculations provide a safety factor for the weld in accordance with the requirements of the ASME Code, Section III, Subsection NF for Class 3 plate and shell supports:

Allowable load per anchor block (2 welds) = $S_a \times 2 \times 0.7071 \times t \times L = 355,072 \text{ lb}$.

Calculated Load (including 15% inertia amplification) = $360,000 \text{ lb} \times 1.15/4 = 103,500 \text{ lb}$.

$$\text{SF(ASME Code)} = 355,072 \text{ lb.}/103,500 \text{ lb.} = 3.43$$

The following calculations provide a safety factor for the weld in accordance with the requirements of Regulatory Guide 3.61 (here we use the yield strength at 300 degrees F since the weld is buried in the concrete (Table 2.2.3)):

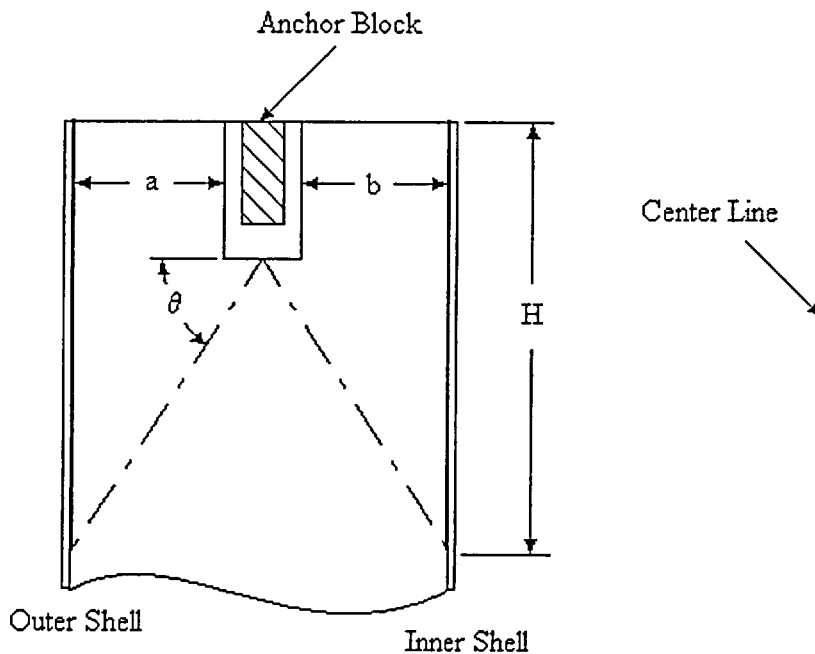
$$\text{Allowable load per anchor block (2 welds)} = 0.6 \times 32,700 \times 2 \times 0.7071 \times t \times L = 353,769 \text{ lb.}$$

$$\text{Calculated Load (3 x weight)} = 360,000 \text{ lb} \times 3/4 \times 1.15 = 310,500 \text{ lb.}$$

$$\text{SF(Reg. Guide 3.61)} = 353,769 \text{ lb.}/310,500 \text{ lb.} = 1.14$$

3.D.7.2 Radial Rib-to-Inner and Outer Shell (Lift from Top)

The load transferred to the radial ribs from the bolt anchor blocks is dispersed through the rib and also transferred to the inner and outer shell of the storage overpacks. A conservative estimate of the safety factors inherent in the vertical welds connecting the radial ribs to the inner and outer shells is obtained by assuming that the entire load is dispersed into the shells. The length of weld assumed to act in the load transfer is based on a dispersion angle (θ) of 65 degrees as shown in the sketch below:



From the geometry of the structure,

$$b = 11.0" \\ a = 11.5"$$

Drawing 1495, sheet 2

The depth of the effective weld to each shell is conservatively computed as

$$H = 6" + (11" + 2.5") \times \tan(65^\circ) = 34.9"$$

St. Venant's principle may be used as an alternate approach to calculate the effective weld length. This principle asserts that the effect of the force acting on the anchor block may be treated as a statically equivalent system which, at a distance approximately equal to the width of the radial rib (27.5"), causes a nearly uniform stress distribution. If we conservatively assume that the average tensile stress in the radial rib diminishes to zero at this distance (i.e., 27.5 inches below the anchor block), the length of weld above this cross section is equal to

$$H = 6" + 27.5" = 33.5"$$

The following calculations are based on this length since it is less than the previous result.

The weld leg area available for load transfer is (double fillet to each of two shells):

$$\text{Weld Area} = 2 \times (2 \times 33.5'' \times 0.1875'') = 25.1 \text{ sq. in.}$$

The following calculations provide a safety factor for the weld in accordance with the requirements of the ASME Code, Section III, Subsection NF for Class 3 plate and shell supports ($S_a = 21,000$ psi for SA516-70):

$$\text{Allowable load per radial rib} = S_a \times 0.7071 \times \text{Weld Area} = 372,712 \text{ lb.}$$

$$\text{Calculated Load (including 15\% inertia amplification)} = 360,000 \text{ lb} \times 1.15/4 = 103,500 \text{ lb.}$$

$$\text{SF(ASME Code)} = 372,712 \text{ lb.}/103,500 \text{ lb.} = 3.60$$

The following calculations provide a safety factor for the weld in accordance with the requirements of Regulatory Guide 3.61. The yield strength of the SA516-70 at 350 degrees F is taken as 33,150 psi per Table Y-1 of ASME Code, Section II, Part D.

$$\text{Allowable load per radial rib} = 0.6 \times 33,150 \times .7071 \times \text{Weld Area} = 353,012 \text{ lb.}$$

$$\text{Calculated Load (3 x weight)} = 360,000 \text{ lb} \times 3/4 \times 1.15 = 310,500 \text{ lb.}$$

$$\text{SF(Reg. Guide 3.61)} = 353,012 \text{ lb.}/310,500 \text{ lb.} = 1.13$$

3.D.7.3 Baseplate-to-Inner Shell (Top Lift (bounds bottom lift))

The weld between the storage overpack baseplate and the storage overpack inner shell is an all-around fillet weld (except at the duct locations (see drawing 1495, sheet 2)). To bound both the top and bottom lift, it is conservatively assumed that this weld supports a lifted load consisting of the weights of the loaded MPC, the pedestal shield concrete and steel, and the MPC baseplate (i.e., the structural action of the weld to the outer shell is conservatively neglected).

Therefore, the weld is subject to the following total load

116,067 lb. (MPC and pedestal shield) + 7967 lb. (baseplate) (from calculation package weight tables)

so that the applied load in the weld is conservatively assumed as:

$$\text{Load} = 124,034 \text{ lb}$$

The weld is a double-sided fillet weld with weld leg size "t" at mean diameter $D = 73.5" + 1.25"$, or

$$t = 0.375"$$

$$D = 74.75"$$

From the Bill-of-Materials for the HI-STORM 100 storage overpack, the width of each inlet vent is

$$w = 16.5"$$

Therefore, the total linear length (around the periphery) of fillet weld available to transfer the load is

$$L = 3.14159 \times D - 4 \times w = 168.83"$$

Therefore, the weld throat area is

$$\text{Area} = 2 \times 0.7071 \times t \times L = 89.53 \text{ sq. inches}$$

The capacity of the weld per the ASME Code Section III Subsection NF is defined as Lc1

$$Lc1 = 21,000 \text{ psi} \times \text{Area} = 1,880,130 \text{ lb.}$$

The capacity of the weld per Regulatory Guide 3.61 is defined as Lc2

$$Lc2 = .6 \times 33,150 \text{ psi} \times \text{Area} = 1,780,752 \text{ lb.}$$

Since 3 x lifted load bounds 1.15 x lifted load, it is clear that the Regulatory Guide 3.61 criteria produce the minimum safety factor. The calculated safety factor at this location is

$$SF = Lc2 / (\text{Load} \times 1.15) = 12.48$$

3.D.7.4 Inlet Vent-to Baseplate Weld (Bottom Lift)

Drawing 1561, sheet 3 identifies the weld available to transfer the lifted load to the hydraulic jacks (not part of the HI-STORM 100 System) used in the bottom lift scenario. Load carrying capacity is assigned only to the fillet welds. The weld leg length "t" and the total length of weld available for load transfer "L" (per inlet vent) are given as:

$$t = 0.5''$$

$$L = 2 \times 29.5'' \text{ (see Bill-of-Materials item 13)} = 59''$$

The load capacity of the weld (Lc3), per the more severe Regulatory Guide 3.61 requirement, is

$$Lc3 = 0.6 \times 33,150 \text{ psi} \times (0.7071 \times t \times L) = 414,894 \text{ lb.}$$

Therefore, the safety factor under three times lifted load (including an inertia amplifier) is

$$SF = 414,894 \text{ lb.} / (3 \times 360,000 \text{ lb.} \times 1.15) / 4 = 1.33$$

3.D.8 Stress Analysis of the Pedestal Shield

The pedestal shield concrete serves to support the loaded MPC and the pedestal platform during normal storage. The pedestal shield concrete is confined by the surrounding pedestal shell that serves, during the lifting operation, to resist radial expansion of the concrete cylinder due to the Poisson Ratio effect under the predominate axial compression of the concrete pedestal shield.

The compressive load capacity of the concrete making up the pedestal shield is the compression area x allowable compressive stress. From Table 3.3.5, the allowable compressive stress in the concrete is

$$\sigma_c = 1266 \text{ psi}$$

The concrete cylinder diameter (see Bill-of-Materials, item 24) is

$$D_c = 67.875''$$

Therefore, the load capacity per the ACI 318.1 concrete code (Reference [3.3.2] in Section 3.8 of this FSAR), defined as Lc4, is

$$Lc4 = \sigma_c \times \text{compression area of concrete cylinder} = 1266 \text{ psi} \times 3618 \text{ sq. inch} = 4,580,388 \text{ lb.}$$

The applied load is conservatively assumed as the summed weight of the loaded MPC plus the pedestal platform plus the pedestal concrete shield.

$$W = 90,000 \text{ lb. (Table 3.2.1)} + 5120 \text{ lb. (weight spreadsheet)} + 5518 \text{ lb. (weight spreadsheet)} \\ = 100,638 \text{ lb.}$$

Conservatively applying the Regulatory Guide 3.61 criteria to the concrete (interpret the allowable compressive stress as the "yield stress" for this evaluation) gives a safety factor

$$SF = Lc4/3W*1.15 = 13.19 \quad (\text{Note that the 1.15 accounts for inertia effects during the lift})$$

The pedestal shell is assumed to fully confine the concrete. Therefore, during compression of the concrete, a maximum lateral (radially oriented) pressure is applied to the pedestal shell due to the Poisson Ratio effect. This pressure varies linearly with concrete depth. Assuming the Poisson's Ratio of the concrete to be $\nu = 0.2$, the maximum pressure on the pedestal shell is

$$p_{\text{confine}} = \nu/(1-\nu) \times (3W \times 1.15/\text{compression area of concrete cylinder}) = 0.25 \times 95.965 \text{ psi} \\ = 23.99 \text{ psi}$$

Conservatively neglecting variations with depth of concrete, the hoop stress in the confining pedestal shell is obtained as follows:

$$t = \text{pedestal shell thickness} = 0.25''$$

$$R = \text{pedestal shell mean radius} = (0.5 \times 68.375'' - .5 \times 0.25'') = 34.0625''$$

$$\text{Hoop Stress} = p_{\text{confine}} \times R/t = 3,269 \text{ psi}$$

This gives a safety factor based on the Regulatory Guide 3.61 criteria equal to

$$SF = 33,150 \text{ psi/Hoop Stress} = 10.14$$

This result is bounding for the HI-STORM 100S since the height and weight of the concrete pedestal is reduced.

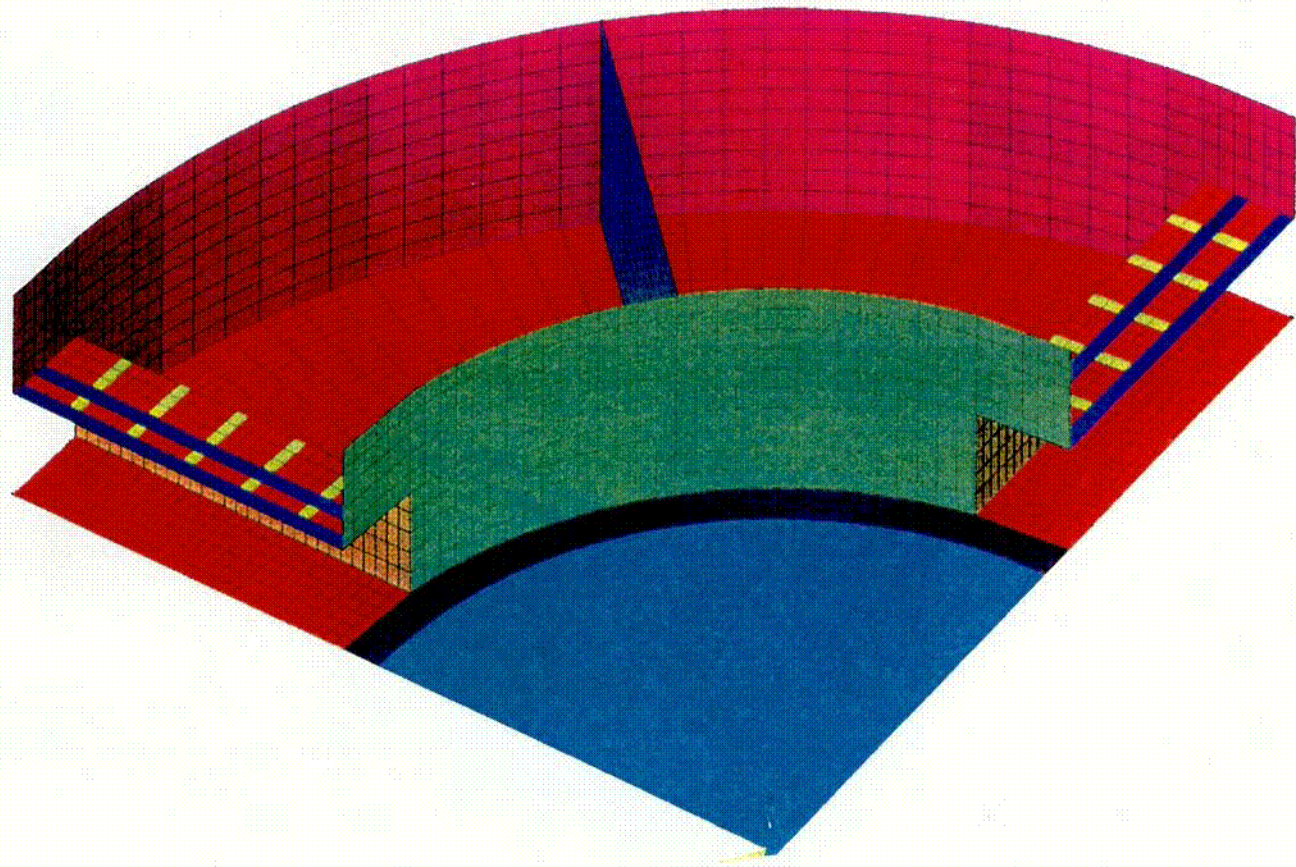
3.D.9 Conclusion

The design of the HI-STORM 100 is adequate for the bottom end lift through the inlet vents. The design of the HI-STORM 100 is also adequate for the top end lift through the lifting lugs. Safety factors are established based on requirements of the ASME Code Section III, Subsection NF for Class 3 plate and shell supports and also on the requirements of USNRC Regulatory Guide 3.61. The conclusions also apply to the HI-STORM 100S.

3.D.10 References

1. ANSYS 5.3, A General Purpose Finite Element Code, ANSYS, Inc.
2. Crane Manufacturer's Association of America (CMAA), Specification #70, 1988, Section 3.3.
3. ASME Code Section III, Subsection NF-3324.5, Table NF-3324.5(a)-1, 1995

ANSYS 5.2
FEB 3 1997
12:22:09
ELEMENTS
REAL NUM
XV =-1
YV =-2
ZV =1
*DIST=50.243
*XF =33.866
*YF =1.749
*ZF =10.107
VUP =Z
CENTROID HIDDEN



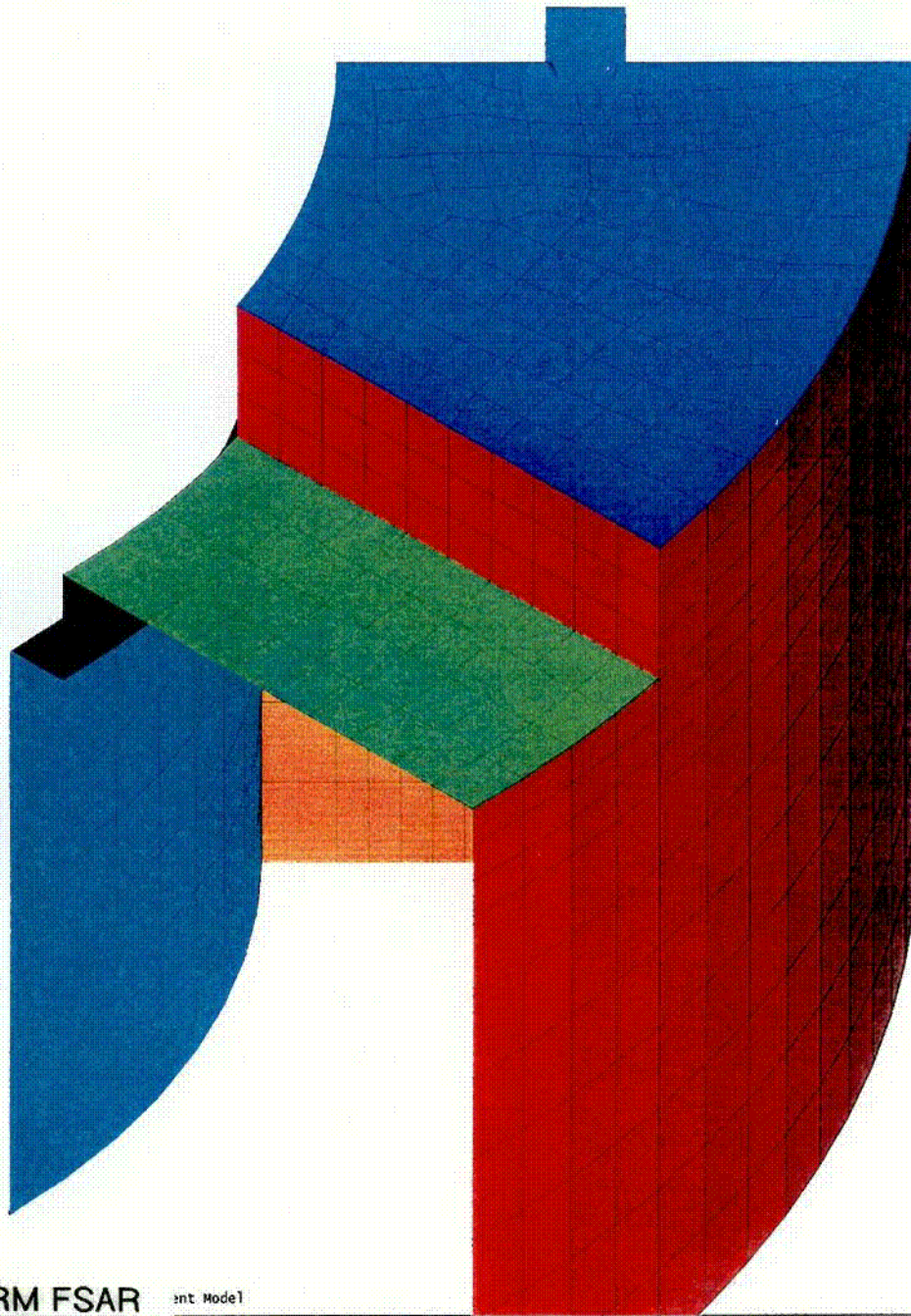
101

HI-STORM FSAR
HI-2002444

ITS.

Figure 3.D.1 Bottom End Lift at the Inlet Vents

Rev. 0



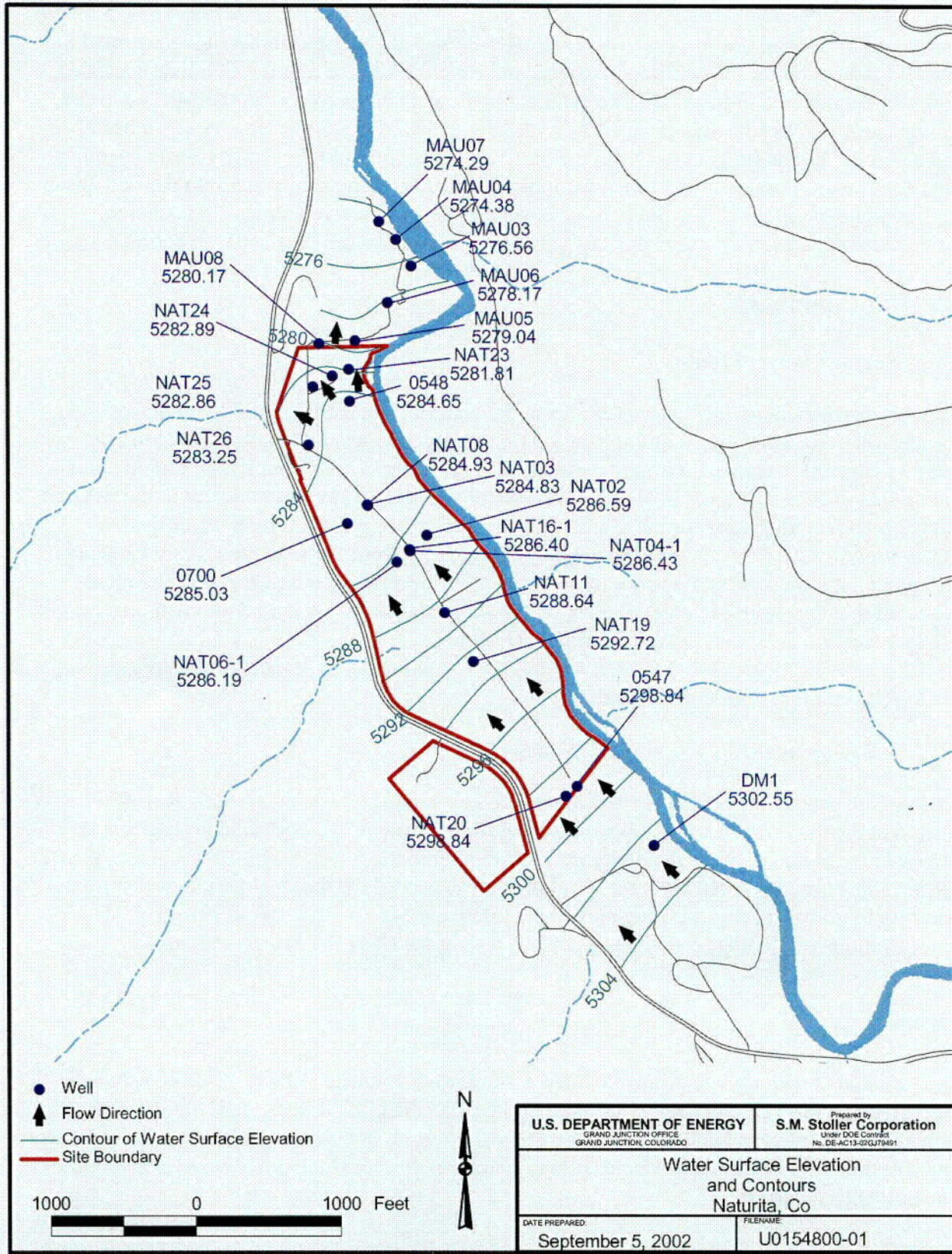
ANSYS 5.2
 FEB 3 1997
 14:48:12
 ELEMENTS
 REAL NUM
 XV =1
 YV =-1
 ZV =1
 *DIST=29.698
 *XF =46.152
 *YF =23.29
 *ZF =-19
 VUP =Z
 CENTROID HIDDEN

HI-STORM FSAR int Model
 HI-2002444

C02

Figure 3.D.2a Top End Lift Finite Element Model

Rev. 0

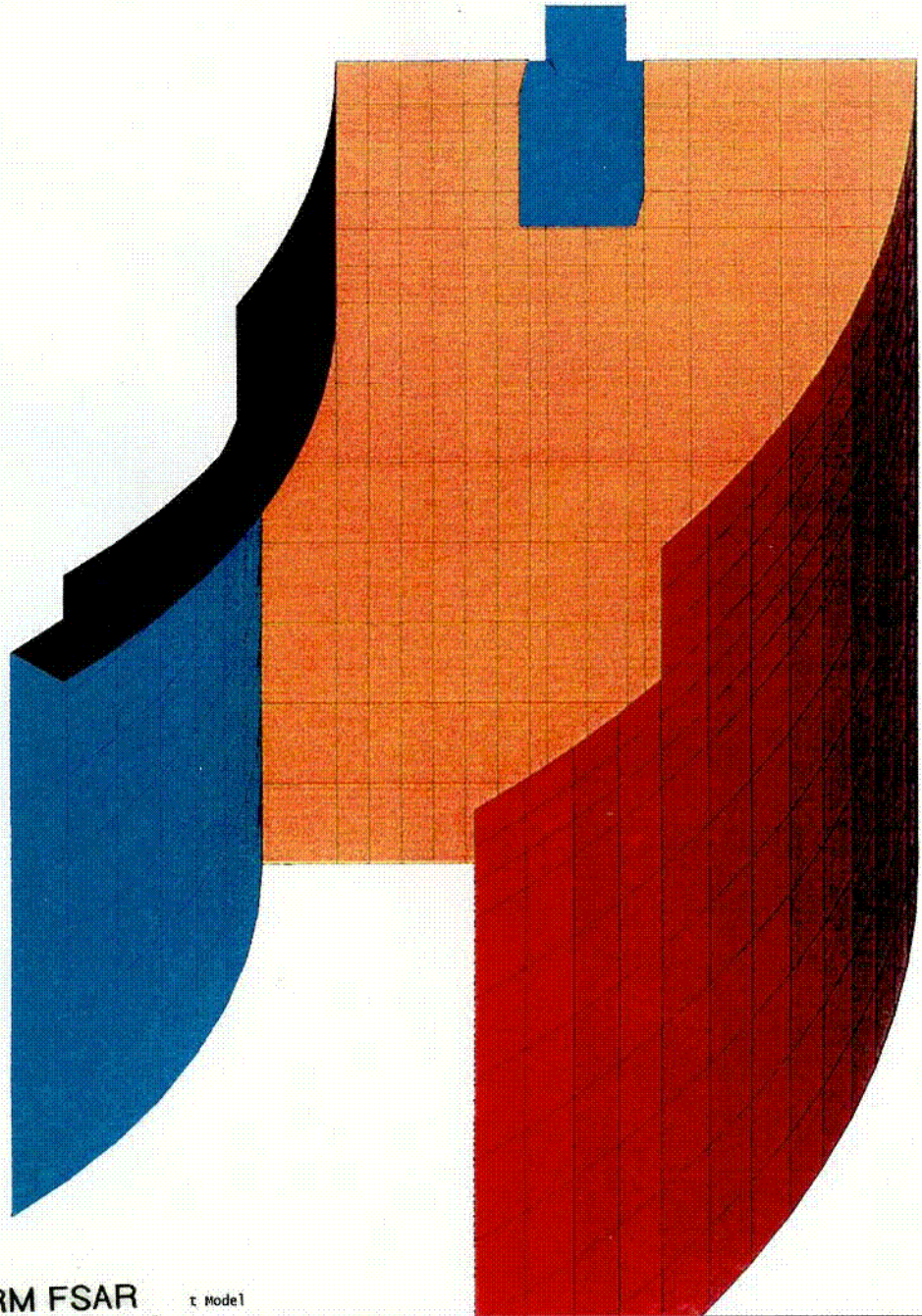


m:\ugw\51110016\13\w\01548\w\0154800.apr r50329 9/5/2002, 15:59

Figure 2-4. Alluvial Water Table Elevations at the Naturita Site

CO3

ANSYS 5.2
FEB 3 1997
14:45:58
ELEMENTS
REAL NUM
XV =1
YV =-1
ZV =1
*DIST=29.698
*XF =46.152
*YF =23.29
*ZF =-19
VUP =2
CENTROID HIDDEN



HI-STORM FSAR
HI-2002444

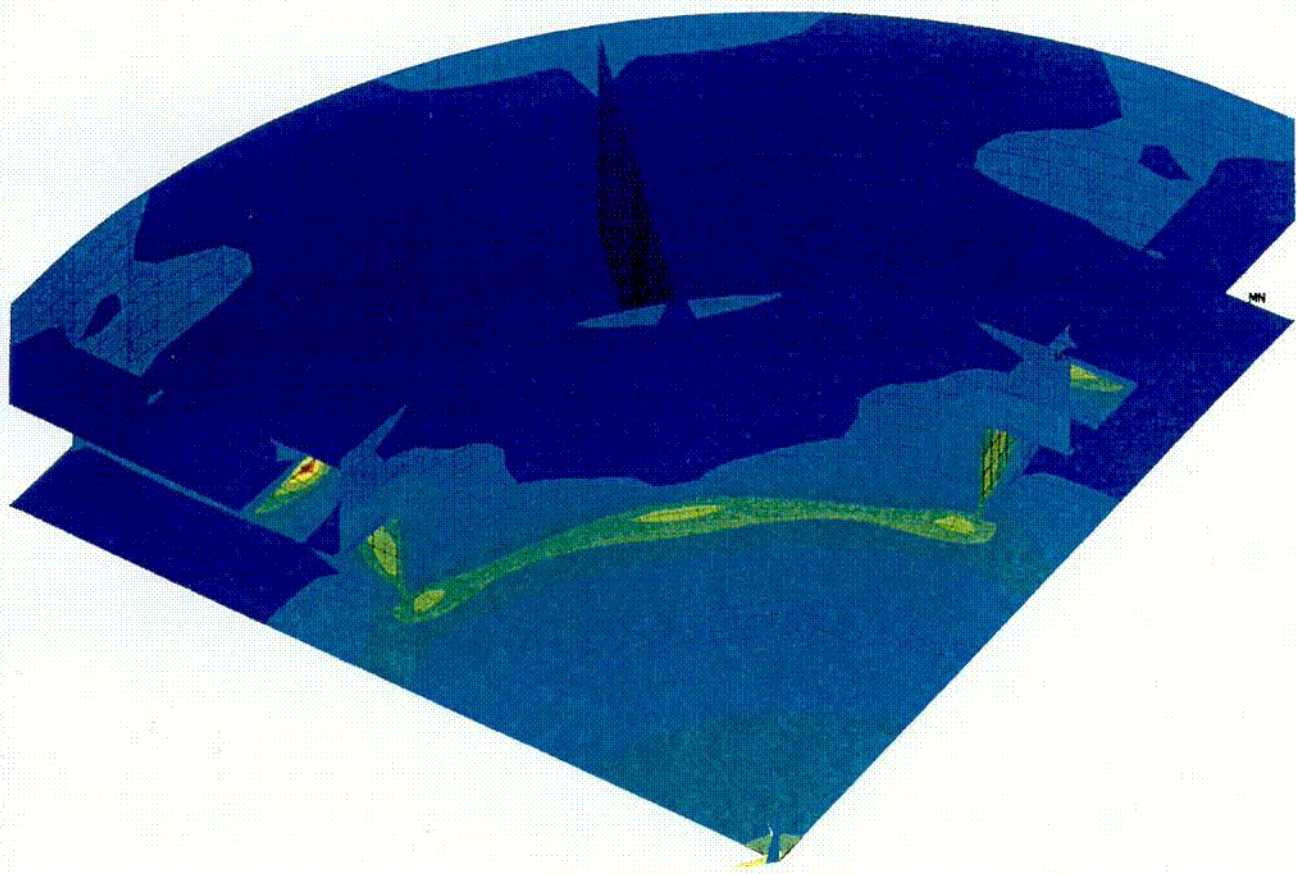
t Model

Figure 3D.2c Top End Lift Finite Element Model

Rev. 0

copy

ANSYS 5.2
 FEB 3 1997
 14:13:28
 NODAL SOLUTION
 STEP=1
 SUB =1
 TIME=1
 SINT (AVG)
 TOP
 DMX = .07113
 SMN =89.219
 SMX =13893
 SMXB=19376
 89.219
 1623
 3157
 4690
 6224
 7758
 9292
 10825
 12359
 13893



HI-STORM FSAR
 HI-2002444

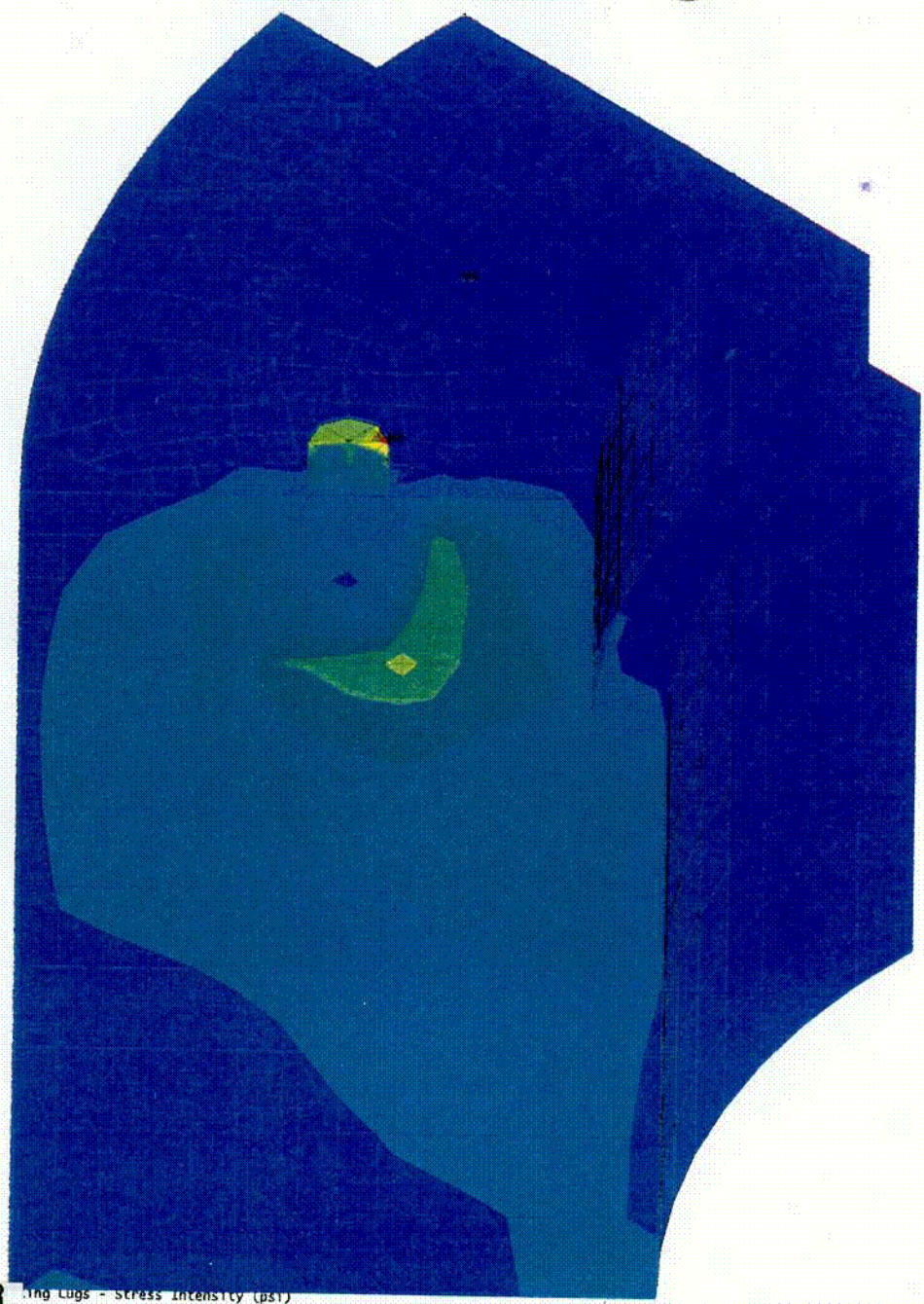
VENTS - STRESS INTENSITY PROF

Figure 3.D.3 Bottom End Lift at the Inlet Vents - Stress Intensity Profile (psi)

Rev. 0

C05

ANSYS 5.2
FEB 3 1997
14:25:47
NODAL SOLUTION
STEP=1
SUB =1
TIME=1
S.INT (AVG)
TOP
DMX =.013705
SMN =115.307
SHX =27380
SPOXB=52027
115.307
3145
6174
9204
12233
15263
18292
21321
24351
27380



HI-STORM FSAR
HI-2002444

Lifting Lugs - Stress Intensity (psi)

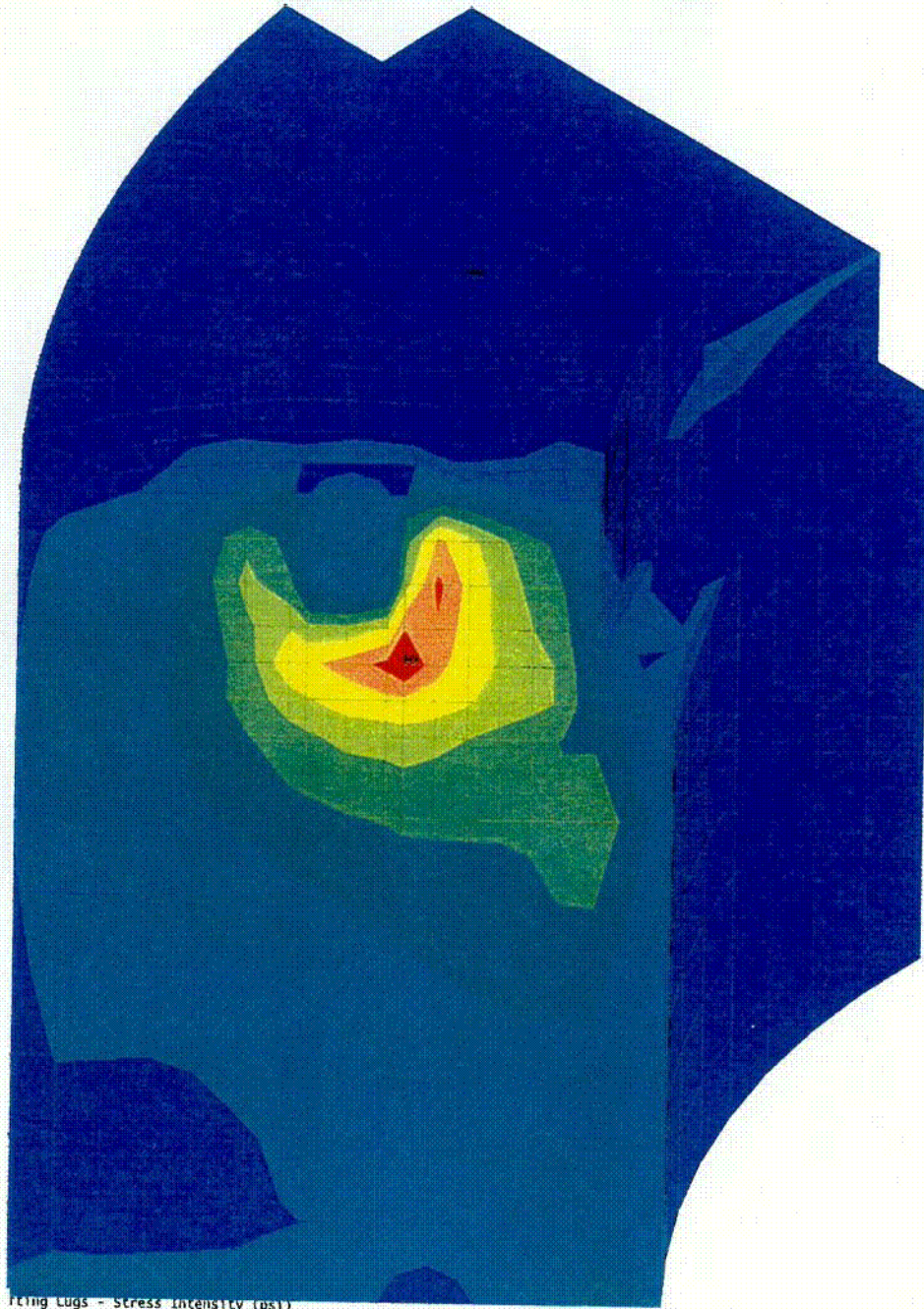
Figure 3.D.4a Top End Lift at the Lifting Lugs - Stress Intensity (psi)

Rev. 0

600

ANSYS 5.2
 FEB 3 1997
 14:27:13
 NODAL SOLUTION
 STEP=1
 SUB =1
 TIME=1
 SINT (AVG)
 TOP
 DMX =.013705
 SMN =115.307
 SMX =16612
 SMXB=20816

115.307
1948
3781
5614
7447
9280
11113
12946
14779
16612



Lifting Lugs - Stress Intensity (psi)

HI-STORM FSAR
 HI-2002444

Figure 3.D.4b Top End Lift at the Lifting Lugs - Stress Intensity (psi)

Rev. 0

007

ANSYS 5.2
 FEB 3 1997
 14:30:33
 NODAL SOLUTION
 STEP=1
 SUB =1
 TIME=1
 SINT (AVG)
 TOP
 DMX = .013705
 SMN =115.307
 SMX =8837
 SMAX=14816
 115.307
 1084
 2054
 3023
 3992
 4961
 5930
 6899
 7868
 8837



Figure 3.D.4. Top End Lift at the Lifting Lugs - Stress Intensity (psi)

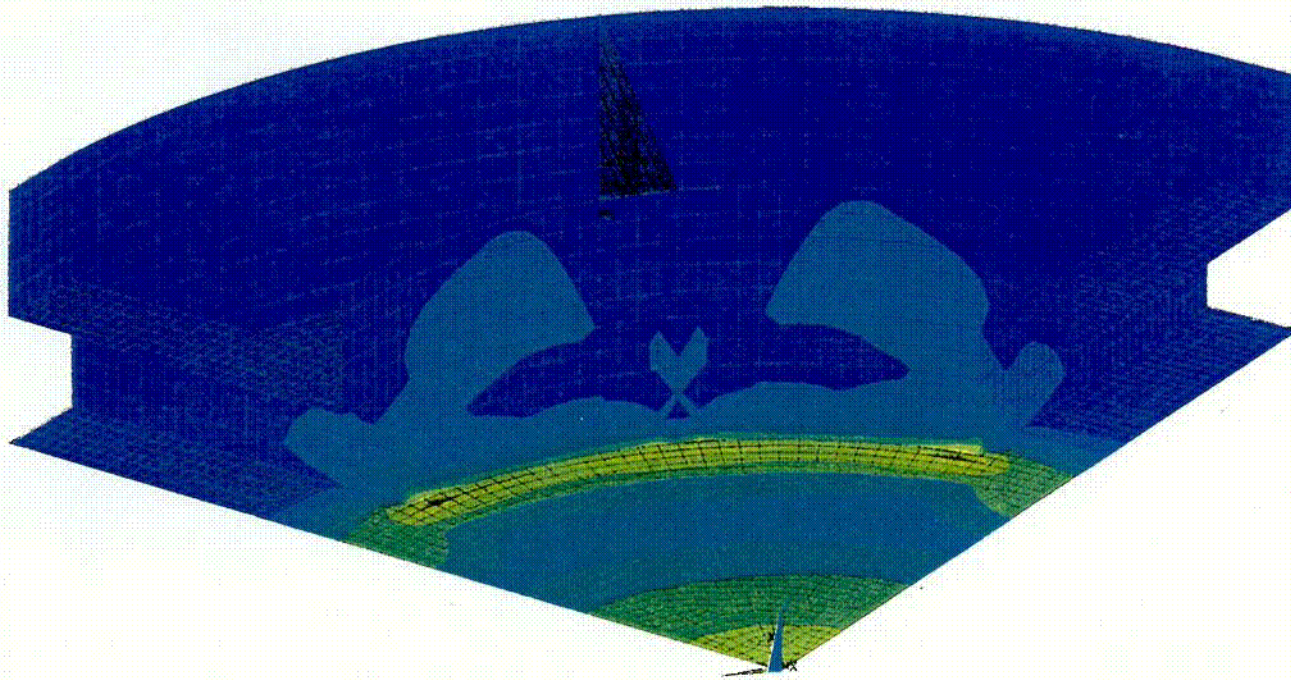
Rev. 0

808

HI-STORM FSAR
 HI-2002444

Figure 3.D.4c Top End Lift at the Lifting Lugs - Stress Intensity (psi)

ANSYS 5.2
FEB 3 1997
15:31:58
NODAL SOLUTION
STEP=1
SUB =1
TIME=1
SINT (AVG)
TOP
DMX =.062175
SMN =29.283
SMX =10070
SMXB=13973
29.283
1145
2261
3376
4492
5608
6723
7839
8955
10070



HI-STORM FSAR
HI-2002444

Intensity (psi)

Figure 3.D.5a Top End Lift - Baseplate Stress Intensity (psi)

Rev. 0

C09

ANSYS 5.2
 FEB 3 1997
 15:43:09
 NODAL SOLUTION
 STEP=1
 SUB =1
 TIME=1
 SINT (AVG)
 TOP
 DMX = .062175
 SMN =20.724
 SMX =10070
 SHXB=13973

20.724
1137
2254
3371
4487
5604
6720
7837
8954
10070



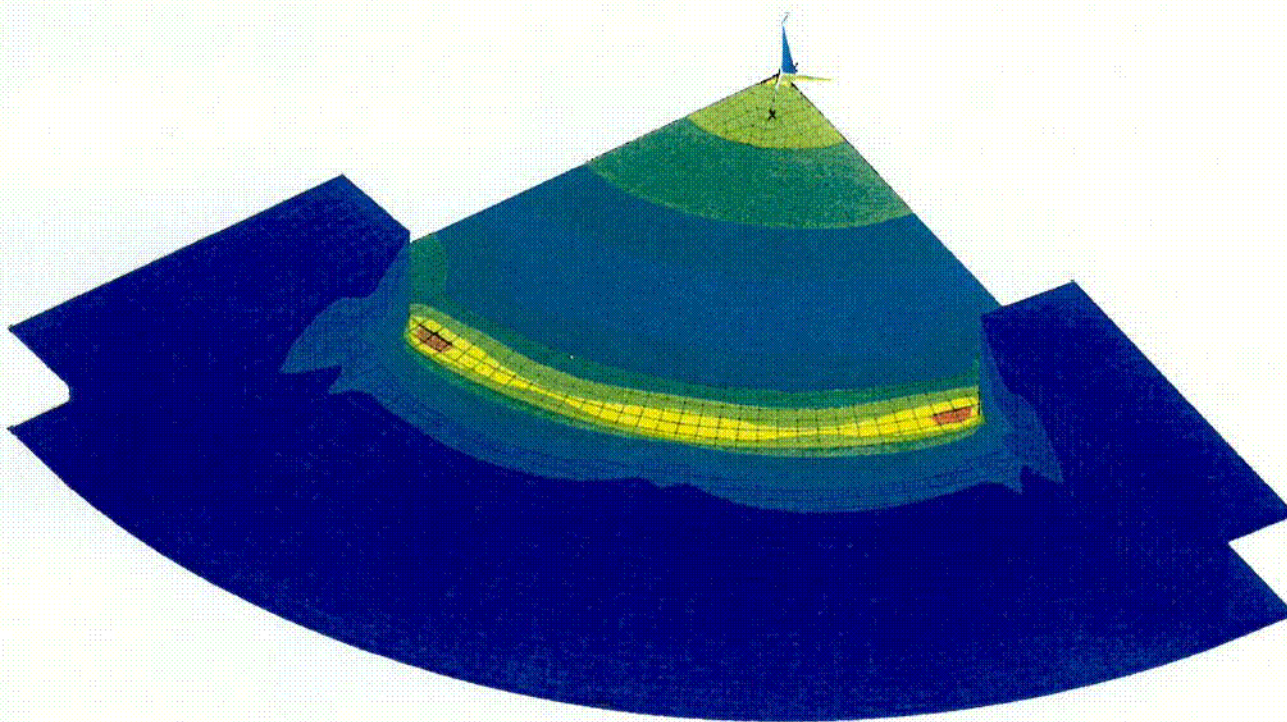
Fi HI-STORM FSAP Intensity (psi)
 HI-2002444

Figure 3.D.5b Top End Lift - Baseplate Stress Intensity (psi)

Rev. 0

C10

ANSYS 5.2
FEB 3 1997
15:38:38
MODAL SOLUTION
STEP=1
SUB =1
TIME=1
SINT (AVG)
TOP
DIX = .062175
SIN = 3.874
SMX = 10070
SMCY = 13778
3.874
1122
2241
3359
4478
5596
6715
7833
8952
10070



HI-STORM FSAR Intensity (psi)
HI-2002444

Figure 3.D.5c Top End Lift - Baseplate Stress Intensity (psi)

Rev. 0

11

APPENDIX 3.E - LIFTING TRUNNION STRESS ANALYSIS FOR HI-TRAC

3.E.1 Introduction and Description

This appendix contains a stress analysis of the upper lifting trunnions on the HI-TRAC transfer cask. The objective of this analysis is to show that under any cask lifting condition, the stress in the trunnions do not exceed allowable limits. The appendix is self contained; all references cited are listed in Section 3.E.5. All input dimensions are obtained from Holtec drawing no. 1880.

The lifting trunnions are threaded into the trunnion block which is welded to the outer and inner shells and the top forging of HI-TRAC. A locking plate, secured with attachment bolts, prevents the trunnions from backing out.

This Appendix is written using the Mathcad computer code [3.E.1]. The notation ":@" represents the equal sign for a defined calculation. The notation "=" represents a computed response or answer.

3.E.2 Methodology and Acceptance Criteria

Methodology

The lifting trunnions are analyzed using a mechanics of materials method with the trunnions considered as short beams. Stresses in both the trunnions and in the HI-TRAC top forging are calculated under the specified load. Sketches at the end of the appendix show the appropriate free body diagrams.

In this analyses, primary bending and shear stresses in the trunnions are determined first. Then, local bearing stress, thread shear stress, and trunnion block weld stresses are computed.

The global effect of the trunnion loadings on the supporting shell structure and top flange is considered by a finite element analysis of the HI-TRAC structure near the trunnions (see Appendix 3.AE).

Acceptance Criteria

The HI-TRAC transfer cask trunnions are part of a non-redundant lifting system. NUREG-0612 [3.E.2], section 5.1.6(3), requires that the lifting trunnions be able to support a load of 10 times the actual lifted load without exceeding the material ultimate strength.

The lifted load should include a dynamic load factor to account for inertia effects. CMAA Specification #70 (1988) [3.E.3], recommends an appropriate minimum hoist load factor for lifted loads. Since cask lifting is a low speed operation the use of a minimum hoist load factor for dynamic effects is conservative.

Where the trunnions and the top forging interface, the top forging allowable strengths are used in the determination of structural margins; the limits on strength are those of the ASME Code, Section III, Subsection NF for the appropriate load combination.

3.E.3 Materials and Material Properties

The trunnions are SB-637-N07718 steel. The transfer cask trunnion block is SA-350-LF3 steel. The trunnion design temperature is set at 150°F; trunnion block properties are also based on a temperature of 200°F. These are appropriate temperatures based on thermal analysis results in Table 4.5.4. Material properties are extracted from the appropriate tables in Section 3.3.

The trunnion material yield strength, $S_y := 147000 \cdot \text{psi}$

The trunnion material ultimate strength, $S_u := 181300 \cdot \text{psi}$

The trunnion block and top forging material yield strength, $S_{yf} := 34200 \cdot \text{psi}$

The trunnion block and top forging material ultimate strength, $S_{uf} := 68500 \cdot \text{psi}$

3.E.4 Assumptions

1. The trunnions are analyzed for strength as beam members.
2. The weight of the extended portion of the trunnion is conservatively neglected since it opposes the lifted load.
3. Any load carrying capacity of the locking plate is conservatively neglected.
4. Trunnions are loaded equally.
5. The lifting yoke is conservatively set at the outer end of the trunnion less 50% of the lifting yoke so as to maximize the moment arm. The minimum thickness of the lifting yoke is specified. Therefore, the maximum value of the moment arm can be established.
6. Trunnion stress analysis is based only on mechanical loads applied laterally to the trunnion axis.

3.E.5 References

[3.E.1] MATHCAD 7.0, Mathsoft, 1997.

[3.E.2] NUREG-0612, Control of Heavy Loads at Nuclear Power Plants Resolution of Generic Technical Activity A-36, Section 5.1.6(3), 1980.

[3.E.3] Crane Manufacturers Association of America (CMAA), Specification #70, 1988, Section 3.3.

[3.E.4] J. Shigley and C. Mischke, Mechanical Engineering Design, McGraw-Hill, 5th Edition, 1989, p.328.

[3.E.5] O.W. Blodgett, Design of Welded Structures, The James F. Lincoln Arc Welding Foundation, 12th Edition, 1982, p.7.4-7.

3.E.6 Analysis

In this section, stresses in the trunnion and the trunnion block material are determined. Stresses in the trunnions are compared to allowable strengths per NUREG-0612, and stresses in the trunnion block are compared with appropriate allowable strengths from Subsection NF of the ASME Code

3.E.6.1 Stresses in the Trunnion

In this subsection, the geometry of the system is defined, and bending and shear stresses in the lifting trunnions are determined. The input lifted load is from Table 3.2.4 less the lift yoke (3,600 lb).

3.E.6.1.1 Input Data

All input dimensions are obtained from Holtec drawing no. 1880.

The trunnion outer diameter, $d := 5.75 \cdot \text{in}$

The minimum lift yoke connecting link yoke width, $t_f := 2.25 \cdot \text{in}$

The bounding lifted weight of the cask and contents (lift yoke not included),

$W := 245000 \cdot \text{lb}$

The number of lifting trunnions, $n := 2$

The dynamic load factor (from 3.E.3), $DLF := 1.15$

The exposed trunnion length, $L := 3.375 \cdot \text{in}$

This minimum lift yoke connecting link width defines the contact patch on the trunnion and establishes the location of the concentrated lifting load. The maximum lifted weight bounds the actual maximum weights of the HI-TRAC 100 systems.

The trunnion cross sectional area (Area), moment of inertia (I) and applied per trunnion load (P) can be determined using the following formulae:

$$\text{Area} := \frac{\pi}{4} \cdot d^2 \qquad I := \frac{\pi}{4} \cdot \left(\frac{d}{2}\right)^4 \qquad P := \frac{W \cdot \text{DLF}}{n}$$

Substituting the input values defined above into these three equations yields the following values:

$$\text{Area} = 25.97 \text{ in}^2 \qquad I = 53.65884 \text{ in}^4 \qquad P = 1.41 \times 10^5 \text{ lbf}$$

3.E.6.1.2 Bending Stress in the Trunnion

The lifting yoke arm is conservatively set at the outer end of the trunnion to maximize the moment arm. The applied moment arm (L_{arm}) is defined as the distance from the root of the trunnion to the centerline of the lifting yoke connecting link (see Figure 3.E.1).

$$L_{\text{arm}} := L - .5 \cdot t_f$$

$$L_{\text{arm}} = 2.25 \text{ in}$$

The applied moment (M) at the root of the trunnion is therefore determined as:

$$M := P \cdot L_{\text{arm}} \qquad M = 3.17 \times 10^5 \text{ in} \cdot \text{lbf}$$

From beam theory, the maximum tensile stress occurs in an outer fiber at the root of the trunnion. The distance from the neutral axis to an outer fiber (y) is one-half of the trunnion diameter:

$$y := \frac{d}{2}$$

and the maximum bending stress due to the applied moment is therefore determined as:

$$\sigma := \frac{M \cdot y}{I} \qquad \sigma = 16982.92 \text{ psi}$$

Comparing the value of the bending stress with 10% of the ultimate strength of the material and 16.7% of the yield strength results in safety factors of:

$$S_{1u} := \frac{.1 \cdot S_u}{\sigma} \qquad S_{1u} = 1.07 \qquad S_{1y} := \frac{.167 \cdot S_y}{\sigma} \qquad S_{1y} = 1.45$$

This safety factor is greater than 1, which is the factor of safety required by [3.E.2]. Note that the safety factor calculated above, and used elsewhere in this appendix, is defined as the allowable strength divided by the calculated strength.

3.E.6.1.3 Shear Stress in the Trunnion

The maximum shear stress in the trunnion, which occurs at the neutral axis, is determined using beam theory. The first moment of the area above the neutral axis is determined as:

$$Q := \int_0^\pi \int_{0-\text{in}}^{\frac{d}{2}} r^2 \cdot \sin(\theta) \, dr \, d\theta \quad \text{or} \quad Q := \frac{1}{12} \cdot d^3$$

$$Q = 15.84 \text{ in}^3$$

The shear load (V) is equal to the applied per trunnion load (P) and the "thickness" of the beam (t) at the neutral axis is equal to the trunnion diameter (d).

$$V := P \quad t := d$$

From beam theory, the maximum shear stress is determined as:

$$\tau := \frac{V \cdot Q}{I \cdot t} \quad \tau = 7233.47 \text{ psi}$$

The ultimate shear strength is defined as 60% of the ultimate tensile strength. Comparing the calculated shear stress value with 10% of the ultimate shear strength, result in a safety factor of:

$$S_4 := \frac{0.1 \cdot (0.6 \cdot S_u)}{\tau} \quad S_4 = 1.5$$

This safety factor is greater than 1, as required by [3.E.2].

3.E.6.2 Stresses in the Trunnion Block

In the following subsection, stresses in the trunnion block due to bearing loads and thread shear loads are determined. Also computed is the average weld shear stress connecting the trunnion block to the HI-TRAC shells and top forging.

3.E.6.2.1 Input Data

The number of threads per inch,	NTI := 4	
The trunnion length inserted into the trunnion block,	$L_w := 4.375 \cdot \text{in}$	(conservative minimum)
The transfer forging outer diameter,	$D_o := 81.25 \cdot \text{in}$	
The transfer forging inner diameter,	$D_i := 68.75 \cdot \text{in}$	
Weld thickness - outer shell,	$t_{wo} := .625 \cdot \text{in}$	
Weld thickness - inner shell,	$t_{wi} := .625 \cdot \text{in}$	
Width of trunnion block,	$w_{block} := 10 \cdot \text{in}$	
Depth of trunnion block,	$d_{block} := 10 \cdot \text{in}$	
Thickness of trunnion block,	$t_{block} := .5 \cdot (D_o - D_i)$	$t_{block} = 6.25 \text{ in}$

3.E.6.2.2 Bearing Stress and Thread Shear Stress

A longitudinal local bearing stress is developed in the base material, during cask handling, at the contact surface between the embedded portion of the trunnion and the cavity in the trunnion block. The effective diameter (for stress evaluation purposes) of the portion of the trunnion that is threaded into the trunnion block is determined as per [3.E.4] as:

$$dd := d - \frac{1.299038}{NTI} \cdot \text{in} \quad dd = 5.43 \text{ in}$$

The projected area supporting the bearing load is determined as:

$$A := L_w \cdot dd \quad A = 23.74 \text{ in}^2$$

and the average bearing stress on the trunnion block is therefore determined as:

$$\sigma_d := \frac{V}{A} \quad \sigma_d = 5935.21 \text{ psi}$$

The bending moment that is transferred from the trunnion to the top forging is reacted by a shear stress distribution on the threads. (see Figure 3.E.2, a free body of the portion of the trunnion inserted into the forging). We recalculate the bending moment using a bounding value for the actual location of the applied load. This bounding value considers that the maximum position of the lifting link on the trunnion will leave a clearance "c" between the edge of the link and the end of the trunnion.

$$c := 0.25 \cdot \text{in}$$

The total bending moment applied to the trunnion threads is therefore defined by:

$$\text{Moment} := M \cdot \frac{(L_{\text{arm}} - c)}{L_{\text{arm}}} + V \cdot \left(\frac{L_w}{2} \right) \quad \frac{(L_{\text{arm}} - c)}{L_{\text{arm}}} = 0.89$$

The average shear stress in the threaded region is assumed to be a sinusoidal distribution around the periphery. Therefore, moment equilibrium yields:

$$\text{Moment} := \int_0^{2\pi} \tau \cdot R \cdot \sin(\text{theta}) \cdot R \cdot (L_w) \, d\text{theta}$$

where the average shear stress along the threaded length, $\tau := \tau_{\text{max}} \cdot \sin(\text{theta})$

Integrating the moment expression above, over the required interval, yields the following expression for the total bending moment:

$$\text{Moment} := \tau_{\text{max}} \cdot \pi \cdot d^2 \cdot \frac{(L_w)}{4}$$

Solving for the maximum shear stress existing around the circumference of the trunnion (averaged along the length of the insert) gives the stress at the root of the trunnion thread.

$$\tau_{\text{max}} := 4 \cdot \frac{\text{Moment}}{\pi \cdot d^2 \cdot (L_w)} \quad \tau_{\text{max}} = 5832.87 \text{ psi}$$

Similarly, the shear stress at the external root of the thread in the trunnion block is:

$$\tau_{\text{froot}} := 4 \cdot \frac{\text{Moment}}{\pi \cdot d^2 \cdot L_w} \quad \tau_{\text{froot}} = 5192.6 \text{ psi}$$

3.E.6.2.3 Comparison with Yield Strength Per Reg.Guide 3.61 and NUREG-0612

The allowable yield stress of the top forging material in the region supporting the lifting trunnions is set forth in Section 3.E.3 of this appendix as:

$$S_{yf} = 34200 \text{ psi}$$

The safety factor against yield in the top forging is calculated for bearing stress and for thread shear stress separately. The same calculation is also performed for the trunnion material at the interface.

We note that Regulatory Guide 3.61 only requires that the material anywhere in the cask not exceed 1/3 of the yield stress.

Safety Factor Against Yielding for Bearing Stress in Trunnion Block at Interface

$$SF_{\text{bearing}} := \frac{0.333 \cdot S_{yf}}{\sigma_d} \quad SF_{\text{bearing}} = 1.92$$

Safety Factor Against Yielding for Thread Shear Stress in Trunnion Block at interface.

$$SF_{\text{thread_shear}} := .6 \cdot \frac{0.333 \cdot S_{yf}}{\tau_{\text{froot}}} \quad SF_{\text{thread_shear}} = 1.32$$

Safety Factor Against Yielding for Bearing Stress in Trunnion

$$SF_{\text{bearing}} := \frac{S_y \cdot 0.1667}{\sigma_d} \quad SF_{\text{bearing}} = 4.13$$

Safety Factor Against Yielding for Thread Shear Stress in Trunnion

$$SF_{\text{thread_shear}} := .6 \cdot \frac{S_y \cdot 0.1667}{\tau_{\text{max}}} \quad SF_{\text{thread_shear}} = 2.52$$

The above calculations demonstrate that the local bearing stress and the thread shear stress at the trunnion-forging interface satisfy NUREG-0612 requirements on trunnion safety factors against material yield and satisfy Regulatory Guide 3.61 requirements on material in the cask (other than the trunnion itself).

3.E.6.2.4 Trunnion Block Weld Stress

Figure 3.E.3 shows the weld array that transfers the load to the top forging and to the outer and inner shells. The weld array transfers the total shear force and the bending moment to the HI-TRAC body.

The areas and the moments of inertia for the outer and inner welds are:

$$\text{Area}_{wo} := t_{wo} \cdot (2 \cdot w_{block} + 2 \cdot d_{block}) \quad \text{Area}_{wo} = 25 \text{ in}^2$$

$$I_{wo} := \frac{2 \cdot d_{block}^3 \cdot t_{wo}}{12} + 2 \cdot w_{block} \cdot t_{wo} \cdot \left(\frac{d_{block}}{2} \right)^2 \quad I_{wo} = 416.67 \text{ in}^4$$

$$\text{Area}_{wi} := t_{wi} \cdot (2 \cdot w_{block} + 2 \cdot d_{block}) \quad \text{Area}_{wi} = 25 \text{ in}^2$$

$$I_{wi} := \frac{2 \cdot d_{block}^3 \cdot t_{wi}}{12} + 2 \cdot w_{block} \cdot t_{wi} \cdot \left(\frac{d_{block}}{2} \right)^2 \quad I_{wi} = 416.67 \text{ in}^4$$

The center of gravity, the total area, and the total moment of inertia of the weld are:

$$x_{wg} := \frac{-\text{Area}_{wo} \cdot \left(\frac{t_{block}}{2} \right) + \text{Area}_{wi} \cdot \left(\frac{t_{block}}{2} \right)}{\text{Area}_{wo} + \text{Area}_{wi}} \quad x_{wg} = 0 \text{ in}$$

$$\text{Area}_w := \text{Area}_{wo} + \text{Area}_{wi} \quad \text{Area}_w = 50 \text{ in}^2$$

$$I_w := I_{wo} + \text{Area}_{wo} \cdot \left(\frac{t_{block}}{2} + x_{wg} \right)^2 + I_{wi} + \text{Area}_{wi} \cdot \left(\frac{t_{block}}{2} - x_{wg} \right)^2 \quad I_w = 1321.61 \text{ in}^4$$

The distance to the extreme weld fiber is:

$$c_{max} := \sqrt{\left(\frac{d_{block}}{2} \right)^2 + \left(\frac{t_{block}}{2} - x_{wg} \right)^2} \quad c_{max} = 5.9 \text{ in}$$

The bending moment and the shear force to be resisted by the weld array are:

$$\text{Moment} := M + V \cdot \left(\frac{t_{\text{block}}}{2} + x_{\text{wg}} \right) \quad \text{Moment} = 7.57 \times 10^5 \text{ lbf}\cdot\text{in} \quad V = 1.41 \times 10^5 \text{ lbf}$$

The average weld stress from the shear force is

$$\tau_V := \frac{V}{\text{Area}_w} \quad \tau_V = 2817.5 \text{ psi}$$

The maximum weld stress due to the bending moment is

$$\tau_M := \frac{\text{Moment} \cdot c_{\text{max}}}{I_w} \quad \tau_M = 3378.17 \text{ psi}$$

Therefore, the maximum weld stress is

$$\tau_{\text{weld}} := \sqrt{\tau_V^2 + \tau_M^2} \quad \tau_{\text{weld}} = 4398.9 \text{ psi}$$

The weld stress safety factor is compared to 1/3 the material yield strength

$$\text{SF}_{\text{weld}} := 0.333 \cdot \frac{S_{yf}}{\tau_{\text{weld}}} \quad \text{SF}_{\text{weld}} = 2.59$$

3.E.7 Conclusion

The HI-TRAC lifting trunnions meet the requirements of NUREG 0612 for lifting heavy loads in a nuclear plant. Primary stresses in the top trunnions are less than the ultimate strength of the trunnion material/10. Local bearing stress, thread shear stress, and weld stress in the top trunnion support block do not exceed the allowable limits imposed by Regulatory Guide 3.61.

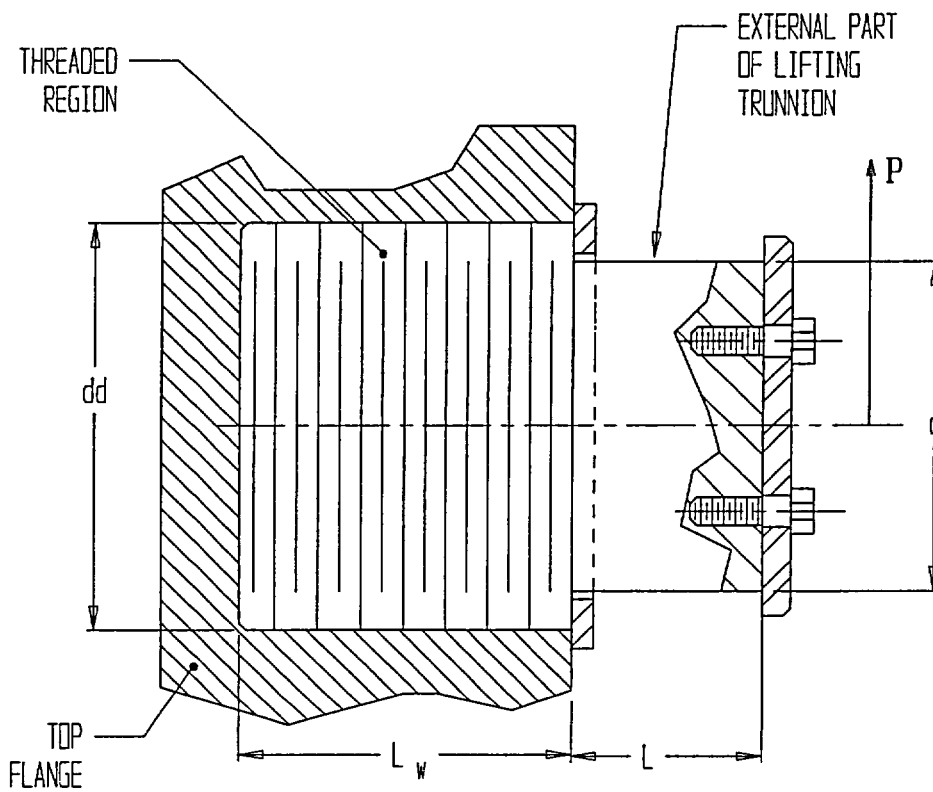


FIGURE 3.E.1; SKETCH OF LIFTING TRUNNION GEOMETRY SHOWING APPLIED LOAD

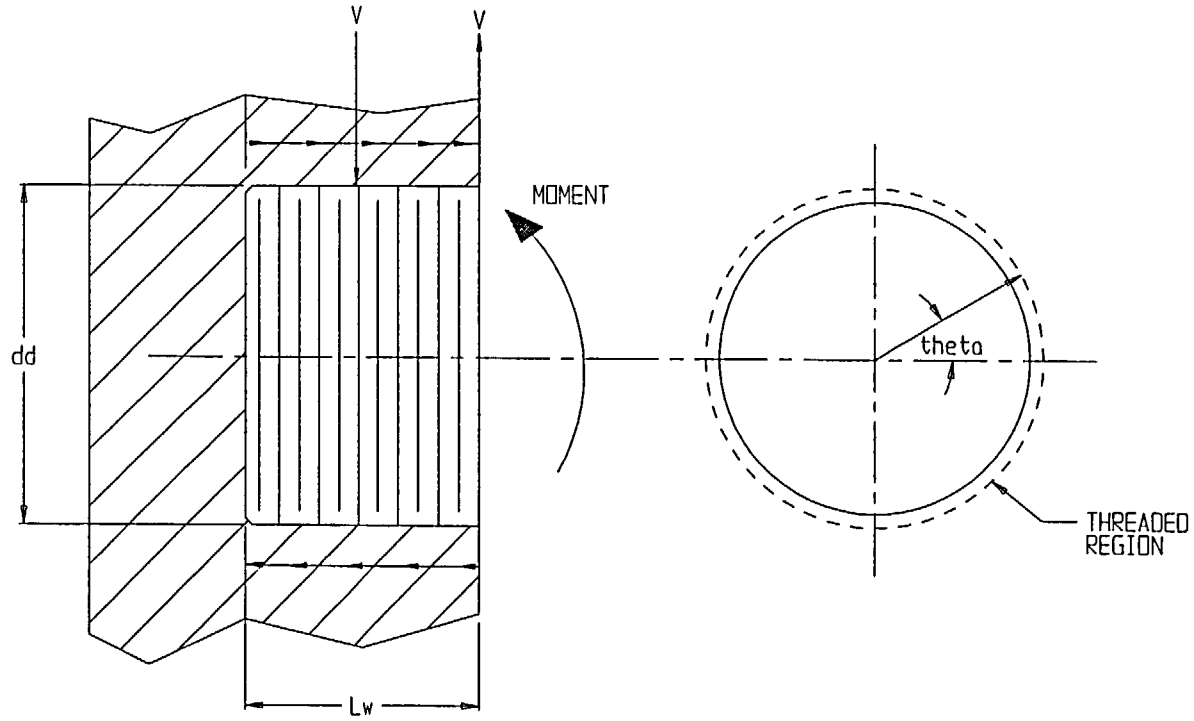


FIGURE 3.E.2; FREE BODY SKETCH OF LIFTING TRUNNION THREADED REGION SHOWING MOMENT BALANCE BY SHEAR STRESSES

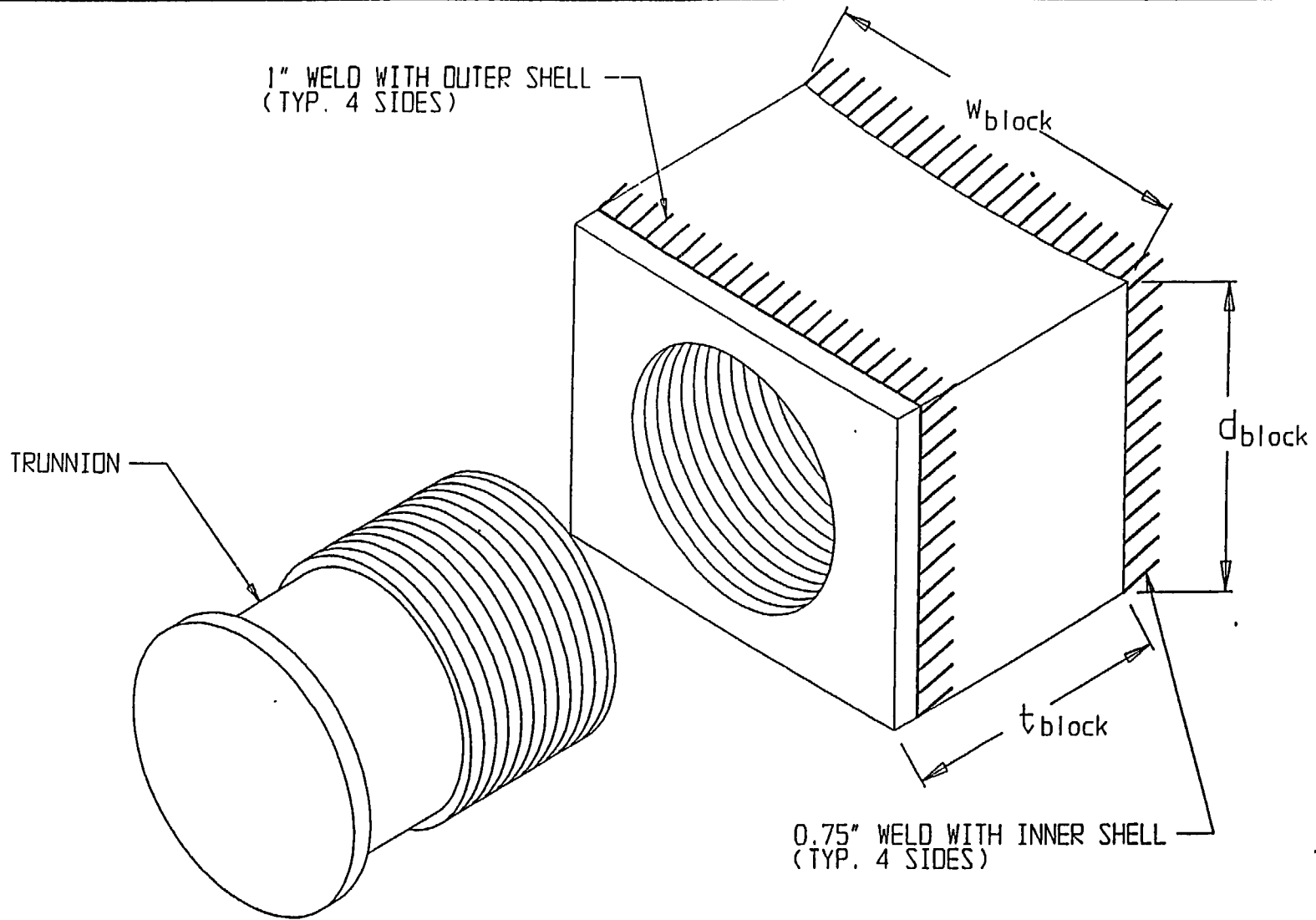


FIGURE 3.E.3; WELD CONFIGURATION IN LIFTING TRUNNION BLOCK

APPENDIX 3.F LEAD SLUMP ANALYSIS (HI-TRAC SIDE DROP)

3.F.1 Introduction

The HI-TRAC 125 transfer cask body consists of a ¾-inch inner metal shell, a 1-inch thick outer metal shell and a 4.5-inch thick lead annulus between the inner and the outer shells. The inner shell and outer shell are fabricated from carbon steel material (SA-516-GR.70). During a postulated handling accident scenario, resulting in a side drop on the ISFSI pad, the HI-TRAC is assumed subjected to a design basis deceleration load of 45 Gs which may result in the slumping of the radial lead shield. Slumping of the radial lead shield from a side drop accident is not considered a probable scenario because of:

- (a) the shape of the interacting surfaces;
- (b) the ovalization of the shell walls at impact;
- (c) the compression of the shell walls by the weight of the MPC at the region of direct impact with the ISFSI pad; and,
- (d) the relatively high friction coefficient of 0.97 between lead-steel surfaces [1].

Nevertheless, an analysis of the potential for lead slump, as a result of a 45G side impact of the HI-TRAC on a storage pad, is investigated in this appendix.

3.F.2 Assumptions

The analysis in this appendix is based on the following assumptions:

- a) Frictionless interfaces are assumed to conservatively increase the propensity for lead slump.
- b) The lead slump starts and ends before the deformation of the shell walls.
- c) The dynamic modulus of lead behaves as predicted in Reference 2.
- d) The temperature of lead during a transfer operation is high enough to support the predicted behavior of lead in Reference 2.
- e) The HI-TRAC shell walls are infinitely long, i.e., the outer and inner shell are uncapped at the top and bottom ends.
- f) The deceleration loads are conservatively assumed to be reacted at a single point of contact (with the ISFSI pad). This results in an overestimation of local stress.

3.F.3 Methodology

The lead slump analysis is split into two phases. The first phase (Phase I) calculates the amount of lead slump and the associated radial forces at the boundaries as a result of a 45G side impact. The second phase (Phase II) imposes the radial forces computed in

Phase I as input load for the calculation of the stresses in the inner shell and the outer shell walls. The lead slump analysis is performed using the ANSYS, 3D, slider-gap-friction element COMBIN40 and the 2-D isoparametric solid element PLANE42. ANSYS[3] is a general purpose finite element computer code. A planar cross section of the HI-TRAC is modeled with PLANE42 and COMBIN40 as shown in Figure 3.F.1.

Phase I.

The compressive and tensile forces on the inner shell and the outer shell, as a result of the hypothetical lead slump, are calculated in this section of the analysis. To accomplish this task, the inner shell and the outer shell are removed, from the overall finite element model and the compression-only gap elements between the lead-shell interfaces grounded.

The following material values are used in the analysis:

The stiffness of the compression-only gap elements is taken as $1.0E+06$ pounds per inch.

The secant modulus of elasticity of the lead is 15,000 psi. This value is based on the quasi-static true stress-strain curves for chemical lead in compression.

The density and poisson's ratio of lead are taken as 0.41 pounds per-cubic-inch and 0.40 respectively.

The results of the Phase I analysis are the radial forces in the interface gap elements where contact is maintained and the deformation of the lead. The radial compression force on the gap elements associated with a 45-G impact is used as loading in the second stage of the analysis. Table 3.F.1 shows these forces for the inner shell and the outer shell used for the stress calculations in Phase II. The values in Table 3.F.1 are plotted in Figure 3.F.3. Figure 3.F.2 shows the radial contraction of the lead shield from the imposed 45G deceleration loading (imposed as an amplified gravitational acceleration).

Phase II:

The full model shown in Figure 3.F.1 is used for this analysis. The deceleration forces in the lead is removed by setting the density of lead to zero since it has been used a priori in the computation of the radial forces on the shell in Phase I. These radial forces are now applied as loads on the inner shell and the outer shell as shown in Figure 3.F.3 along with the 45G side impact deceleration load on the metal shells. It is noted that these forces are overestimated because of the approach used in Phase I.

The material properties for the inner and outer metal shells are:

The modulus of elasticity for the inner shell and the outer shell is taken as $28.0E+06$ psi, the poisson's ratio taken as 0.29, and the weight density taken as 0.288 pounds per-cubic-inch.

The resulting stresses in the shells are shown in Figure 3.F.4.

3.F.4 Slump Evaluation

Figure 3.F.2, shows that, even with the conservative assumptions employed in the model, the maximum predicted gap between lead and outer shell, at the location 180° from the impact point, is 0.1 inches. This gap decreases gradually to a zero value at approximately 25 degrees from the Y-axis. The maximum local stress intensity of 51,000 psi occurs at the inner shell as shown in Figure 3.F.4. The location of this stress intensity is directly above the assumed point of impact. It is noted, however, that the magnitude of this local stress intensity still remains below the material strength allowable of 58,700 psi (for primary membrane plus primary bending), in accordance with the ASME Code Subsection NF, Level D criteria at 400°F (Table 3.1.12).

The deformation of the inner and outer shells that contain the lead are negligibly small. The decrease in the diameter of the inner shell of the HI-TRAC transfer cask (in the direction of the deceleration) is approximately $0.00054''$. This result demonstrates that ovalization of the shell, due to forces from the contained lead, is negligible.

It is noted that in an actual drop scenario, the water jacket (not included here) would suffer the effects of the direct impact; the reaction load balancing the deceleration loads would not be a point load (as has been modeled herein), but would be spread over a small but finite circumferential length of the outer shell. Thus, in the actual scenario, the stress intensity will be reduced from the value computed here.

3.F.5 Conclusion

The conservative lead slump analysis demonstrates that there is no appreciable change in the status and state of lead after a 45G side impact of the HI-TRAC. The stress intensity levels predicted from this conservative model preclude any permanent global deformations of the configuration. Deformations due to the drop decelerations are primarily confined to the lead; there is no appreciable ovalization of the confining shells.

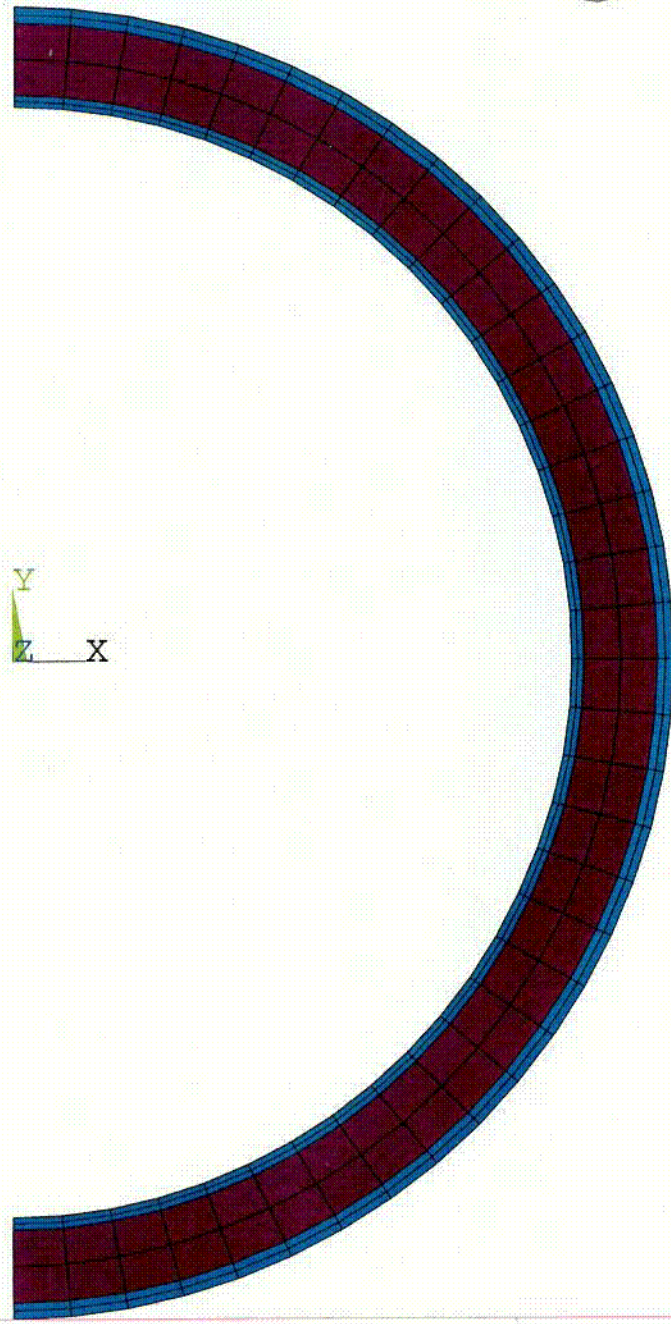
It is concluded that lead slump is not a concern and there will be no impediment to ready retrievability of the MPC and its fuel load in the event of a side drop with a 45G deceleration.

3.F.6 References

1. "Marks' Standard Handbook for Mechanical Engineers", Table 3.2.1, Eugene A. Avallone Theodore Baumeiser III., McGraw-Hill, 1987.

2. Evans, J.H., "Structural Analysis of Shipping Casks, Volume 8, Experimental Study of Stress-Strain Properties of Lead Under Specified Impact Conditions." ORNL/TM-1312, Vol. 8, Oak Ridge National Laboratory, Oak Ridge, TN, August 1970.
3. ANSYS, A general Purpose Finite Element Code, ANSYS Inc. Version 5.3, 1996.

1



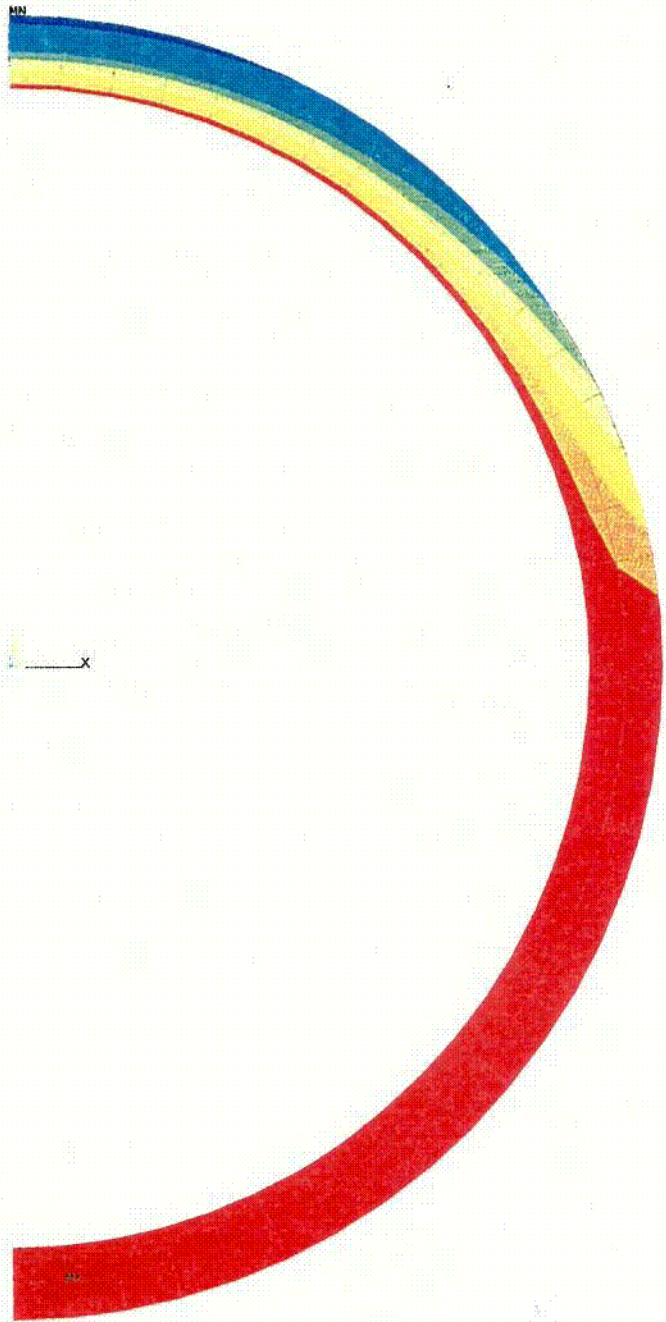
ANSYS 5.4
JAN 15 1999
11:25:50
ELEMENTS
MAT NUM

ZV =1
DIST=44.688
XF =20.313
CENTROID HIDDEN

C12

Figure 3.F.1 Lead Slump Finite Element Model

ANSYS 5.2
 FEB 4 1997
 09:57:55
 NODAL SOLUTION
 STEP=2
 SUB =10
 TIME=2
 UX
 RSYS=1
 DMX =1.769
 SMN =-.100962
 SMX =.004431
 .004431
 .007279
 .01899
 .0307
 .04241
 .054121
 .065831
 .077542
 .089252
 .100962
 .104431



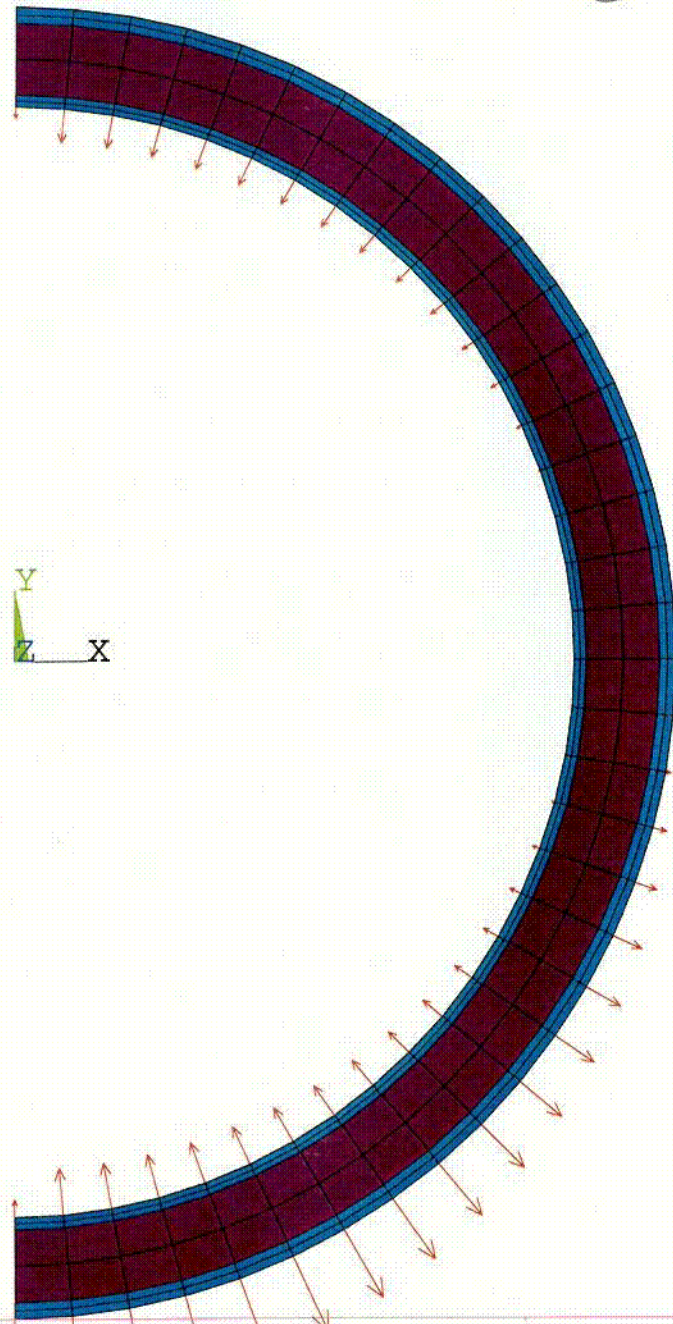
HI-STORM FSAR
 HI-2002444

FIGURE 3F2

Rev. 0

Figure 3.F.2 Lead Slump Analysis (Phase I) Lead Contraction.

1



ANSYS 5.4
JAN 15 1999
11:22:10
ELEMENTS
MAT NUM
F

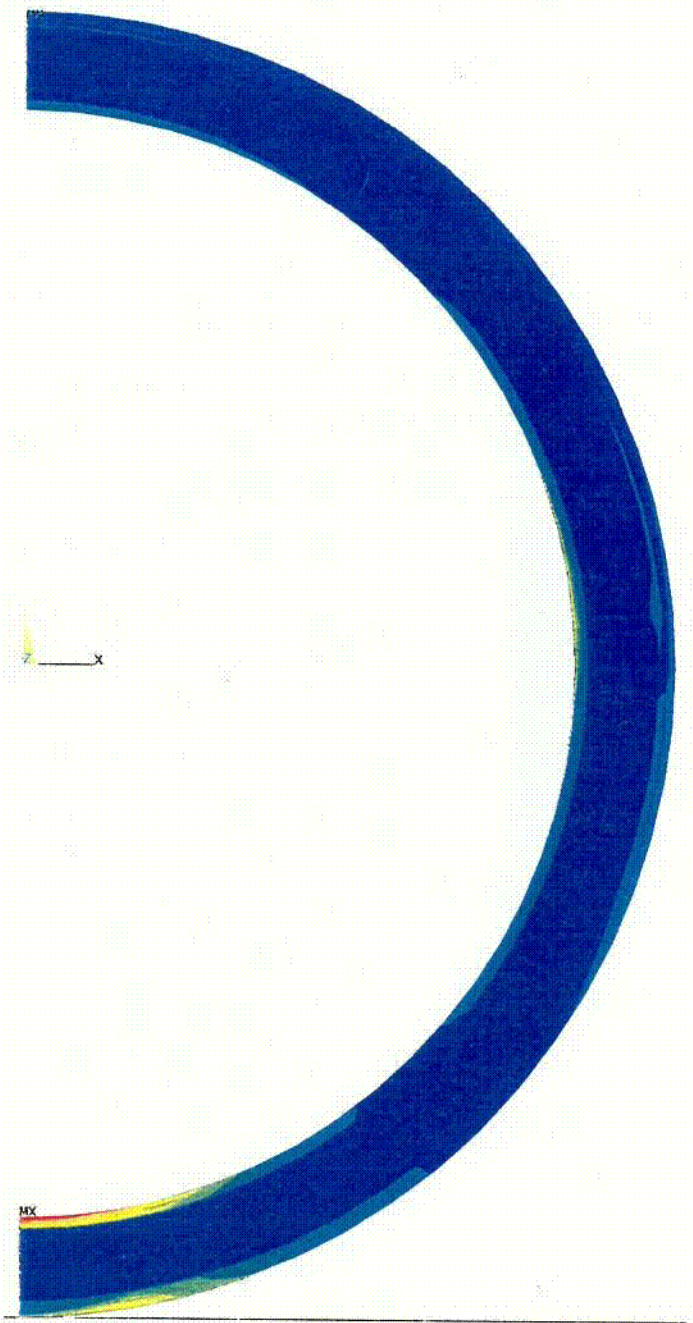
ZV =1
DIST=44.688
XF =20.313
CENTROID HIDDEN

C14

Figure 3.F.3 Lead Slump Analysis (Phase II)
HI-STORM FSAR
HI-2002444

Rev. 0

ANSYS 5.2
 FEB 4 1997
 11:25:20
 NODAL SOLUTION
 STEP=2
 SUB =5
 TIME=2
 SINT (AVG)
 DMX = 508234
 SMN =41.462
 SMX =50626
 41.462
 5662
 11282
 16903
 22523
 28144
 33764
 39385
 45005
 50626



HI-STORM FSAR
 HI-2002444

FIGURE 3.F.4

Rev. 0

Figure 3.F.4 Lead Slump Analysis (Phase II) Stress Intensity

215

APPENDIX 3.G - MISSILE PENETRATION ANALYSES FOR HI-STORM 100

3.G.1 Introduction

In this appendix, deformations and stresses in the HI-STORM 100 Overpack due to two missile strikes are investigated. The objective of the analysis is to show that deformations in the HI-STORM 100 system due to the missile strike events do not compromise the containment boundary of the system, and that global stresses in the overpack that arise from the missile strikes do not exceed the appropriate limits.

The two missiles considered are a 1-in. diameter steel sphere and an 8-in. diameter rigid cylinder, traveling at 126 miles per hour per Table 3.3.2. The two missile impacts are separate events.

3.G.2 References

[3.G.1] Young, Warren C., *Roark's Formulas for Stress and Strain*, 6th Edition, McGraw-Hill, 1989.

[3.G.2] Rothbart, H., *Mechanical Design and Systems Handbook*, 2nd Edition, McGraw Hill, 1985.

[3.G.3] ACI-318.1-89, *Building Code Requirements for Structural Plain Concrete*, American Concrete Institute, 1989 (Revised 1992).

[3.G.4] Working Model, v.4.0, Knowledge Revolution, 1997.

3.G.3 Composition

This appendix was created using the Mathcad (version 8) software package. Mathcad uses the symbol ':=' as an assignment operator, and the equals symbol '=' retrieves values for constants or variables. Mathcad's built-in equation solver is also used.

3.G.4 General Assumptions

General assumptions that apply to all analyses in this appendix are stated here. Further assumptions are stated in the subsequent text.

1. Formulae taken from Reference 3.G.1 are based on assumptions that are delineated in that reference.
2. The missiles are assumed to strike the cask at the most vulnerable location, in a manner that imparts the largest amount of energy to the cask surface.

3. For missile strikes on the side of the overpack, structural resistance in compression is offered by the concrete material that backs the outer shell.

4. All material property data are specified at the anticipated operating temperature of the particular component.

3.G.5 1-in. Diameter Steel Sphere Impact

3.G.5.1 Method

The first step in the 1-in. diameter sphere missile impact analysis is an investigation of the elastic behavior of the cask component being impacted. By balancing the kinetic energy of the missile with the work done deforming the impacted surface, it is shown that the missile's energy will not be entirely absorbed by elastic deformation. Therefore, the small missile will dent the cask. The elastic impact of the sphere is treated as a contact problem. The geometry is shown in Figure 3.G.1.

Following the elastic investigation of the impact, a plastic analysis is performed to determine the depth of the dent.

3.G.5.2 Elastic Analysis

The input data is specified as

The diameter of the sphere, $D := 1 \cdot \text{in}$

The velocity of sphere before impact, $V_0 := 126 \cdot \text{mph}$

The weight density of steel, $\rho := 0.283 \cdot \frac{\text{lbf}}{\text{in}^3}$

The modulus of elasticity, SA-516,Gr.70 (from Table 3.3.2 @ 350 deg.F), $E := 28.0 \cdot 10^6 \cdot \text{psi}$

The Poisson's ratio of steel, $\nu := 0.3$

The yield stress of SA516,Gr.70 (from Table 3.3.2 @ 350 deg. F), $S_y := 33150 \cdot \text{psi}$

In the 1-in. diameter sphere impact problem, the final velocity at which elastic deformation ends must be assumed. This velocity is conservatively assumed to be 99.5% of the pre-impact velocity of the missile. Thus, the velocity at which the average surface stress reaches the yield stress of the material (V_f) is:

$$V_f := .995 \cdot V_0$$

The mass of the missile is calculated using: $M := \frac{\rho}{g} \cdot \frac{4}{3} \cdot \pi \cdot \left(\frac{D}{2}\right)^3$

Using Table 33, case 1 (p. 650) of reference 3.G.1 for a sphere penetrating a flat plate, the spring constant K_2 relating the contact load to the local target deformation (raised to the power 1.5) is defined as:

$$K_2 := \left(\frac{E^2 \cdot D}{1.55^3}\right)^{0.5}$$

Balancing the kinetic energy with the work done deforming the bodies, we obtain the relation:

$$\frac{1}{2} \cdot M \cdot d(V^2) := F dx$$

Note that the small block is the Mathcad notation that this equation is part of the text and is not evaluated.

where:

$$F := K_2 \cdot x^{\frac{3}{2}}$$

and x is the depth of penetration.

Integrating and applying the condition that $V=V_0$ at $x=0$ gives:

$$\frac{M}{2} \cdot (V^2 - V_0^2) := \frac{2}{5} \cdot K_2 \cdot x^{2.5}$$

Solving this equation for x , the depth of penetration $x := \left[\frac{M \cdot \left(\frac{V_0^2 - V_f^2}{2}\right)^{0.4}}{0.4 \cdot K_2} \right]^{0.4}$

and the peak impact force $F := K_2 \cdot x^{1.5}$ Thus, the depth of penetration $x = 0.005$ in

and the peak impact force $F = 4871.664$ lbf.

The surface area of the cask/missile contact patch is determined as:

$$\text{Area} := \pi \cdot (D \cdot x - x^2) \qquad \text{Area} = 0.015 \text{ in}^2$$

and the average pressure on the patch to elastically support the load is approximately given as:

$$P_{avg} := \frac{F}{Area}$$

$$P_{avg} = 322566 \text{ psi}$$

This average pressure is greater than the yield stress of the impacted material. Therefore, the impact produces an inelastic deformation at the missile/cask contact location and local yielding occurs almost immediately after impact. From this conclusion, the change in kinetic energy of the missile must be assumed to be entirely absorbed by plastic deformation.

3.G.5.3 Plastic Analysis

Disregarding the small amount of energy absorbed in elastic deformation, the kinetic energy of the missile is entirely balanced by the plastic work done in forming a spherically shaped dent in the surface. Perfectly plastic behavior of the impacted material is assumed. The kinetic energy of the missile just before impact is determined as:

$$KE := \frac{1}{2} \cdot M \cdot V_0^2$$

$$KE = 78.642 \text{ ft}\cdot\text{lb}$$

Using Mathcad's built-in solver, determination of the depth of penetration begins with an estimate:

Assume $d := 0.18 \text{ in}$

$$\text{Given} \quad KE = S_y \cdot \pi \cdot \left(D \cdot \frac{d^2}{2} - \frac{d^3}{3} \right)$$

where the right hand side is the plastic work. The final deformation is characterized by the depth (d1) of the spherical dent in the cask surface, which is obtained as the value d (which solves the energy balance equation):

$$d1 := \text{Find}(d)$$

$$d1 = 0.141 \text{ in}$$

Note that the solution to the equation, d1, that is obtained by using the "Find(d)" command, can be checked by direct substitution of d1 for d in the equation. The maximum load, assuming that a constant stress is maintained until all of the impact energy is absorbed, is therefore:

$$P_{max} := S_y \cdot \pi \cdot (D \cdot d1 - d1^2)$$

$$P_{max} = 12648 \text{ lbf}$$

3.G.5.4 Conclusion: 1-in. Diameter Sphere Missile Impact

The depth of penetration of the small missile, which is required to absorb all of the impact energy, is less than the thinnest section of material on the exterior surface of the cask. Therefore, the small missile will dent, but not penetrate, the cask. Global stresses in the overpack that arise from the 1-in. missile strike are assumed to be negligible.

The calculation applies equally well to a 1" diameter missile which enters an inlet or outlet duct. In either case, there is no penetration from a normal impact since the dent in the casing surrounding the concrete is less than the thickness of the steel casing. If the small missile enters the duct at an angle, geometry of the duct suggests that multiple impacts with the steel casing or with the inner duct walls will occur with each impact causing a loss of kinetic energy. If the small missile does finally impact the MPC wall, any MPC denting will be less than the depth computed from the analysis, and will not breach confinement. Impacts at higher temperatures do not change the conclusions since the depth of denting caused by the small sphere is less than the minimum thickness of any metal target in the HI-STORM System.

3.G.6 Impact of an 8-in. Diameter Rigid Cylinder

3.G.6.1 Method

An 8-in. diameter cylindrical missile is postulated to impact the cask at the most vulnerable location, as shown in Figure 3.G.2. The deformed shape is shown for the case where a steel shell forming the overpack outer shell is backed by concrete shielding. Since impact may occur at the most vulnerable location, an impact may also occur where there is no backing of the steel plate.

The following two impact locations are investigated:

- a. Impact on the outer overpack shell (with concrete backing)
- b. Impact on the overpack top lid (no concrete backing)

Penetration is examined by balancing the kinetic energy of the missile with the work required to punch out a slug of the target material. Both the outer shell and the concrete neutron absorber material are considered to be active in resisting missile penetration in the case of a side strike.

Finally, global stresses in the overpack due to the 8-in. cylindrical missile impact are considered. Two impact locations are investigated, a side strike and an end strike.

3.G.6.2 Determination of Input Kinetic Energy

The input data is specified as follows:

The diameter of the missile, $D := 8 \cdot \text{in}$

The weight of the missile (125 kg, from Table 2.2.5), $\text{Weight} := 125 \cdot 2.204 \cdot \text{lbf}$

The velocity of the missile before impact, $V_0 := 126 \cdot \text{mph}$

The yield stress of the shell material at 350°F (from Table 3.3.2), $S_y := 33150 \cdot \text{psi}$

The ultimate stress of the shell material at 350°F (from Table 3.3.2), $S_u := 70000 \cdot \text{psi}$

The design membrane stress intensity of the shell material at 350°F (from Table 3.1.12),

$$S_m := 39750 \cdot \text{psi}$$

For the top lids (SA-516 Gr70) material, the following material properties are used:

The yield stress of the top lid material at 350°F (from Table 3.3.2), $S_{yt} := 33150 \cdot \text{psi}$

The ultimate stress of the top lid material at 350°F (from Table 3.3.2), $S_{ut} := 70000 \cdot \text{psi}$

The design membrane plus bending stress intensity of the top lid material at 350°F (from Table 3.1.12), $S_{mt} := 59650 \cdot \text{psi}$

The compressive strength of the concrete shielding (Table 3.3.5) $f_c := 3300 \cdot \text{psi}$

The kinetic energy that is required to be absorbed is calculated as:

$$\text{KE} := \frac{1}{2} \cdot \frac{\text{Weight}}{g} \cdot V_0^2 \quad \text{KE} = 1.755 \times 10^6 \text{ lbf} \cdot \text{in}$$

3.G.6.3 Local Penetration

Local penetration is examined by requiring that the impact force developed be balanced by only the resistance force developed in shear along the side area of a plug that would be punched out from an otherwise rigid material. That is, a "shear plug" type failure mechanism is assumed. The failure mode is based on achievement of the ultimate stress in shear. If the steel plug is backed by additional load resisting material (the concrete shielding), then the confined compressive strength of the backing material also acts to resist the strike. The following two impact locations are examined:

- a. Penetration of the overpack outer shell,
- b. Penetration of the overpack top lid.

a. Penetration of the overpack outer shell:

The thickness of overpack outer shell, $t := 0.75 \text{ in}$

The energy balance equation to determine the depth of local penetration (d in Figure 3.G.2) is

$KE = \text{Work done by shearing force in steel shell} + \text{Work done by compression force in the backing material (if present)}$

The unknown to be determined is the depth of penetration, d . In the equation, the ultimate shear strength of the steel material is assumed conservatively as 50% of the ultimate strength in tension. The compressive strength of the backing material (if present) is taken as the allowable strength of confined concrete under bearing. From Table 3.3.5 and ACI-318.1, the unconfined bearing strength is related to the concrete compressive strength by the relation

$$f_{cus} := 1 \cdot (0.65 \cdot 0.85 \cdot f_c) \qquad f_{cus} = 1823.3 \text{ psi}$$

For confined concrete bearing strengths, the American Concrete Institute Code for Plain Concrete [3.G.3, Section 6.2] allows a doubling of the bearing strength. Therefore, the allowable bearing strength for confined concrete is

$$f_{ccs} := 2 \cdot f_{cus} \qquad f_{ccs} = 3646.5 \text{ psi}$$

Assume that the maximum depth of penetration d is greater than the outer shell thickness t ; i.e., the outer shell is penetrated. If the compression strength of the concrete material is included, then the impacting missile is resisted by both the outer shell in shear and by the underlying concrete in compression and the energy balance equation is solvable for the penetration depth in the form:

$$\delta := \frac{KE - .5 \cdot S_u \cdot \pi \cdot D \cdot t^2}{f_{ccs} \cdot \pi \cdot \frac{D^2}{4}} \qquad \text{which has the solution:}$$

$$\delta = 6.87 \text{ in}$$

The initial assumption is confirmed; namely, the outer steel shell is penetrated, and the concrete backing acts to absorb the necessary energy to stop the missile. The overpack experiences a maximum impact load of P_i , where

$$P_i := .5 \cdot S_u \cdot \pi \cdot D \cdot t + f_{ccs} \cdot \pi \cdot \frac{D^2}{4} \qquad P_i = 8.43 \times 10^5 \text{ lbf}$$

This value for impact force is used later to evaluate a global stress state in the overpack.

A similar analysis can be performed for the case when the 8" diameter missile goes directly into the inlet vent and impacts the pedestal shield. In this case, the steel outer shell is penetrated, and the concrete backing the steel plate will absorb the kinetic energy.

For a pedestal steel shell thickness of

$$t_{ss} := 0.25 \cdot \text{in}$$

$$\delta := \frac{KE - .5 \cdot S_u \cdot \pi \cdot D \cdot t_{ss}^2}{f_{ccs} \cdot \pi \cdot \frac{D^2}{4}}$$

which has the solution:

$$\delta = 9.27 \text{ in} < \text{radius of pedestal}$$

b. Penetration of the HI-STORM 100 top lid

Input geometry of the top lids (per nomenclature in Figure 3.G.3)

thickness of each lid $t_{lid} := 2 \cdot \text{in}$ 2 lids act to resist the impact

unsupported lid diameter $D_{lid} := 80.5 \cdot \text{in}$ (Dwg. 1945 and BM-1575)

Figure 3 G.3 shows the impact of the 8" missile on the top lid consisting of two flat plate. Under the impact, the top lid will deform globally as two simply supported plate; with the minimal lid bolting (4 attachment locations), it is nonconservative to assume any other outer boundary condition. To examine local penetration, the assumption that the lids are rigid is made and that all energy is absorbed by the target forming a shear plug. Using the methodology applied to the side strike, if the lid is considered rigid in the vicinity of the support, then the kinetic energy of the strike is absorbed by the lid developing a shear plug. The maximum energy that can be developed by the outer of the two top lids is

$$IE := \frac{S_{ut}}{2} \cdot \pi \cdot D \cdot (t_{lid})^2 \qquad IE = 3.519 \times 10^6 \text{ lbf} \cdot \text{in}$$

Note that in the calculation of maximum energy, it is assumed that the total shear surface area supporting shear moves by an amount equal to the total depth of the lid.

$$\frac{KE}{IE} = 0.499$$

Since the ratio of energy to be absorbed is much less than the energy that can be absorbed prior to a complete shear plug becoming itself a missile, it is concluded that the outer of the two top lids will not be completely penetrated by the intermediate missile.

The results of the investigation of penetration at the limiting locations demonstrate that the HI-STORM 100 Overpack adequately protects the MPC from a direct missile strike. The following section demonstrates that the global stresses in the overpack remain below allowable limits in the missile strike event.

3.G.6.4 Stresses in the Overpack Due to 8-in. Diameter Missile Strike

Global stresses in the overpack due to missile strikes at two locations are examined in this subsection.

The first location is a side strike at the level of the top of the cask, where the entire force is reacted by the overpack inner and outer shells acting as a cantilever beam (see Figure 3.G.4).

The second location is an end strike at the center of the overpack top lid.

a. First Location: Side Strike on Overpack

The distance from the missile strike to the base, $L := 227 \cdot \text{in}$

The mean diameter of the overpack inner shell, $D_1 := 74.75 \cdot \text{in}$

The mean diameter of the outer shell, $D_o := 131.75 \cdot \text{in}$

The thickness of the inner shell, $t_i := 1.25 \cdot \text{in}$

The thickness of the outer shell, $t_o := 0.75 \cdot \text{in}$

The applied force, $P_i = 8.43 \times 10^5 \text{ lbf}$

Conservatively neglecting any stiffening from the radial ribs or from the concrete shielding, the total moment of inertia provided by the inner and outer shells to resist beam bending is

$$I := \pi \cdot \left(\frac{D_1}{2} \right)^3 \cdot t_i + \pi \cdot \left(\frac{D_o}{2} \right)^3 \cdot t_o \quad I = 8.786 \times 10^5 \text{ in}^4$$

The applied moment and resultant stress in the outer shell can then be determined as:

$$\text{Moment} := P_i \cdot L$$

$$\text{Moment} = 1.914 \times 10^8 \text{ in} \cdot \text{lbf}$$

$$\text{Stress} := \text{Moment} \cdot \frac{D_o}{2 \cdot I}$$

$$\text{Stress} = 14349 \text{ psi}$$

A safety factor for the level D condition is obtained by comparing the calculated stress to the membrane stress intensity for the material.

$$SF := \frac{S_m}{\text{Stress}} \quad SF = 2.77$$

b. Second Location: End Strike on Overpack Top Lids

The stress state near the center of the top lids is investigated by performing a dynamic analysis to ascertain the maximum load applied to the two top lids as they undergo a global mode of deflection. It is assumed that each lid deforms like a simply supported plate for this analysis and it is conservatively assumed that none of the energy is absorbed by local plastic deformation. The radius of simple support is approximately equal to the radius of the inner shell of the storage overpack. The initial striking velocity and the striking weight of the missile are known. It is determined from [3.G.2], p.5-55, that 50% of the lid weight acts during the subsequent deformation. It remains to establish an appropriate spring constant to represent the plate elastic behavior in order to establish all of the necessary input for solving the dynamic problem representing the post-strike behavior of the lid-missile system. To determine the spring rate, we apply Case 16 of Table 24 in [3.G.1] which is the static solution for a circular plate, simply supported at the edge, and subject to a load applied over a small circular region. Using the notation of [3.G.1] for the case in question, and assuming deformation only inboard of the overpack inner shell, allows us to perform the following analysis:

$$\text{The radius of simple support, } a := \frac{D_{\text{lid}}}{2} \quad a = 40.25 \text{ in}$$

Calculate an overestimate of the lid stiffness (conservative), by using a bounding Young's Modulus:

$$E_b := 29.1 \cdot 10^6 \cdot \text{psi}$$

$$\text{The lid stiffness, } D := \frac{E_b \cdot t_{\text{lid}}^3}{12 \cdot (1 - \nu^2)} \quad D = 2.132 \times 10^7 \text{ lbf}\cdot\text{in}$$

The global stiffness of each of the two lids (K) is simply the total load divided by the corresponding displacement at the plate center. From the classical solution referenced:

$$K := \frac{16 \cdot \pi \cdot D \cdot (1 + \nu)}{(3 + \nu) \cdot a^2} \quad K = 2.606 \times 10^5 \frac{\text{lbf}}{\text{in}}$$

Each of the two lids develops this spring constant.

To establish the appropriate structural damping value associated with the stiffness, a post-impact natural frequency is determined as follows:

The weight of each of the two identical top lid plates that participate in the dynamic analysis is assumed equal; the mass of the shielding and shielding confining metal is included and assumed equally distributed between the two lids;

Table 3.2.1

$$W_{clp} := \frac{.5 \cdot 23000 \cdot \text{lbf}}{2}$$

Using the appropriate expression from [3.G.2], the natural frequency of each lid can be determined as:

$$f := \frac{1}{2 \cdot \pi} \cdot \sqrt{K \cdot \frac{g}{(\text{Weight} + W_{clp})}} \quad f = 20.565 \text{ Hz}$$

We assume 4% structural damping based on stiffness :

$$c := \left(\frac{.04}{\pi \cdot f} \right) \cdot K \quad c = 161.327 \text{ lbf} \cdot \frac{\text{sec}}{\text{in}}$$

The dynamics problem is solved using the Working Model program [3.G.4], with the impacting missile striking a target mass (the outer top lid) which is supported by two springs having spring constant $K/2$ to ground and is also in contact with a target mass representing the inner top lid which is also supported by two springs having spring constant $K/2$. The system is constrained to move vertically subsequent to the impact by the striking mass, and gravitational forces are included in the solution. The objective of the analysis is to determine the forces in each spring and to determine the maximum vertical movement of the lower of the two lids. Figure 3.G.5 shows the model and the corresponding results. Plots of the spring forces associated with each lid, the vertical movement of each lid, and the vertical velocity of the striking missile. The results of the analysis predict that the peak value of the maximum force developed in each of the lids is (sum of two spring-damper elements per lid), $W := 2 \cdot 52430 \cdot \text{lbf}$.

The stress near the center of the closure plate is obtained by computing the bending moment due to W. For Level D conditions, only primary bending stress intensities are required to be compared to the allowable strength value. The stress directly under the loaded region, by the very nature of the form of solution ($\ln(a/r)$), should not be considered as a primary stress. The primary stress intensity state is considered to be fully established in the plate cross section at a radius equal to 100% of the load contact radius. Therefore, the bending moment and the stress are computed just outboard of the contact circle :

Define the contact diameter as $d_{con} := 8 \cdot \text{in}$

$$r := 1.0 \cdot \left(\frac{d_{con}}{2} \right) \quad r = 4 \text{ in}$$

$$M_t := \frac{W}{16 \cdot \pi} \cdot \left[(1 + \nu) \cdot \ln\left(\frac{a}{r}\right) \cdot 4 + (1 - \nu) \cdot \left[4 - \left(\frac{d_{con}}{2 \cdot r} \right)^2 \right] \right]$$

$$M_r := \frac{W}{16 \cdot \pi} \cdot \left[(1 + \nu) \cdot \ln\left(\frac{a}{r}\right) \cdot 4 + (1 - \nu) \cdot \left[1 - \left(\frac{r}{.5 \cdot D_{hd}} \right)^2 \right] \cdot \left(\frac{d_{con}}{2 \cdot r} \right)^2 \right]$$

The above formulas come from Table 24, Case 16 in [3 G.1].

$$M_t = 2.943 \times 10^4 \text{ lbf} \cdot \frac{\text{in}}{\text{in}} \quad M_r = 2.649 \times 10^4 \text{ lbf} \cdot \frac{\text{in}}{\text{in}}$$

The tangential moment exceeds the radial moment at this location and the moments have the same sign, so the maximum moment and corresponding stress are:

$$\sigma_t := 6 \cdot \frac{M_t}{t_{lid}} \quad \sigma_t = 4.414 \times 10^4 \text{ psi}$$

This stress represents a stress intensity. As a measure of the safety factor, we compare this primary bending stress intensity with the allowable primary membrane plus primary bending strength at the design temperature.

$$\frac{S_{mt}}{\sigma_t} = 1.351$$

Note that this definition of safety factor is appropriate since the component is being designed in accordance with ASME Section III, Subsection NF for a Level D event.

From the numerical solution, the predicted maximum deflection of the two lids is 0.4" under the impact of the missile. Therefore, the MPC lid is protected from the effects of the impact.

3.G.7 Conclusion

The above calculations demonstrate that the HI-STORM 100 Overpack provides an effective containment barrier for the MPC after being subjected to various missile strikes. No missile strike compromises the integrity of the boundary; further, global stress intensities arising from the missile strikes satisfy ASME Code Level D allowable strengths away from the immediate vicinity of the loaded region.

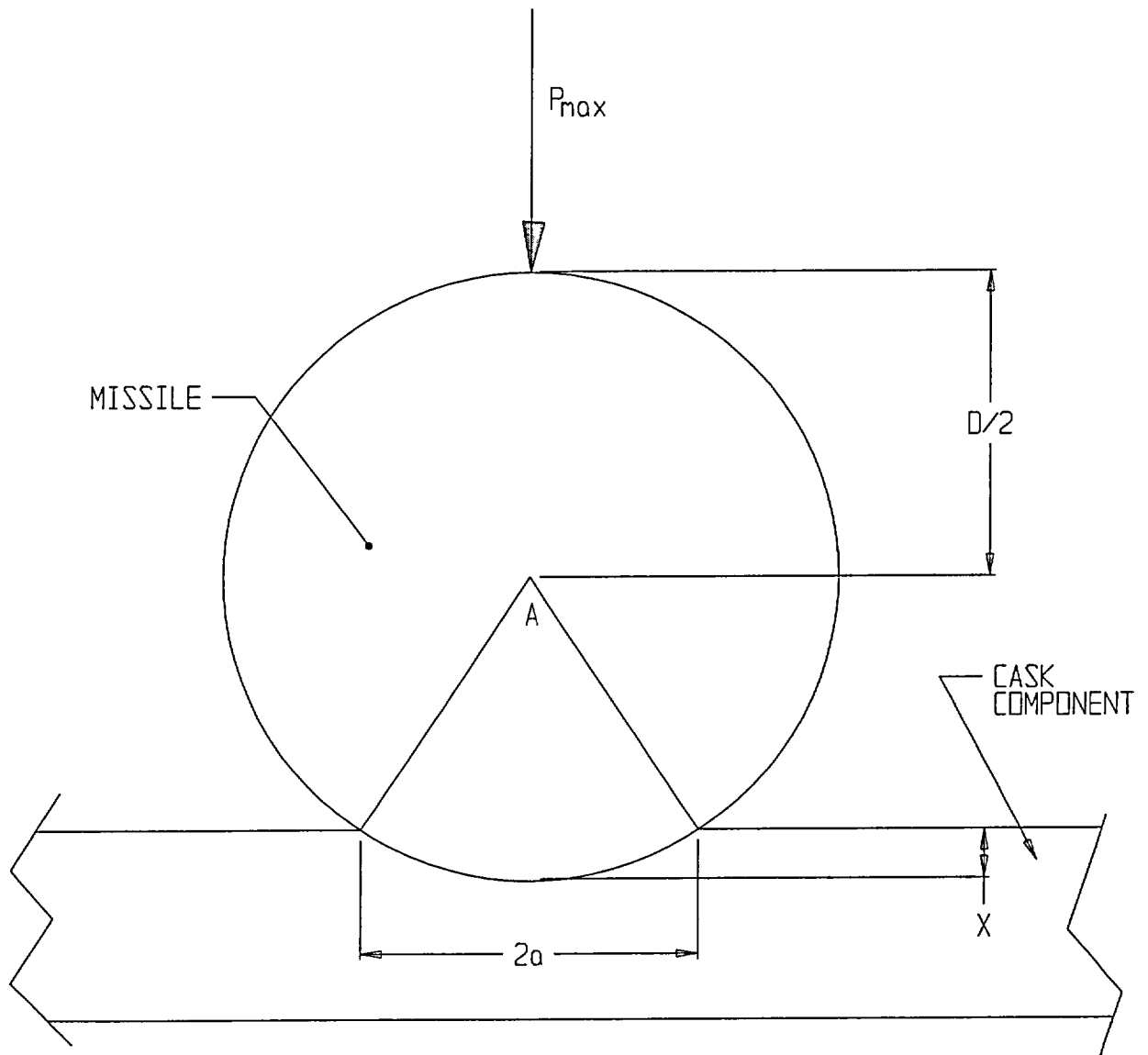
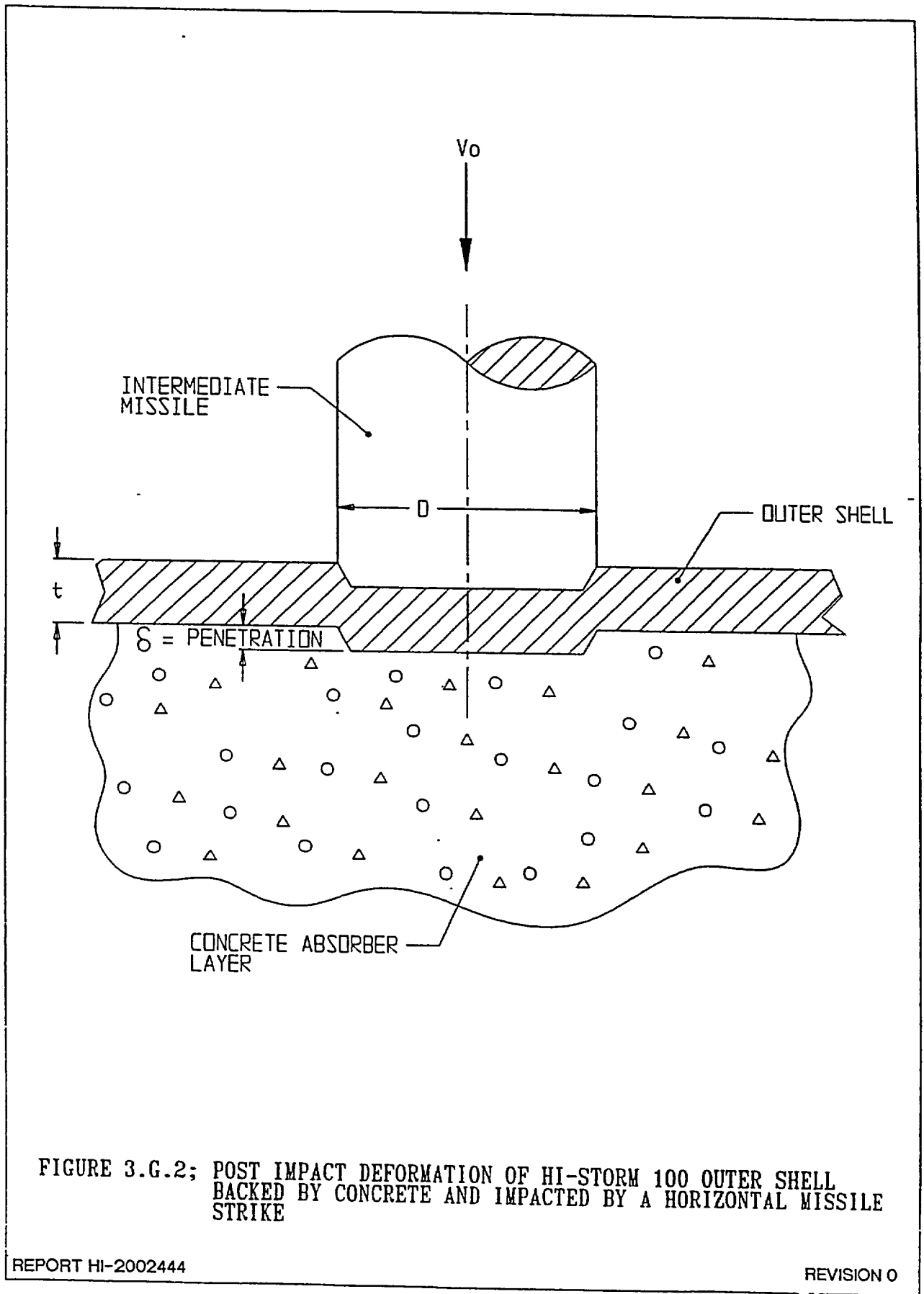


FIGURE 3.G.1; SMALL MISSILE IMPACT



REPORT HI-2002444

PROJECTS\5014\HI2002444\CH_3\3_G_3

REVISION 0

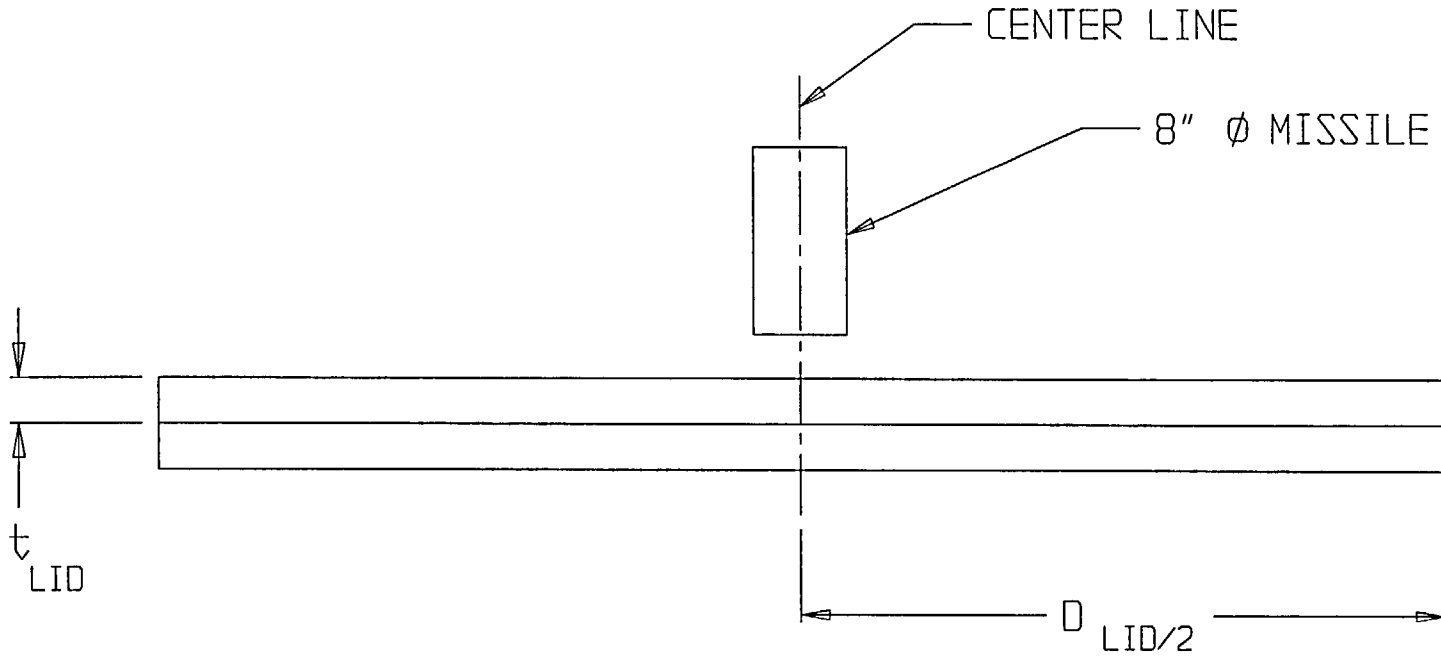


FIGURE 3.G.3; MISSILE IMPACT ON TOP LID

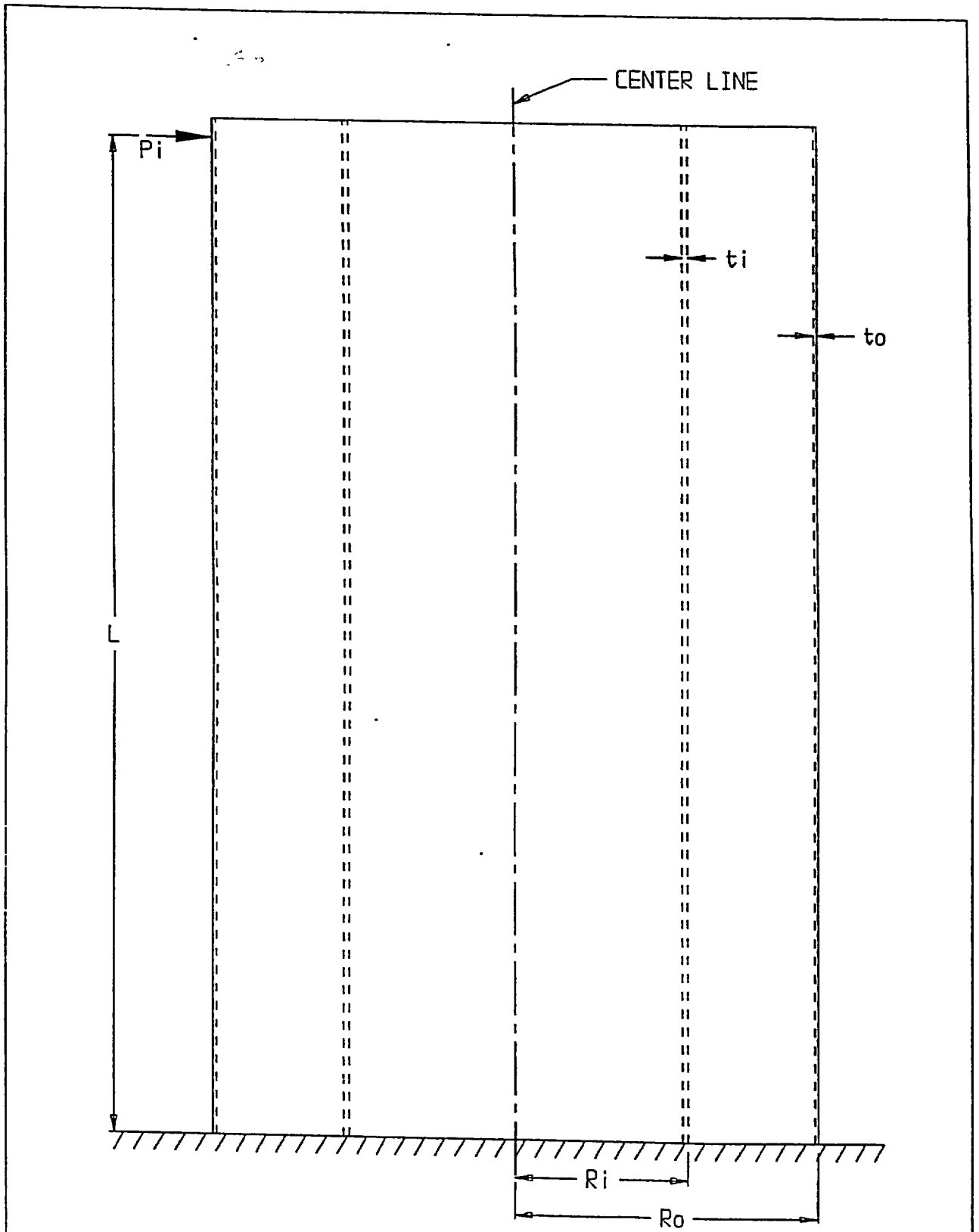
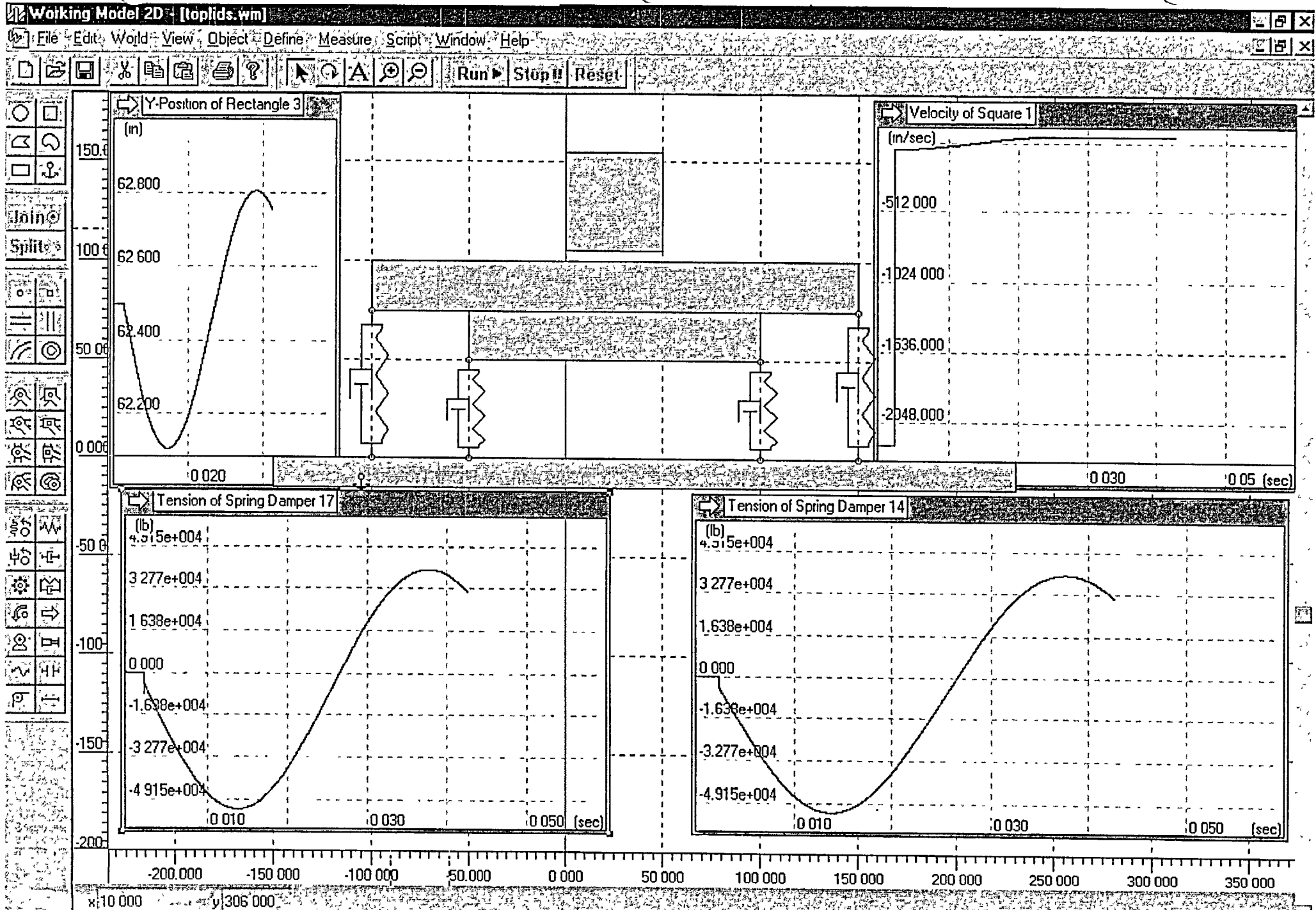


FIGURE 3.G.4; MISSILE STRIKE AT TOP OF HI-STORM



HI-STORM FSAR
HI-2002444

Fig. 3.G.5 Top Lid Missile Impact

APPENDIX 3.H - MISSILE PENETRATION ANALYSES FOR HI-TRAC

3.H.1 Introduction

In this appendix, deformations and stresses in the HI-TRAC transfer cask due to two types of missiles are investigated. The objective of the analysis is to show that deformations in the HI-TRAC system, due to the missile strike events, do not compromise the MPC confinement boundary of the system.

The two missiles considered are a 1-in. diameter steel sphere and an 8-in. diameter cylinder, both traveling at 126 miles per hour. The two missile impacts are separate events.

The locations on the transfer cask that are investigated are strikes on the outer shell and top lid of HI-TRAC and strikes on the bottom transfer lid doors. The outer shell of HI-TRAC is 1" thick and is backed by a substantial thickness (4.5") of lead which is itself contained by an inner shell of thickness 0.75". The bottom transfer lid door of the 125 ton HI TRAC, used while HI-TRAC is outside the fuel building, is a composite structure consisting (from outside to inside) of 3/4" steel plate, 2" of lead, a .5" thick intermediate plate, Holtite-A, and finally a 2.25" thick inner plate. The 100 ton HI TRAC is a composite structure consisting (from outside to inside) of 1/2" steel plate, 1.5" of lead, and finally a 2.25" thick inner plate. Figure 3.H.1 shows locations of the missile strikes (side and transfer lid) examined for the 125 ton HI-TRAC.

3.H.2 References

[3.H.1] Nelms, H.A., Structural Analysis of Shipping Casks, Effect of Jacket Physical Properties and Curvature on Puncture Resistance, Vol. 3, ORNL TM-1312, Oak Ridge National Laboratories, Oak Ridge, TN, June, 1968.

[3.H.2] Young, Warren C., Roark's Formulas for Stress and Strain, 6th Edition, McGraw-Hill, 1989.

[3.H.3] Design of Structures for Missile Impact, Topical Report BC-TOP-9A, Revision 2, 9/74 (accepted by the USNRC by letter of 11/25/74).

[3.H.4] Kar, A. K., "Residual Velocity for Projectiles", Nuclear Engineering and Design, Vol. 53, North-Holland Publishing Company, 1979, p. 87-95.

[3.H.5] ASME Code, Section III, Subsection NG, Table NG-3352-1, 1995.

3.H.3 Composition

This appendix was created using the Mathcad (version 7) software package. Mathcad uses the symbol ':=' as an assignment operator, and the equals symbol '=' retrieves values.

3.H.4 General Assumptions

General assumptions that apply to all analyses in this appendix are stated here. Further assumptions are stated in the subsequent text.

1. Formulae taken from Reference 3.H.1 are based on assumptions that are delineated in that reference.
2. The missiles are assumed to strike the transfer cask at the most vulnerable location, in a manner that imparts the largest amount of energy to the cask surface.
3. All material property data are specified at the anticipated design temperature of the particular component.
4. Resistance from the outside water jacket is conservatively neglected.
5. The 1-in diameter steel sphere and the 8-in diameter cylinder are formed from Grade 60 steel material; the ultimate stress of which is 60,000 psi.

3.H.5 Missile Strike on the Outer Shell

3.H.5.1 Method

Empirical formulas [3.H.1] for lead backed shells are used to examine the impacts on the side of the transfer cask. It is demonstrated that the penetration distance is less than the metal thickness of the outer shell.

3.H.5.2 Penetration Analysis

Since there are no openings on the side of the HI-TRAC, the missile strike calculations are governed by the 8" diameter missile.

The input data is specified as:

The density of the steel is (from Section 3.3), $\rho := .283 \frac{\text{lbf}}{\text{in}^3}$

The thickness of the outer steel shell (from Holtec drawing no. 1880), $t_o := 1.0 \cdot \text{in}$

The diameter of the missile, $D := 8 \cdot \text{in}$

The weight of the missile (125 kg, from Table 2.2.5), $\text{Weight} := 125 \cdot 2.204 \cdot \text{lbf}$

The velocity of the missile before impact, $V_0 := 126 \cdot \text{mph}$

The ultimate stress of the steel material at 350°F (from Table 3.3.2), $S_u := 70000 \cdot \text{psi}$

The kinetic energy that is required to be absorbed is calculated as:

$$\text{KE} := \frac{1}{2} \cdot \frac{\text{Weight}}{g} \cdot V_0^2 \qquad \text{KE} = 1.755 \times 10^6 \text{ lbf} \cdot \text{in}$$

Using [3.H.1], the thickness required to prevent penetration is

$$t_{\text{pen}} := \left[\frac{\left(\frac{\text{KE}}{\text{in} \cdot \text{lbf}} \right)}{2.4 \cdot \left(\frac{S_u}{\text{psi}} \right) \cdot \left(\frac{D}{\text{in}} \right)^{1.6}} \right]^{0.71} \qquad t_{\text{pen}} = 0.498 \text{ inch}$$

3.H.5.3 Conclusion

Since the penetration predicted is less than the outer shell thickness, protection of containment is assured.

3.H.6 Missile Strike on Bottom Transfer Lid Door of the 125 ton HI TRAC

3.H.6.1 Methodology

When HI-TRAC is transported horizontally outside of the fuel building, the potential exists for a missile strike on the bottom transfer lid door. The lid door is a composite structure shown in Holtec drawing 1928. The analysis is performed using the following formula for penetration of steel plates from the Bechtel Topical Report [3.H.3, p.2-3] (accepted by the USNRC):

$$T := \frac{\left(\frac{M \cdot V^2}{2}\right)^{\frac{2}{3}}}{672 \cdot D}$$

Note that the square block with any formula is the Mathcad notation that the formula is used in text at this point in the document and not evaluated.

where T is the steel thickness to be perforated (in);
M is the mass of the missile (lbf-sec²/ft);
D is the diameter of the missile (in);
V is the striking velocity (ft/sec).

For multi-element missile barriers, such as the transfer lid, procedures for prediction of local damage are acceptable if the residual velocity of the missile perforating the first element is considered as the striking velocity for the next element. For determining this residual velocity, the following equation presented in [3.H.3] is used (note that [3.H.4] has a similar formula; we use the NRC accepted formulation in the Topical Report):

$$V_r := \left(V_i^2 - V_p^2\right)^{\frac{1}{2}}$$

where V_p is the velocity required to perforate the barrier thickness;
V_i is the striking velocity of the missile;
V_r is the residual velocity of the missile.

The Holtite material is assumed not to resist the missile impact, but the outer and intermediate plates, plus the lead shielding, if necessary, are assumed to be able to resist the missile strike.

3.H.6.2 Data Input

The thickness of the outer plate of the transfer lid door for the 125 ton HI TRAC is taken from Holtec drawing 1928:

$$t_3 := 0.75 \cdot \text{in}$$

3.H.6.3 Impact Analysis

The kinetic energy that is required to be absorbed by the transfer lid is (eliminate the units so results can be substituted into the empirical formulas).

$$M := \frac{\text{Weight}}{g} \cdot \frac{\text{ft}}{\text{lbf} \cdot \text{sec}^2} \quad M = 8.563$$

$$V_i := V_0 \cdot \frac{\text{sec}}{\text{ft}} \quad V_i = 184.8$$

$$D := \frac{D}{\text{in}} \quad D = 8$$

$$T := \frac{\left(\frac{M \cdot V_i^2}{2} \right)^{\frac{2}{3}}}{672 \cdot D} \quad T = 0.516 \text{ inch} \quad < t_3 = 0.75 \text{ in (outer plate of transfer lid for the 125 ton HI TRAC)}$$

$V_r = 0$ ft/sec for the 125 ton HI TRAC. For the 100 ton HI TRAC, the outer transfer lid will be penetrated. The remaining kinetic energy to be absorbed is computed as follows:

First determine the velocity to penetrate the 1/2" outer plate of the 100 ton HI TRAC.

$$T_1 := 0.5$$

$$C_1 := 672 \cdot D \cdot T_1 \quad C_1 = 2688$$

$$K_p := C_1^{1.5} \quad K_p = 1.394 \times 10^5$$

$$V_p := \sqrt{2 \cdot \frac{K_p}{M}} \quad V_p = 180.418$$

Then the residual velocity is

$$V_r := \left(V_i^2 - V_p^2 \right)^{\frac{1}{2}} \quad V_r = 40.007$$

Without further calculations, it is clear that the residual is small enough to be absorbed by the combination of lead, and the inner plate without puncture of the inner plate.

3.H.6.4 Conclusion

The transfer lid door acts as a barrier against penetration by the postulated missile. Based on the above calculation for the 125 ton HI TRAC, the missile does not penetrate the first steel layer, the outer plate; for the 100 ton HI TRAC, the outer plate may be penetrated, but the residual velocity is not sufficient to completely penetrate the remaining structure of the transfer lid.

3.H.7 Direct Missile Strike at Center of MPC Top Closure

The top lid of the HI-TRAC has a central hole for rigging the MPC. During transport, this opening can be protected with a missile shield plate. If we conservatively neglect any energy absorption or stopping of the missile by such a protective plate, then we demonstrate that a 5/8" J-groove weld around the periphery of the MPC lid will not exceed postulated level D weld stress limits.

Since the weld in question is located around the top surface periphery of the MPC lid, it is assumed to be at the design temperature of the shell rather than the design temperature conservatively set for the MPC top lid. We conservatively, use a reduced weld efficiency 0.45 to be consistent with other evaluations.

ASME Section III, Subsection NG [3.H.5] gives the weld efficiency for the groove weld as

$$e := 0.45$$

The ultimate strength of the base metal at 350 deg. F is $S_u := 65200 \cdot \text{psi}$

For the weld metal ultimate strength, we conservatively assume the same value. We now compare the allowable weld stress with the allowable base metal shear stress to determine the governing section:

$$\tau_{\text{all}} := \text{if}(.72 \cdot S_u \cdot e < .42 \cdot S_u, .72 \cdot S_u \cdot e, .42 \cdot S_u) \quad \tau_{\text{all}} = 2.112 \times 10^4 \text{ psi}$$

where the above formula is built into the Mathcad solution algorithm.

The allowable load supported by the weld is calculated as follows:

Conservatively base the weld area on the MPC lid outside diameter $D := 67.25 \cdot \text{in}$

$$t_{\text{weld}} := 0.625 \cdot \text{in} \quad (\text{Note the actual weld thickness is } 0.75 \text{''})$$

$$P_{\text{all}} := \tau_{\text{all}} \cdot \pi \cdot D \cdot t_{\text{weld}} \quad P_{\text{all}} = 2.789 \times 10^6 \text{ lbf}$$

The applied load from the missile is assumed to be based on a flow stress for a mild steel bar assumed as

$$\sigma_{\text{flow}} := 45000 \cdot \text{psi}$$

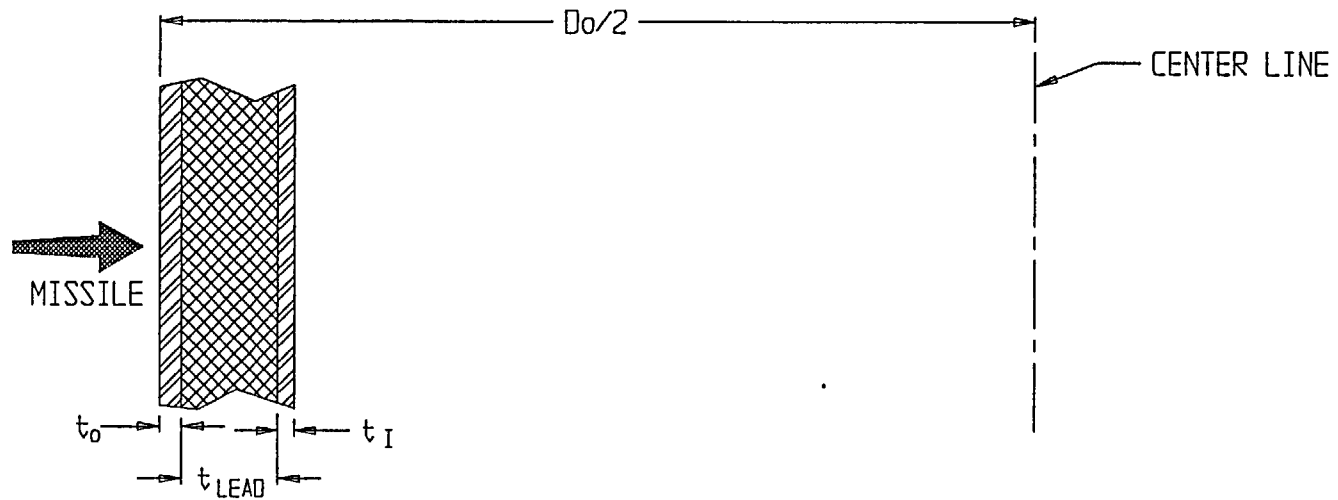
Therefore the force developed at the interface is

$$P_{\text{missile}} := \sigma_{\text{flow}} \cdot \frac{\pi \cdot 8^2 \cdot \text{in}^2}{4} \quad P_{\text{missile}} = 2.262 \times 10^6 \text{ lbf}$$

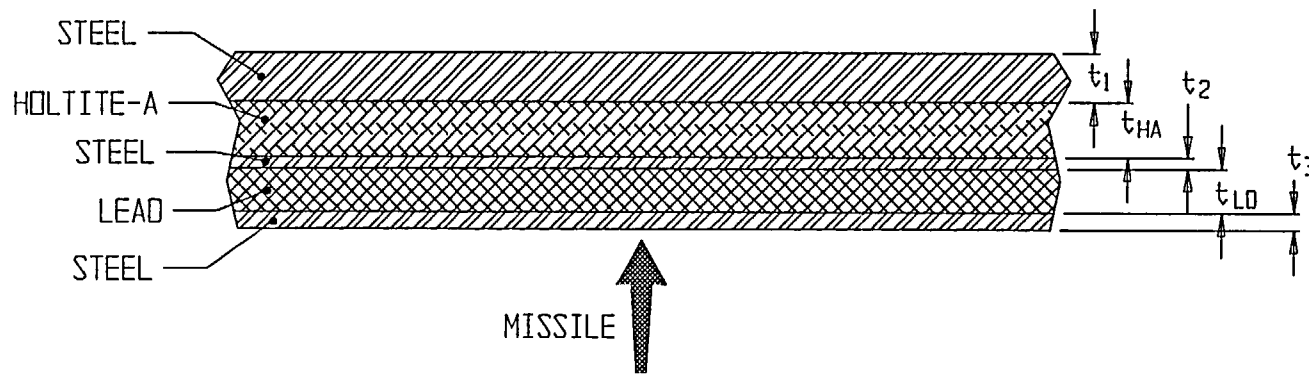
The safety factor against failure of the peripheral weld is

$$\text{SF}_{\text{weld}} := \frac{P_{\text{all}}}{P_{\text{missile}}} \quad \text{SF}_{\text{weld}} = 1.233$$

The presence of the protective plate to absorb energy will increase this safety factor. For a missile strike directly on the top lid plate (away from the hole), the calculations given in 3.H.6.3 demonstrate that the plate will not be punctured by the missile.



3.H.1(a) SIDE STRIKE



3.H.1(b) BOTTOM STRIKE

FIGURE 3.H.1; HI-TRAC MISSILE STRIKE LOCATIONS

APPENDIX 3.I: HI-TRAC FREE THERMAL EXPANSIONS

3.I.1 Scope

In this calculation, estimates of operating gaps, both radially and axially, are computed for the fuel basket-to-MPC shell, and for the MPC shell-to-HI-TRAC. The temperature distribution used as input is derived from a hypothetical worst case MPC thermal load. This calculation is in support of the results presented in Section 3.4.4.2.

3.I.2 Methodology

Bounding temperatures are used to construct temperature distributions that will permit calculation of differential thermal expansions both radially and axially for the basket-to-MPC gaps, and for the MPC-to-HI-TRAC gaps. Reference temperatures are set at 70°F for all components. Temperature distributions are computed at the axial location of the HI-TRAC System where the temperatures are highest. A comprehensive nomenclature listing is provided in Section 3.I.6.

3.I.3 References

[3.I.1] Boley and Weiner, Theory of Thermal Stresses, John Wiley, 1960, Sec. 9.10, pp. 288-291.

[3.I.2] Burgreen, Elements of Thermal Stress Analysis, Arcturus Publishers, Cherry Hill NJ, 1988.

3.I.4 Calculations for Hot Components (Middle of System)

3.I.4.1 Input Data

Based on thermal calculations in Chapter 4, the following temperatures are appropriate at the hottest location of the HI-TRAC (see Figure 3.I.1 and Table 4.5.2).

The temperature change at the inside surface of the HI-TRAC, $\Delta T_{1h} := 322 - 70$ |

The temperature change at the inside of the water jacket, $\Delta T_{2h} := 314 - 70$ |

The temperature change at the mean radius of the MPC shell, $\Delta T_{3h} := 455 - 70$ |

The temperature change at the outside of the MPC basket, $\Delta T_{4h} := (600 - 70) \cdot 1.1$ |

The temperature change at the center of the basket, $\Delta T_{5h} := 852 - 70$ |

Note that the outer basket temperature is conservatively amplified by 10% to insure a bounding parabolic distribution. This conservatism serves to maximize the growth of the basket. The geometry of the components are as follows (referring to Figure 3.I.1)

The outer radius of the outer shell, $b := 40.625 \text{ in}$

The inner radius of the HI-TRAC, $a := 34.375 \text{ in}$

The mean radius of the MPC shell, $R_{\text{mpc}} := \frac{68.375 \text{ in} - 0.5 \text{ in}}{2}$ $R_{\text{mpc}} = 33.938 \text{ in}$

The initial MPC-to-overpack minimal radial clearance, $RC_{\text{mo}} := .5 \cdot (68.75 - 68.5) \text{ in}$ |

$$RC_{\text{mo}} = 0.125 \text{ in} \quad |$$

For axial growth calculations of the MPC-to-HI-TRAC top flange clearance, the axial length of the HI-TRAC is defined as the distance from the bottom flange to the top flange, and the axial length of the MPC is defined as the overall MPC height.

The axial length of the HI-TRAC, $L_{\text{ovp}} := 191.25 \text{ in}$

The axial length of the MPC, $L_{\text{mpc}} := 190.5 \text{ in}$

The initial MPC-to-HI-TRAC nominal axial clearance, $AC_{\text{mo}} := L_{\text{ovp}} - L_{\text{mpc}}$

$$AC_{\text{mo}} = 0.75 \text{ in}$$

For growth calculations for the fuel basket-to-MPC shell clearances, the axial length of the basket is defined as the total length of the basket and the outer radius of the basket is defined as the mean radius of the MPC shell minus one-half of the shell thickness minus the initial basket-to-shell radial clearance.

The axial length of the basket, $L_{\text{bas}} := 176.5 \text{ in}$

The initial basket-to-MPC lid nominal axial clearance, $AC_{\text{bm}} := 1.8125 \text{ in}$ |

The initial basket-to-MPC shell nominal radial clearance, $RC_{\text{bm}} := 0.1875 \text{ in}$

The outer radius of the basket, $R_{\text{b}} := R_{\text{mpc}} - \frac{0.5}{2} \text{ in} - RC_{\text{bm}}$ $R_{\text{b}} = 33.5 \text{ in}$

The coefficients of thermal expansion used in the subsequent calculations are based on the mean temperatures of the MPC shell and a bounding mean temperature for the basket.

The coefficient of thermal expansion for the MPC shell, $\alpha_{\text{mpc}} := 9.338 \cdot 10^{-6}$

The coefficient of thermal expansion for the basket, $\alpha_{\text{bas}} := 9.90 \cdot 10^{-6}$ 800 deg. F

3.I.4.2 Thermal Growth of the Overpack

Results for thermal expansion deformation and stress in the overpack are obtained here. The system is replaced by a equivalent uniform hollow cylinder with approximated average properties.

Based on the given inside and outside surface temperatures, the temperature solution in the cylinder is given in the form:

$$C_a + C_b \cdot \ln\left(\frac{r}{a}\right)$$

where,

$$C_a := \Delta T_{1h} \quad C_a = 252$$

$$C_b := \frac{\Delta T_{2h} - \Delta T_{1h}}{\ln\left(\frac{b}{a}\right)} \quad C_b = -47.889$$

Next, form the integral relationship:

$$\text{Int} := \int_a^b \left[C_a + C_b \cdot \ln\left(\frac{r}{a}\right) \right] \cdot r \, dr$$

The Mathcad program, which was used to create this appendix, is capable of evaluating the integral "Int" either numerically or symbolically. To demonstrate that the results are equivalent, the integral is evaluated both ways in order to qualify the accuracy of any additional integrations that are needed.

The result obtained through numerical integration, $\text{Int} = 5.807 \times 10^4 \text{ in}^2$

To perform a symbolic evaluation of the solution the integral "Ints" is defined. This integral is then evaluated using the Maple symbolic math engine built into the Mathcad program as:

$$\text{Int}_s := \int_a^b \left[C_a + C_b \cdot \ln\left(\frac{r}{a}\right) \right] \cdot r \, dr$$

$$\text{Int}_s := \frac{1}{2} \cdot C_b \cdot \ln\left(\frac{b}{a}\right) \cdot b^2 + \frac{1}{2} \cdot C_a \cdot b^2 - \frac{1}{4} \cdot C_b \cdot b^2 + \frac{1}{4} \cdot C_b \cdot a^2 - \frac{1}{2} \cdot C_a \cdot a^2 \quad \text{Int}_s = 5.807 \times 10^4 \text{ in}^2$$

We note that the values of Int and Ints are identical. The average temperature in the overpack cylinder (T_{bar}) is therefore determined as:

$$T_{\text{bar}} := \frac{2}{(b^2 - a^2)} \cdot \text{Int}$$

$$T_{\text{bar}} = 247.778$$

We estimate the average coefficient of thermal expansion for the HI-TRAC by weighting the volume of the various layers. A total of three layers are identified for this calculation. They are:

- 1) the inner shell
- 2) the radial lead shield
- 3) the outer shell

Thermal properties are based on estimated temperatures in the component and coefficient of thermal expansion values taken from the tables in Chapter 3. The following averaging calculation involves the thicknesses (t) of the various components, and the estimated coefficients of thermal expansion at the components' mean radial positions. The results of the weighted average process yields an effective coefficient of linear thermal expansion for use in computing radial growth of a solid cylinder (the overpack).

The thicknesses of each component are defined as:

$$t_1 := 0.75 \cdot \text{in}$$

$$t_2 := 4.5 \cdot \text{in}$$

$$t_3 := 10 \cdot \text{in}$$

and the corresponding mean radii can therefore be defined as:

$$r_1 := a + 0.5 \cdot t_1$$

$$r_2 := r_1 + 0.5 \cdot t_1 + 0.5 \cdot t_2$$

$$r_3 := r_2 + 0.5 \cdot t_2 + 0.5 \cdot t_3$$

To check the accuracy of these calculations, the outer radius of the HI-TRAC is calculated from r_3 and t_3 , and the result is compared with the previously defined value (b).

$$b_1 := r_3 + 0.5 \cdot t_3$$

$$b_1 = 40.625 \text{ in}$$

$$b = 40.625 \text{ in}$$

We note that the calculated value b_1 is identical to the previously defined value b . The coefficients of thermal expansion for each component, estimated based on the temperature gradient, are defined as:

$$\begin{aligned}\alpha_1 &:= 6.3382 \cdot 10^{-6} \\ \alpha_2 &:= 17.2 \cdot 10^{-6} \quad @300 \text{ deg F} \\ \alpha_3 &:= 6.311 \cdot 10^{-6}\end{aligned}$$

Thus, the average coefficient of thermal expansion of the HI-TRAC is determined as:

$$\begin{aligned}\alpha_{\text{avg}} &:= \frac{r_1 \cdot t_1 \cdot \alpha_1 + r_2 \cdot t_2 \cdot \alpha_2 + r_3 \cdot t_3 \cdot \alpha_3}{\frac{a+b}{2} \cdot (t_1 + t_2 + t_3)} \\ \alpha_{\text{avg}} &= 1.413 \times 10^{-5}\end{aligned}$$

Reference 3.I.1 gives an expression for the radial deformation due to thermal growth. At the inner radius of the HI-TRAC ($r = a$), the radial growth is determined as:

$$\Delta R_{\text{ah}} := \alpha_{\text{avg}} \cdot a \cdot T_{\text{bar}} \quad \Delta R_{\text{ah}} = 0.12 \text{ in}$$

Similarly, an overestimate of the axial growth of the HI-TRAC can be determined by applying the average temperature (T_{bar}) over the entire length of the overpack as:

$$\begin{aligned}\Delta L_{\text{ovph}} &:= L_{\text{ovp}} \cdot \alpha_{\text{avg}} \cdot T_{\text{bar}} \\ \Delta L_{\text{ovph}} &= 0.669 \text{ in}\end{aligned}$$

Estimates of the secondary thermal stresses that develop in the HI-TRAC due to the radial temperature variation are determined using a conservatively high value of E as based on the temperature of the steel. The circumferential stress at the inner and outer surfaces (σ_{ca} and σ_{cb} , respectively) are determined as:

The Young's Modulus of the material, $E := 28600000$ psi

$$\sigma_{\text{ca}} := \alpha_{\text{avg}} \cdot \frac{E}{a^2} \cdot \left[2 \cdot \frac{a^2}{(b^2 - a^2)} \cdot \text{Int} - (C_a) \cdot a^2 \right] \quad \sigma_{\text{ca}} = -1706 \text{ psi}$$

$$\sigma_{cb} := \alpha_{avg} \cdot \frac{E}{b^2} \cdot \left[2 \cdot \frac{b^2}{(b^2 - a^2)} \cdot \text{Int} - \left[C_a + C_b \cdot \left(\ln \left(\frac{b}{a} \right) \right) \right] \right] \cdot b^2 \quad \sigma_{cb} = 1526 \text{ psi}$$

The radial stress due to the temperature gradient is zero at both the inner and outer surfaces of the HI-TRAC. The radius where a maximum radial stress is expected, and the corresponding radial stress, are determined by trial and error as:

$$N := 0.47$$

$$r := a \cdot (1 - N) + N \cdot b$$

$$r = 37.313 \text{ in}$$

$$\sigma_r := \alpha_{avg} \cdot \frac{E}{r^2} \cdot \left[\frac{r^2 - a^2}{2} \cdot T_{bar} - \int_a^r \left[C_a + C_b \cdot \left(\ln \left(\frac{y}{a} \right) \right) \right] \cdot y \, dy \right]$$

$$\sigma_r = -67.389 \text{ psi}$$

The axial stress developed due to the temperature gradient is equal to the sum of the radial and tangential stresses at any radial location. (see eq. 9.10.7) of [3.I.1]. Therefore, the axial stresses are available from the above calculations. The stress intensities in the HI-TRAC due to the temperature distribution are below the Level A membrane stress.

3.I.4.3 Thermal Growth of the MPC Shell

The radial and axial growth of the MPC shell (ΔR_{mpch} and ΔL_{mpch} , respectively) are determined as:

$$\Delta R_{mpch} := \alpha_{mpc} \cdot R_{mpc} \cdot \Delta T_{3h}$$

$$\Delta R_{mpch} = 0.122 \text{ in}$$

$$\Delta L_{mpch} := \alpha_{mpc} \cdot L_{mpc} \cdot \Delta T_{3h}$$

$$\Delta L_{mpch} = 0.685 \text{ in}$$

3.I.4.4 Clearances Between the MPC Shell and HI-TRAC

The final radial and axial MPC shell-to-HI-TRAC clearances (RG_{moh} and AG_{moh} , respectively) are determined as:

$$RG_{\text{moh}} := RC_{\text{mo}} + \Delta R_{\text{ah}} - \Delta R_{\text{mpch}}$$

$$RG_{\text{moh}} = 0.123 \text{ in}$$

$$AG_{\text{moh}} := AC_{\text{mo}} + \Delta L_{\text{ovph}} - \Delta L_{\text{mpch}}$$

$$AG_{\text{moh}} = 0.735 \text{ in}$$

Note that this axial clearance (AG_{moh}) is based on the temperature distribution at the top end of the system.

3.I.4.5 Thermal Growth of the MPC Basket

Using formulas given in [3.I.2] for a solid body of revolution, and assuming a parabolic temperature distribution in the radial direction with the center and outer temperatures given previously, the following relationships can be developed for free thermal growth.

$$\text{Define } \Delta T_{\text{bas}} := \Delta T_{5\text{h}} - \Delta T_{4\text{h}}$$

$$\Delta T_{\text{bas}} = 199$$

$$\text{Then the mean temperature can be defined as } T_{\text{bar}} := \frac{2}{R_b^2} \cdot \int_0^{R_b} \left(\Delta T_{5\text{h}} - \Delta T_{\text{bas}} \cdot \frac{r^2}{R_b^2} \right) r \, dr$$

Using the Maple symbolic engine again, the closed form solution of the integral is:

$$T_{\text{bar}} := \frac{2}{R_b^2} \cdot \left(\frac{-1}{4} \cdot \Delta T_{\text{bas}} \cdot R_b^2 + \frac{1}{2} \cdot \Delta T_{5\text{h}} \cdot R_b^2 \right)$$

$$T_{\text{bar}} = 682.5$$

The corresponding radial growth at the periphery (ΔR_{bh}) is therefore determined as:

$$\Delta R_{\text{bh}} := \alpha_{\text{bas}} \cdot R_b \cdot T_{\text{bar}} \quad \Delta R_{\text{bh}} = 0.226 \text{ in}$$

and the corresponding axial growth (ΔL_{bas}) is determined from [3.I.2] as:

$$\Delta L_{\text{bh}} := \Delta R_{\text{bh}} \cdot \frac{L_{\text{bas}}}{R_b} \quad \Delta L_{\text{bh}} = 1.193 \text{ in}$$

Note that the coefficient of thermal expansion for the hottest basket temperature has been used, and the results are therefore conservative.

3.I.4.6 Clearances Between the Fuel Basket and MPC Shell

The final radial and axial fuel basket-to-MPC shell and lid clearances (RG_{bmh} and AG_{bmh} , respectively) are determined as:

$$RG_{bmh} := RC_{bm} - \Delta R_{bh} + \Delta R_{mpch}$$

$$RG_{bmh} = 0.083 \text{ in}$$

$$AG_{bmh} := AC_{bm} - \Delta L_{bh} + \Delta L_{mpch}$$

$$AG_{bmh} = 1.305 \text{ in}$$

3.1.5 Summary of Results

The previous results are summarized here.

MPC Shell-to-HI-TRAC

$$RG_{moh} = 0.123 \text{ in}$$

$$AG_{moh} = 0.735 \text{ in}$$

Fuel Basket-to-MPC Shell

$$RG_{bmh} = 0.083 \text{ in}$$

$$AG_{bmh} = 1.305 \text{ in}$$

3.1.6 Nomenclature

a is the inner radius of the HI-TRAC

AC_{bm} is the initial fuel basket-to-MPC axial clearance.

AC_{mo} is the initial MPC-to-HI-TRAC axial clearance.

AG_{bmh} is the final fuel basket-to-MPC shell axial gap for the hot components.

AG_{moh} is the final MPC shell-to-HI-TRAC axial gap for the hot components.

b is the outer radius of the HI-TRAC

L_{bas} is the axial length of the fuel basket.

L_{mpc} is the axial length of the MPC.

L_{ovp} is the axial length of the HI-TRAC.

r_1 (r_2, r_3) is mean radius of the HI-TRAC inner shell (radial lead shield, outer shell).

R_b is the outer radius of the fuel basket.

R_{mpc} is the mean radius of the MPC shell.

RC_{bm} is the initial fuel basket-to-MPC radial clearance.

RC_{mo} is the initial MPC shell-to-HI-TRAC radial clearance.

RG_{bmh} is the final fuel basket-to-MPC shell radial gap for the hot components.

RG_{moh} is the final MPC shell-to-HI-TRAC radial gap for the hot components.

t_1 (t_2, t_3) is the thickness of the HI-TRAC inner shell (radial lead shield, outer shell).

T_{bar} is the average temperature of the HI-TRAC cylinder.

α_1 (α_2, α_3) is the coefficient of thermal expansion of the HI-TRAC inner shell (radial lead shield, outer shell).

α_{avg} is the average coefficient of thermal expansion of the HI-TRAC.

α_{bas} is the coefficient of thermal expansion of the HI-TRAC.

α_{mpc} is the coefficient of thermal expansion of the MPC.

ΔL_{bh} is the axial growth of the fuel basket for the hot components.

ΔL_{mpch} is the axial growth of the MPC for the hot components.
 ΔL_{ovph} is the axial growth of the HI-TRAC for the hot components.
 ΔR_{ah} is the radial growth of the HI-TRAC inner radius for the hot components.
 ΔR_{bh} is the radial growth of the fuel basket for the hot components.
 ΔR_{mpch} is the radial growth of the MPC shell for the hot components.
 ΔT_{1h} is the temperature change at the HI-TRAC inside surface for hot components.
 ΔT_{2h} is the temperature change at the inside of the water jackets for hot components.
 ΔT_{3h} is the temperature change at the MPC shell mean radius for hot components.
 ΔT_{4h} is the temperature change at the MPC basket periphery for hot components.
 ΔT_{5h} is the temperature change at the MPC basket centerline for hot components.
 ΔT_{bas} is the fuel basket centerline-to-periphery temperature gradient.
 σ_{ca} is the circumferential stress at the HI-TRAC inner surface.
 σ_{cb} is the circumferential stress at the HI-TRAC outer surface.
 σ_r is the maximum radial stress of the HI-TRAC.

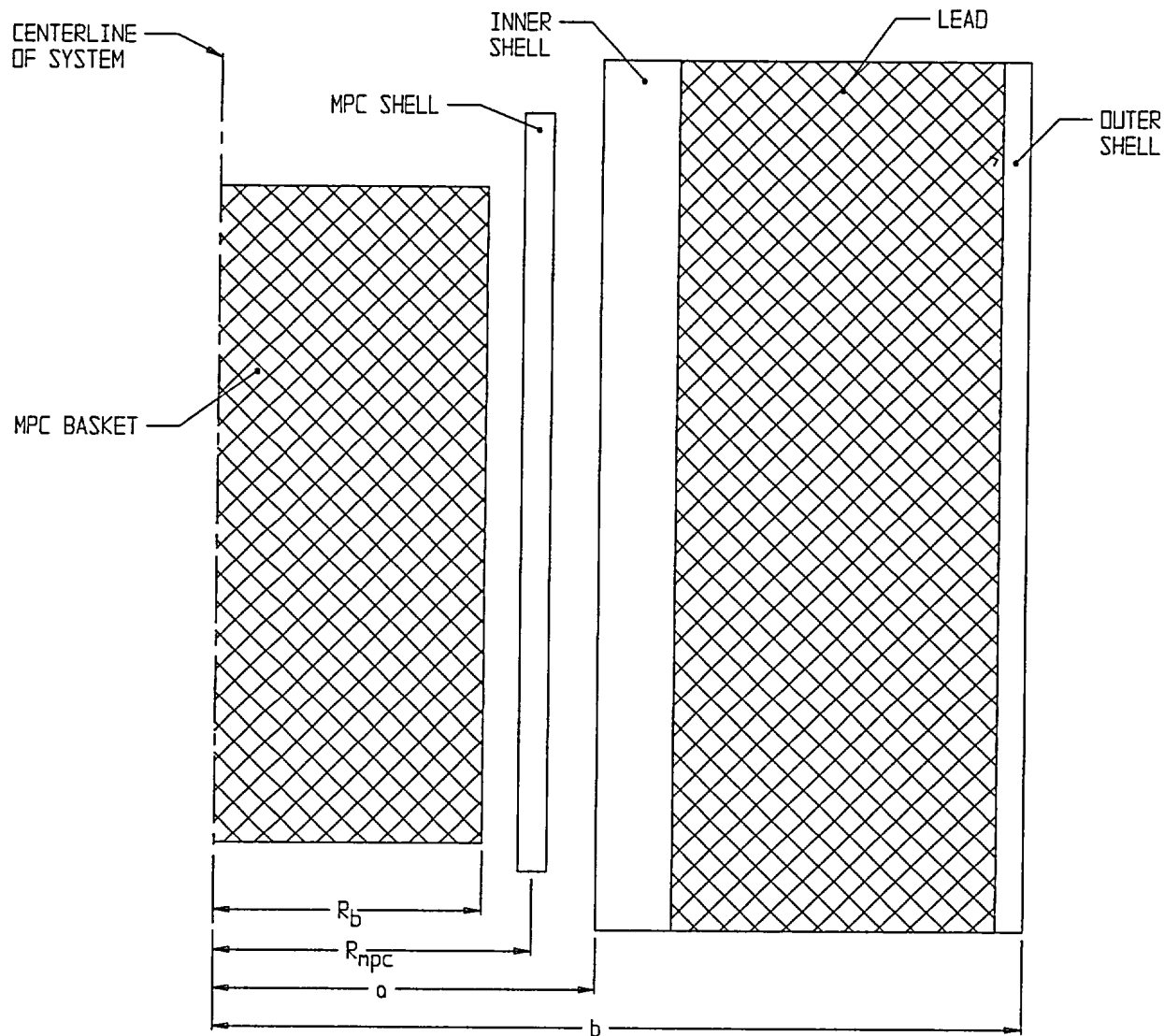


FIGURE 3.1.1; GEOMETRY OF SECTION FOR THERMAL EXPANSION CALCULATIONS

Appendix 3.J

Intentionally Deleted

APPENDIX 3.K HI-STORM TIPOVER - LID ANALYSIS

3.K.1 Introduction

The fully loaded HI-STORM, with the top lid in place, hypothetically tips over onto the ISFSI pad generating a resultant deceleration load of 45 G's at the top of the fuel basket and 49 G's at the top of the storage overpack lid, per Appendix 3.A. In this appendix, the necessary stress analyses are performed to insure that the concrete shielding maintains its position after a non-mechanistic tipover event. A similar evaluation of the lid for the vertical bottom end drop of the HI-STORM 100 is documented in Appendix 3M, Section 3.M.3. Of particular interest in are the concrete shields on the inside and outside of the lid. It is required that the shielding remain in place subsequent to any accident condition of storage.

3.K.2 Methodology

Strength of materials formulations are used to estimate weld stress and shell stresses in the enclosing metal shells surrounding the concrete shielding.

3.K.3 Input Data (from BM-1575 and related drawings in Chapter 1)

3.K.3.1 Geometry

Lid bolt diameter	$d_{\text{bolt}} := 3\text{-in}$	Number of bolts	NB := 4
Lid top plate thickness	$t_{\text{lid}} := 4\text{-in}$	Lid top plate diameter	$d_{\text{lid}} := 126\text{-in}$
Note that the top lid is really two 2" thick plates			
Lid bottom plate thickness	$t_{\text{lidbot}} := 1.25\text{-in}$		
Lid bottom plate diameter	$d_{\text{lidbot}} := 69\text{ in}$		
Lid shell thickness	$t_{\text{lidshell}} := 1\text{-in}$		
Lid shell length	$L_{\text{lidshell}} := 10.5\text{-in}$		
Shield block shell thickness	$t_{\text{block}} := 0.5\text{-in}$		
Shield block height	$L_{\text{shieldblock}} := 8\text{-in}$		
Shield block inner shell OD	$d_{\text{ib}} := 64\text{ in}$	Shield Block outer shell OD	$d_{\text{ob}} := 86\text{-in}$
Shield Block Ring Thickness	$t_{\text{ring}} := 0.25\text{-in}$		
Fillet weld size	$t_{\text{weld}} := 0.25\text{-in}$		

3.K.3.2 Weight Densities

$$\text{Concrete} \quad \gamma_c := 155 \cdot \frac{\text{lbf}}{\text{ft}^3}$$

$$\text{Steel} \quad \gamma_s := 0.283 \cdot \frac{\text{lbf}}{\text{in}^3}$$

3.K.4 Analyses

3.K.4.1 Lid top plate stress analysis

First compute the total load resisted by the four lid bolts when the lid is decelerated by

$$G := 49 \quad \text{Design basis deceleration per Table 3.A.4 of Appendix 3.A}$$

Weight of top plate

$$W_{\text{lid}} := \gamma_s \cdot t_{\text{lid}} \cdot \pi \cdot \frac{d_{\text{lid}}^2}{4} \quad W_{\text{lid}} = 1.411 \times 10^4 \text{ lbf}$$

Weight of bottom plate

$$W_{\text{bot}} := \gamma_s \cdot t_{\text{lidbot}} \cdot \pi \cdot \frac{d_{\text{lidbot}}^2}{4} \quad W_{\text{bot}} = 1.323 \times 10^3 \text{ lbf}$$

Weight of Lid shell

$$W_{\text{shell}} := \gamma_s \cdot t_{\text{lidshell}} \cdot L_{\text{lidshell}} \cdot \pi \cdot (d_{\text{lidbot}} - t_{\text{lidshell}}) \quad W_{\text{shell}} = 634.796 \text{ lbf}$$

Weight of Lid Shield

$$W_{\text{shield}} := \gamma_c \cdot \pi \cdot \frac{(d_{\text{lidbot}} - 2 \cdot t_{\text{lidshell}})^2}{4} \cdot L_{\text{lidshell}} \quad W_{\text{shield}} = 3.321 \times 10^3 \text{ lbf}$$

Weight of shield block shells

$$W_{\text{sblocks}} := \gamma_s \cdot t_{\text{block}} \cdot \pi \cdot (d_{\text{ib}} - t_{\text{block}} + d_{\text{ob}} - t_{\text{block}}) \cdot L_{\text{shieldblock}} \quad W_{\text{sblocks}} = 529.886 \text{ lbf}$$

Weight of Shield block Ring

$$W_{\text{ring}} := \gamma_s \cdot t_{\text{ring}} \cdot \pi \cdot \frac{(d_{\text{ib}}^2 + d_{\text{ob}}^2)}{4} \quad W_{\text{ring}} = 638.575 \text{ lbf}$$

Weight of Shield Block

$$W_{\text{block}} := \gamma_c \cdot L_{\text{shieldblock}} \cdot \frac{\pi}{4} \cdot [(d_{\text{ob}} - 2 \cdot t_{\text{block}})^2 - d_{\text{ib}}^2]$$

$$W_{\text{block}} = 1.763 \times 10^3 \text{ lbf}$$

The total weight of the assemblage is

$$W_{\text{total}} := W_{\text{lid}} + W_{\text{bot}} + W_{\text{shell}} + W_{\text{shield}} + W_{\text{sbs shells}} + W_{\text{ring}} + W_{\text{block}}$$

$$W_{\text{total}} = 2.233 \times 10^4 \text{ lbf}$$

This confirms the bounding weight in Table 3.2.1

For subsequent calculations where the total weight is required, use the bounding weight from Table 3.2.1.

$$W_{\text{lid}} := 23000 \text{ lbf}$$

Compute the bearing stress in the lid at each of the four bolt holes due to the accident load.

$$\text{Area}_{\text{bearing}} := 4 \cdot d_{\text{bolt}} \cdot t_{\text{lid}}$$

$$\text{Area}_{\text{bearing}} = 48 \text{ in}^2$$

$$\sigma_{\text{bearing}} := \frac{W_{\text{total}} \cdot G}{\text{Area}_{\text{bearing}}}$$

$$\sigma_{\text{bearing}} = 2.279 \times 10^4 \text{ psi}$$

Noting that this local stress is less than the Level D allowable membrane stress for the lid material (39,700 psi per Table 3.1.12) and is less than the material yield stress permits us to conclude that if the lid bolts remain intact, the lid top plate will not suffer gross distortion. The calculation just performed assumes that both top plates are in contact with the bolt and that the total load is shared equally. In the event that only one of the two plates takes all of the load, then the calculated stress will be doubled, local yielding will occur near the holes, and the load will be redistributed to both plates.

3.K.4.2 Lid Shell-to-Lid Top Plate Weld

Drawing 1561, sheet 2 shows the weld detail in this region

$$d_{\text{weld}} := d_{\text{lidbot}} + 0.667 \cdot t_{\text{weld}}$$

$$\text{Area}_{\text{weld}} := \pi \cdot d_{\text{weld}} \cdot (0.7071 \cdot t_{\text{weld}})$$

The load to be resisted by this weld is the weight of the lid shield, the shield shell and the lid bottom plate.

$$W_{lw} := W_{bot} + W_{shell} + W_{shield}$$

$$W_{lw} = 5.278 \times 10^3 \text{ lbf}$$

The shear stress in the weld is

$$\tau_{weld2} := \frac{W_{lw} \cdot G}{Area_{weld}}$$

$$\tau_{weld2} = 6.733 \times 10^3 \text{ psi}$$

From Table 3.3.2, the ultimate strength of the steel material (@ 350 degrees F) is

$$S_u := 70000 \text{ psi}$$

The weld stress limit under faulted conditions is taken as the minimum of 42% of the ultimate strength.

$$\tau_{allowable} := .42 \cdot S_u$$

$$\tau_{allowable} = 2.94 \times 10^4 \text{ psi}$$

Therefore, the safety factor for this weld, under the postulated accident, is

$$SF_2 := \frac{\tau_{allowable}}{\tau_{weld2}}$$

$$SF_2 = 4.367$$

Note that we assume that any additional component adding to the weld stress is negligible. This will be corrected, if necessary, in a later section.

Note that ASME Section III, Subsection NF does not impose any weld efficiency factors.

3.K.4.3 Shield Block Shells-to-Lid Top Plate Weld

Drawing 1561, sheet 2 shows the weld detail in this region

$$d_{weldi} := d_{ib} - 0.667 \cdot t_{weld}$$

$$d_{weldi} = 63.833 \text{ in}$$

$$d_{weldo} := d_{ob} - 0.667 \cdot t_{weld}$$

$$d_{weldo} = 85.833 \text{ in}$$

$$Area_{weld} := \pi \cdot (d_{weldi} + d_{weldo}) \cdot (0.7071 \cdot t_{weld})$$

The load to be resisted by this weld is the weight of the shield block, the shield block shells, and the shield block ring.

$$W_{lw} := W_{sbshells} + W_{ring} + W_{block}$$

$$W_{lw} = 2.932 \times 10^3 \text{ lbf}$$

The shear stress in the weld is

$$\tau_{\text{weld}} := \frac{W_{\text{lw}} \cdot G}{\text{Area}_{\text{weld}}} \quad \tau_{\text{weld}} = 1.728 \times 10^3 \text{ psi}$$

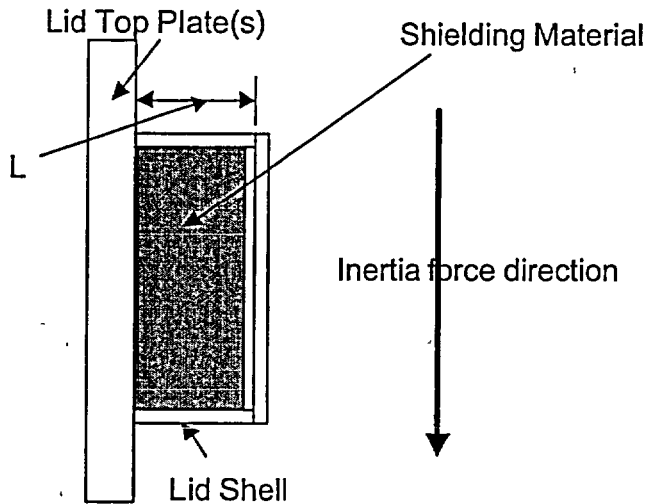
Therefore, this weld does not govern.

3.K.5 Lid Shell Stress Evaluation

The previous section has demonstrated that no welds will experience overstress under the postulated event. To finally conclude that the shielding remains effective after the tipover, an assessment of the stress level in the lid shell is performed in this section.

3.K.5.1 Consideration of the shell as a short beam cantilevered from the lid top plate and subject to the amplified weight of the shielding material plus its own amplified weight.

We consider the following sketch that shows a "side" view of the lid top plate and the lid shell:



The following analysis computes the "axial" stress in the shield shell due to bending as a short beam.

$$\begin{aligned} L &:= L_{\text{ldshell}} & L &= 10.5 \text{ in} \\ t &:= t_{\text{ldshell}} & t &= 1 \text{ in} & t_{\text{weld}} &= 0.25 \text{ in} \\ d &:= d_{\text{ldbot}} & d &= 69 \text{ in} \end{aligned}$$

The load applied to the "beam" is

$$\text{Load} := (W_{\text{bot}} + W_{\text{shell}} + W_{\text{shield}}) \cdot G \quad \text{Load} = 2.586 \times 10^5 \text{ lbf}$$

The area moment of inertia of the weld metal is

$$I := \frac{\pi}{64} \cdot \left[(d + .667 \cdot .7071 \cdot t_{\text{weld}})^4 - (d)^4 \right] \quad I = 7.625 \times 10^3 \text{ in}^4$$

The stress induced by the bending moment is

$$\sigma_{\text{bending}} := \frac{\text{Load} \cdot (0.5 \cdot L) \cdot d}{2 \cdot I} \quad \sigma_{\text{bending}} = 6.144 \times 10^3 \text{ psi}$$

This stress is significant so the safety factor on the weld needs to be reevaluated

$$\text{SF}_2 := \frac{\tau_{\text{allowable}}}{\sqrt{\tau_{\text{weld}}^2 + \sigma_{\text{bending}}^2}} \quad \text{SF}_2 = 3.226$$

3.K.5.2 Consideration of circumferential stress in the lid shell

The lid shell is prevented from departing from a circular shape by the lid top and bottom plates. The effect of these end restraints is felt through an axial distance equal to the so called "bending boundary layer". The bending boundary layer extends along the shell axis approximately a distance equal to $2(td/2)^{1/2}$.

$$L_{\text{bl}} := 2 \cdot \sqrt{\frac{d}{2} \cdot t} \quad L_{\text{bl}} = 11.747 \text{ in}$$

Since the bending boundary layer extends from each end a distance more than the shell length, it is concluded that the shell does not experience any peripheral stresses due to ring type deformation modes.

3.K.6 Shield Block Shells Stress Evaluation

For this configuration, the applied load is less than that for the lid, shell, the length of the shell is less, and the section moment of inertia of the composite structure is increased. Therefore, this component is not governing. The calculations are included, however, for completeness.

The area moment of inertia of the weld metal from the two shells is

$$I_{\text{sb}} := \frac{\pi}{64} \cdot \left[(d_{\text{ob}} + .667 \cdot .7071 \cdot t_{\text{weld}})^4 - (d_{\text{ob}})^4 \right] + \frac{\pi}{64} \cdot \left[(d_{\text{ib}} + .667 \cdot .7071 \cdot t_{\text{weld}})^4 - (d_{\text{ib}})^4 \right]$$

$$I_{\text{sb}} = 2.084 \times 10^4 \text{ in}^4$$

$$L := L_{\text{shieldblock}} \quad L = 8 \text{ in}$$

The load applied to the "beam" is

$$\text{Load} := (W_{\text{sbs shells}} + W_{\text{ring}} + W_{\text{block}}) \cdot G \quad \text{Load} = 1.437 \times 10^5 \text{ lbf}$$

The stress induced by the bending moment is

$$\sigma_{\text{bending}} := \frac{\text{Load} \cdot (0.5 \cdot L) \cdot d_{\text{ob}}}{2 \cdot I_{\text{sb}}} \quad \sigma_{\text{bending}} = 1.186 \times 10^3 \text{ psi}$$

The safety factor is computed noting that there are two components of stress in the weld

$$SF_2 := \frac{\tau_{\text{allowable}}}{\sqrt{\tau_{\text{weld}}^2 + \sigma_{\text{bending}}^2}} \quad SF_2 = 14.027$$

As noted, this location does not govern

3.K.6 Conclusions

The analysis has shown that the stress in the lid remains below the Level A allowable value for the lid material. Therefore, no gross deformation of the lid occurs during the non-mechanistic tipover event.

Stress in the shells remains below Level A values.

All welds connecting the shield block shells and the shield shell to the lid have stress levels below the Level A limit for welds from ASME Section III, Subsection NF. Therefore, the shield materials remain in place.

APPENDIX 3.L HI-STORM LID TOP PLATE BOLTING

3.L.1 Introduction

This appendix provides a calculation that shows that the studs holding the lid top plate in place have sufficient strength to keep the top lid plate(s) in place during a HI-STORM tip over if one stud loses its load carrying ability.

3.L.2 Methodology

Force equilibrium relations are used to calculate the stud shear force resisting movement of the lid top plates, relative to the body of HI-STORM, under the design basis deceleration. Only three of four studs carries load. As described in Subsection 3.4.4.3.2.2, the ASME Code does not apply to the construction of the HI-STORM top plate-to-overpack connection (the lid studs, nuts, and the through holes in the top plate). However, for conservatism, the stress limits from ASME III, Subsection NF are used for this analysis.

3.L.3 Input Data

From the tipover analysis (Table 3.A.4), the deceleration on the lid at the top of the storage overpack is

$$G_{level} := 48.5$$

From Table 3.2.1, the bounding weight for the overpack top lid is

$$Weight := 23000 \cdot \text{lb}$$

Stud material: SA564-630 (Age Hardened at 1075 degrees F)

Stud Material Ultimate Tensile and Yield Strengths

@ 300 deg. F, Table 3.3.4 $S_u := 145000 \cdot \text{psi}$ $S_y := 110700 \cdot \text{psi}$

The allowable stress in the stud is limited to 42% of the ultimate strength or 60% of the yield strength per NF-3225 and Appendix F, F-1335.2.

$$.42 \cdot S_u = 6.09 \times 10^4 \text{ psi} \qquad .6 \cdot S_y = 6.642 \times 10^4 \text{ psi}$$

Therefore, 42% of the ultimate strength governs the stud stress analysis.

Stud diameter (excluding threads) (see BOM No. 1575) $d_{bolt} := 3.25 \cdot \text{in}$



Minimum diameter (including threads) $d_{min} := .99 \cdot d_{bolt}$

This minimum diameter is estimated from Table 3 of Machinery's Handbook, 23rd Edition, Industrial Press, p. 1283.

Therefore the bolt area in the threaded region at the nut is obtained from the equation in the above cited reference (p. 1279).

$$A_{min} := \pi \cdot \left(.5 \cdot d_{min} - \frac{0.16238 \cdot \text{in}}{4} \right)^2 \quad A_{min} = 7.726 \text{ in}^2$$

This is based on 4-UNC threads

The bolt area at the interface with the anchor block is

$$A_{bolt} := \frac{\pi \cdot d_{bolt}^2}{4} \quad A_{bolt} = 8.296 \text{ in}^2$$

Thickness of 2 lid plates $L := 4 \cdot \text{in}$

Thickness of overpack top cover plate $t := 0.75 \cdot \text{in}$ BOM for HI-STORM 100

3.L.4 Calculations

If optional shims are used, all lid studs will support the load in a hypothetical tip-over event; that is, all clearances are closed by shims to ensure contact of stud surface to lids. Shims, if used, provide additional conservatism to the design. Regardless of the presence or absence of shims, we first evaluate what is likely to happen if one stud contacts the lid plates first. Will the hole open or will the stud take all of the load? For the lid, we conservatively assume that opening of the hole takes place at a flow stress equal to the average of the room temperature yield and ultimate strengths for the lid material (as opposed to using the minimum yield strength of the lid).

$$\text{Force} := \text{Weight} \cdot G_{level}$$

$$\text{Force} = 1.115 \times 10^6 \text{ lbf} \quad \text{Number_of_bolts} := 4$$

$$\text{Force_per_bolt} := \frac{\text{Force}}{\text{Number_of_bolts}} \quad \text{Force_per_bolt} = 2.789 \times 10^5 \text{ lbf}$$



Calculate the stud area resisting shear. Consider failure of stud based on 42% of ultimate strength (the allowable strength value per ASME Code, Section III, Appendix F considering the event to be a Level D event). |

The capacity of one stud is computed as follows: $A_b := \pi \cdot \frac{d_{bolt}^2}{4}$ |

Shear_capacity := .42 · S_u · A_b Shear_capacity = 5.052 × 10⁵ lbf |

The bearing capacity of the hole (based on average of yield and ultimate strength of SA516-Grade 70 at 100 degrees F - see Table 3.3.2) is: |

Bearing_Capacity := (70000 + 38000) · psi · d_{bolt} · L · 0.5 |

Bearing_Capacity = 7.02 × 10⁵ lbf |

The ratio $\frac{Bearing_Capacity}{Shear_capacity} = 1.39$

demonstrates that the loaded hole will not enlarge prior to the stud exceeding its shear failure stress. Therefore, assume a single bolt fails. Subsequently, three bolts will contact (lid will rotate to maintain equilibrium). |

Force_per_bolt = 2.789 × 10⁵ lbf Based on all studs active |

Force_per_bolt := $\frac{4}{3}$ · Force_per_bolt Based on three remaining studs active |

Stud shear stress at the anchor block interface

$\tau_{bolt} := \frac{Force_per_bolt}{A_b}$ $\tau_{bolt} = 4.482 \times 10^4$ psi

The safety factor for direct shear at the interface, based on Level D allowable strength, is

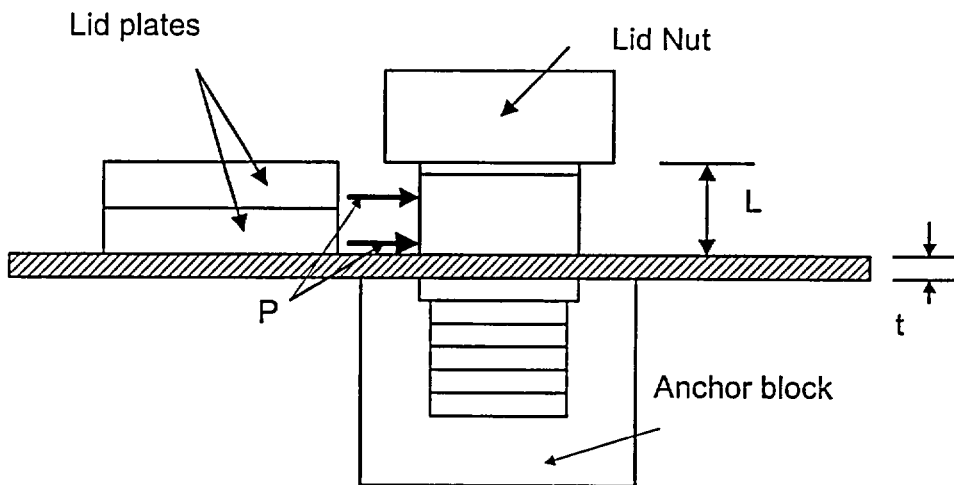
$$SF_s := .42 \cdot \frac{S_u}{\tau_{\text{bolt}}} \quad SF_s = 1.359$$

There is no requirement that the stud be other than "hand-tight" for storage. We conservatively use 300 ft-lb. as the initial torque to be applied for the lid studs during storage (not lifting). Assuming a lubricated surface, this imposes an initial average stud stress conservatively computed below:

$$T := 300 \cdot \text{ft} \cdot \text{lb} \quad \sigma_{\text{initial}} := \frac{T}{.12 \cdot A_b \cdot d_{\text{min}}} \quad \sigma_{\text{initial}} = 1.124 \times 10^3 \text{ psi}$$

(see Shigley and Mischke, Mechanical Engineering Design, McGraw Hill, 5th Edition, pp346-347)

In addition to the mean stress, during a side drop, the stud can experience a bending moment that is computed using the following figure:



$$L = 4 \text{ in}$$

$$t = 0.75 \text{ in}$$

BOM for HI-STORM 100

The presence of the lid nut provides the resistance of a "guided" cantilever for the stud. Therefore, the moment induced is computed as follows using the lid force "P":

$$P := \frac{\text{Force_per_bolt}}{2} \qquad P = 1.859 \times 10^5 \text{ lbf}$$

The weld connecting the two lids together is a 1/4" fillet weld. The capacity of this weld is "Cap", where:

$$\text{Cap} := \pi \cdot 128 \cdot \text{in} \cdot 0.25 \cdot \text{in} \cdot 7071 \cdot (.6 \cdot 38000 \cdot \text{psi}) \qquad [\text{F1334.2}]$$

$$\text{Cap} = 1.621 \times 10^6 \text{ lbf}$$

Since "Cap" is greater than "P", all of the side load will be imposed at the interface between the lower lid plate and the HI-STORM top closure plate.

Using the beam calculation from Roark's Handbook, 6th Edition, given at the end of this Appendix, the moment at the base of the stud, at the anchor block interface, due to the load 2P acting at "t" from the root, is:

$$\text{Moment} := 2.569 \cdot 10^5 \cdot \text{in} \cdot \text{lbf}$$

At the anchor block interface, the moment of inertia is

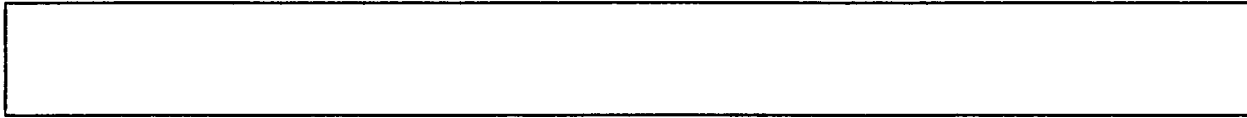
$$\text{Inertia} := \frac{\pi}{64} \cdot d_{\text{bolt}}^4$$

The stress induced by bending of the stud during a side drop is

$$\sigma_{\text{pl}} := \frac{\text{Moment} \cdot d_{\text{bolt}}}{2 \cdot \text{Inertia}} \qquad \sigma_{\text{pl}} = 7.623 \times 10^4 \text{ psi}$$

Under the accident condition, the outer fiber tensile stress in the stud cannot exceed the material ultimate strength (F-1335.1) Assuming that a combined state of tension and shear is present in the stud at the interface with the anchor block, then F-1335.3 imposes an interaction criteria that must be satisfied

$$\text{SF}_t := 1 \cdot \frac{S_u}{\sigma_{\text{pl}} + \sigma_{\text{initial}}} \qquad \text{SF}_t = 1.875$$



$$\text{Interaction_factor} := \left(\frac{1}{\text{SF}_s}\right)^2 + \left(\frac{1}{\text{SF}_t}\right)^2 \quad \text{Interaction_factor} = 0.826$$

Therefore the safety factor for combined tension and shear is

$$\text{SF}_{ts} := \frac{1}{\text{Interaction_factor}} \quad \text{SF}_{ts} = 1.21$$

At the nut, there is no shear force and the maximum axial stress in the stud from the bending is computed below using the moment result from the Roark solution:

$$\text{Inertia}_1 := \frac{\pi}{64} \cdot d_{\min}^4 \quad \text{Moment} := 22020 \cdot \text{in} \cdot \text{lbf}$$

The stress induced by bending of the stud during a side drop is

$$\sigma_{pl} := \frac{\text{Moment} \cdot d_{\min}}{2 \cdot \text{Inertia}_1} \quad \sigma_{pl} = 6.734 \times 10^3 \text{ psi}$$

Under the accident condition, the outer fiber tensile stress in the stud cannot exceed the material ultimate strength (F-1335.1).

$$\text{SF}_t := 1 \cdot \frac{S_u}{\sigma_{pl} + \sigma_{\text{initial}}} \quad \text{SF}_t = 18.453$$

3.L.5 Conclusion

Using the Level D allowables for the non-mechanistic tipover condition, the overpack lid will be normally held in place by the four studs. However, if tolerances cause initial loading of only a single stud, then if we conservatively assume that the stud fails before the remaining studs support the load, it is concluded that the three remaining studs support the entire load and meet the allowable stress limits of the ASME Code, Section III, Appendix F for Level D conditions. To provide additional assurances, the installation procedure may include shims "as necessary" to reduce final tolerance clearances after the lid is installed.

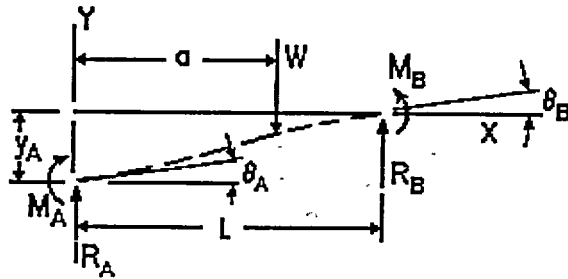
Table 3 Shear, Moment, Slope and Deflection Formulas for Elastic Straight Beams

From Roark's Handbook

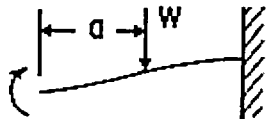


Case 1b Concentrated Intermediate Load; Left End Guided, Right End Fixed

Concentrated intermediate load



Left end guided, right end fixed



Enter dimensions, properties and loading Table 1

Before progressing further, calculate the moment of inertia (I) for your cross section by flipping to Table 1. Enter the computed value below:

Area moment of inertia: $I \equiv 5.477 \cdot \text{in}^4$
Length of beam: $L \equiv 4.75 \cdot \text{in}$
Distance from left edge to load: $a \equiv 4 \cdot \text{in}$
Modulus of elasticity: $E \equiv 28 \cdot 10^6 \cdot \frac{\text{lbf}}{\text{in}^2}$
Load: $W \equiv 371867 \cdot \text{lbf}$

Boundary values

The following specify the reaction forces (R), moments (M), slopes (θ) and deflections (y) at the left and right ends of the beam (denoted as A and B, respectively).

At the left end of the beam (guided):

$$R_A := 0 \cdot \text{lbf}$$

$$M_A := \frac{W \cdot (L - a)^2}{2 \cdot L} \quad M_A = 2.202 \times 10^4 \text{ lbf} \cdot \text{in}$$

$$\theta_A := 0 \cdot \text{deg}$$

$$y_A := \frac{-W}{12 \cdot E \cdot I} \cdot (L - a)^2 \cdot (L + 2 \cdot a) \quad y_A = -1.449 \times 10^{-3} \text{ in}$$

At the right end of the beam (fixed):

$$R_B := W \quad R_B = 3.719 \times 10^5 \text{ lbf}$$

$$M_B := \frac{-W \cdot (L^2 - a^2)}{2 \cdot L} \quad M_B = -2.569 \times 10^5 \text{ lbf} \cdot \text{in}$$

$$\theta_B := 0 \cdot \text{deg} \quad y_B := 0 \cdot \text{in}$$

General formulas and graphs for transverse shear, bending moment, slope and deflection as a function of x

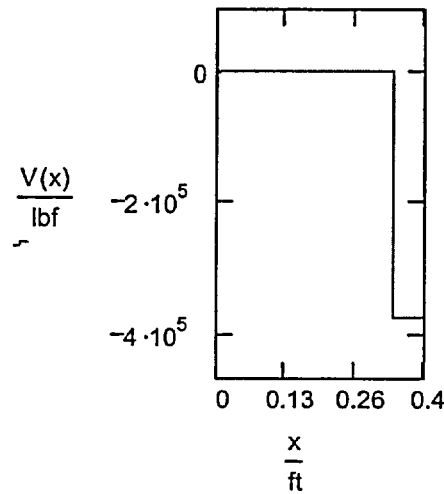
Note: To find the maximum and minimum values of a graphed function, simply **click** once on the graph and read the extreme values to the left of the plot.

$x := 0 \cdot L, .01 \cdot L .. L$ x ranges from 0 to L , the length of the beam.

$x_1 := 15 \cdot \text{ft}$ Define a point along the length of the beam.

Transverse shear $V(x) := R_A - (x > a) \cdot W$

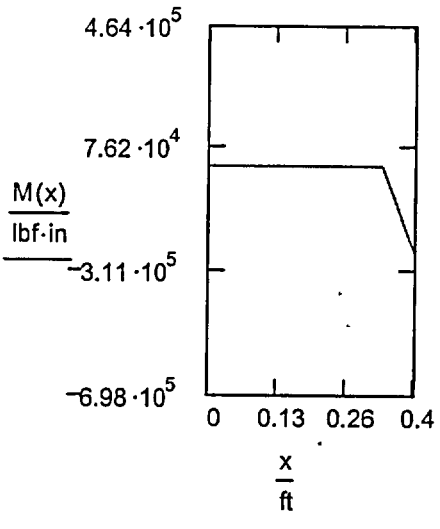
$$V(x_1) = -3.719 \times 10^5 \text{ lbf}$$



Bending moment

$$M(x) := M_A + R_A \cdot x - (x > a) \cdot (x - a) \cdot W$$

$$M(x_1) = -5.452 \times 10^6 \text{ lbf} \cdot \text{ft}$$

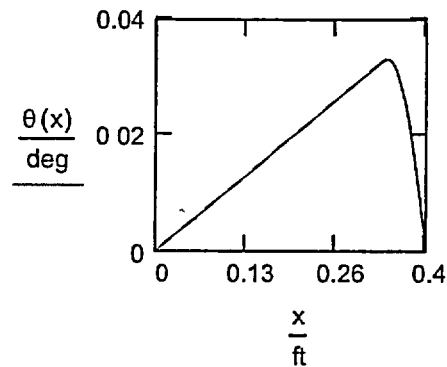




Slope

$$\theta(x) := \theta_A + \frac{M_A \cdot x}{E \cdot I} + \frac{R_A \cdot x^2}{2 \cdot E \cdot I} - \frac{(x > a) \cdot (x - a)^2 \cdot W}{2 \cdot E \cdot I}$$

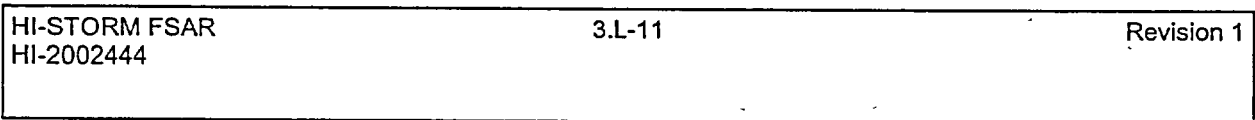
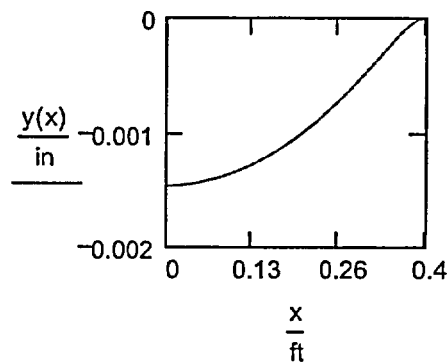
$$\theta(x_1) = -2.15 \times 10^3 \text{ deg}$$



Deflection

$$y(x) := y_A + \theta_A \cdot x + \frac{M_A \cdot x^2}{2 \cdot E \cdot I} + \frac{R_A \cdot x^3}{6 \cdot E \cdot I} - (x > a) \cdot \left[\frac{W}{6 \cdot E \cdot I} \cdot (x - a)^3 \right]$$

$$y(x_1) = -2.201 \times 10^3 \text{ in}$$





Selected maximum values of moments and deformations

Note: The signs in this section correspond to direction.

The subscripts **maxpos/neg** refer to the maximum magnitude of the most positive/negative value for the given parameters.

$$M_{\text{maxpos}} := M_A \qquad M_{\text{maxpos}} = 2.202 \times 10^4 \text{ lbf}\cdot\text{in}$$

$$M_{\text{maxneg}} := M_B \qquad M_{\text{maxneg}} = -2.569 \times 10^5 \text{ lbf}\cdot\text{in}$$

$$Y_{\text{maxneg}} := Y_A \qquad Y_{\text{maxneg}} = -1.449 \times 10^{-3} \text{ in}$$

The subscripts **(p/n)maxval** refer to the maximum attainable value when $a = 0$.

$$M_{\text{pmaxval}} := \frac{W \cdot L}{2} \qquad M_{\text{pmaxval}} = 8.832 \times 10^5 \text{ lbf}\cdot\text{in}$$

$$M_{\text{nmaxval}} := \frac{-W \cdot L}{2} \qquad M_{\text{nmaxval}} = -8.832 \times 10^5 \text{ lbf}\cdot\text{in}$$

$$Y_{\text{maxval}} := \frac{-W \cdot L^3}{12 \cdot E \cdot I} \qquad Y_{\text{maxval}} = -0.022 \text{ in}$$

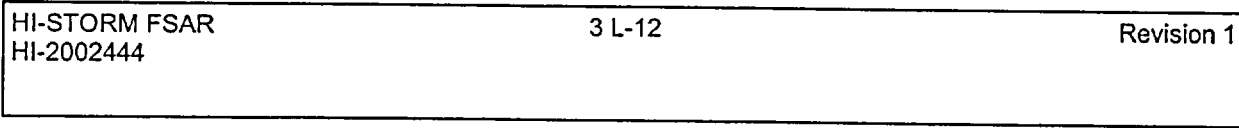
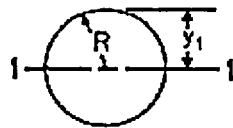




Table 1 Properties of Sections

Case 14 Solid Circle Section

Solid circle section



Notation file

Provides a description of Table 1 and the notation used.

Enter dimensions	Radius:	$R \equiv \frac{3.25}{2} \cdot \text{in}$
Area	$A := \pi \cdot R^2$	$A = 8.296 \text{in}^2$
Distance from centroid to extremities	$y_1 := R$	$y_1 = 1.625 \text{in}$
Moment of inertia	$I_1 := \frac{\pi}{4} \cdot R^4$	$I_1 = 5.477 \text{in}^4$
Radius of gyration about central axes	$r_1 := \frac{R}{2}$	$r_1 = 0.812 \text{in}$
Plastic section modulus	$Z_1 := 1.333 \cdot R^3$	$Z_1 = 5.72 \text{in}^3$
Shape factor	$SF_1 := 1.698$	$SF_1 = 1.698$

APPENDIX 3.M VERTICAL DROP OF OVERPACK

3.M.1 Introduction

The fully loaded HI-STORM 100 storage overpack, with the top lid in place, is assumed to fall vertically from a limiting carry height (see Appendix 3.A) onto the ISFSI pad and is brought to rest with a vertical deceleration of 45 g's. This appendix evaluates the stresses induced on the various elements in the load path as a result of this handling accident. Appendix 3.D has considered vertical handling of the storage overpack; where applicable, results from that analysis are simply amplified by appropriate factors to simulate the loads induced by the vertical drop.

3.M.2 Methodology

Strength of materials formulations are used to establish the state of stress in the various components of the load path. The structural components of the storage overpack considered here as potentially limiting are:

- Lid bottom plate
- Lid shell
- Lid top plate
- Inner shell
- Inlet vent horizontal plates
- Inlet vent vertical plates
- Pedestal shield
- Pedestal shell
- Structural welds in the load path

3.M.3 Analyses

3.M.3.1 Lid Bottom Plate

Under the maximum deceleration load of 45g, the lid bottom plate and the shielding material act together as a composite structure to resist the bending moment. Conservatively evaluate the state of stress in this plate by assuming simple support conditions at the outer periphery where the connection is made to the lid shell. This analysis leads to the maximum stress occurring at the center of the lid bottom plate. Figure 3.M.1 is a sketch of the configuration to be analyzed.

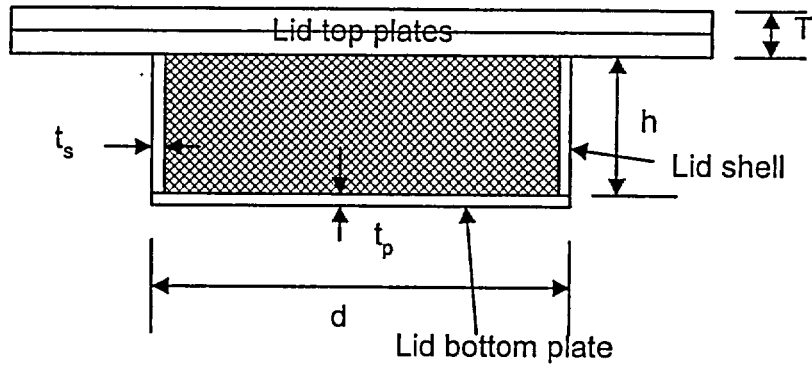


FIGURE 3.M.1 Geometry of Lid Shield

Input Data: (from BM-1575 and Appendix 3.K)

$$d := 69 \cdot \text{in} \quad t_p := 1.25 \cdot \text{in} \quad t_s := 1 \cdot \text{in}$$

$$h = 10.5 \cdot \text{in} \quad T := 4 \cdot \text{in}$$

The weight of the shield material is $W_{\text{shield}} := 3321 \cdot \text{lbf}$

The weight of the bottom plate is $W_{\text{bot}} := 1323 \cdot \text{lbf}$

The weight of the lid shell is

$$W_{\text{shell}} := 0.283 \cdot \frac{\text{lbf}}{\text{in}^3} \cdot \pi \cdot (d - t_s) \cdot h \cdot t_s$$

$$W_{\text{shell}} = 634.796 \text{ lbf}$$

see calculations in Appendix 3.K

Design basis deceleration $G := 45$ Table 2.2.8

For the Level D event, the allowable stress intensity of SA-516 Grade 70, at 350 degrees F, is obtained from Table 3.1.12.

$S_a := 59650 \cdot \text{psi}$ Primary membrane plus primary bending

$S_{\text{apm}} = 39750 \cdot \text{psi}$ Primary membrane only

The ultimate strength of the material is

$$S_u := 70000 \cdot \text{psi}$$

The Young's modulus and Poisson's ratio of the material are

$$E_s := 28.0 \cdot 10^6 \cdot \text{psi} \quad \nu_s := 0.3$$

The compressive strength of the concrete shielding is

$$f_c := 3300 \cdot \text{psi} \quad \text{Table 3.3.5}$$

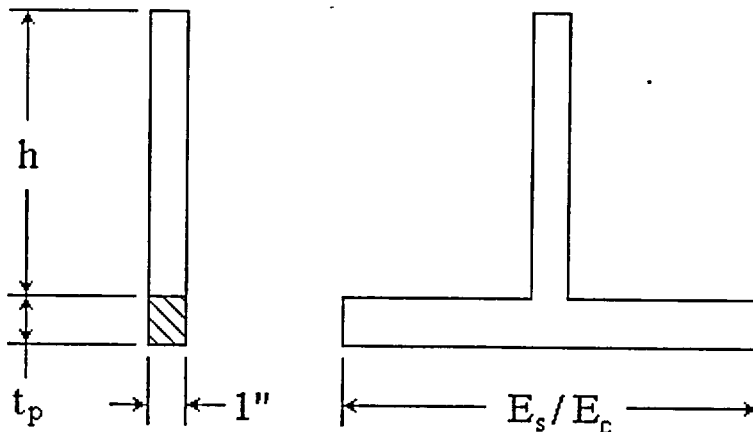
Per the ACI Code, the elastic modulus of concrete is

$$E_c := 57000 \cdot \sqrt{\frac{f_c}{\text{psi}}} \cdot \text{psi}$$

Poisson's ratio for concrete is

$$\nu_c := 0.17$$

First we consider a 1-inch wide cross section through the concrete shielding and the lid bottom plate. Beams that are constructed of more than one material can be treated by using an equivalent width technique. We can develop an equivalent concrete cross section in which the width of lid bottom plate is increased in the same proportion that the modulus of elasticity of steel makes with the modulus of concrete. A sketch of the equivalent cross section is provided below.



Next we compute the centroid location and the moment of inertia of the equivalent cross section

$$y_c := \frac{h \cdot (1 \cdot \text{in}) \cdot \left(t_p + \frac{h}{2} \right) + t_p \cdot \left(\frac{E_s}{E_c} \cdot 1 \text{ in} \right) \cdot \frac{t_p}{2}}{h \cdot (1 \cdot \text{in}) + \left(\frac{E_s}{E_c} \cdot 1 \text{ in} \right) \cdot t_p} \quad y_c = 3.536 \text{ in}$$

$$I_c := \frac{1}{12} \cdot h^3 + h \cdot \left(t_p + \frac{h}{2} - y_c \right)^2 + \frac{1}{12} \cdot \left(\frac{E_s}{E_c} \right) \cdot t_p^3 + t_p \cdot \left(\frac{E_s}{E_c} \right) \cdot \left(y_c - \frac{t_p}{2} \right)^2 \quad I_c = 280 \, 684 \frac{\text{in}^4}{\text{in}}$$

The amplified lateral pressure load on the plate under the vertical handling event is computed as:

$$p := G \cdot \frac{(W_{\text{shield}} + W_{\text{bot}})}{\left(\frac{\pi \cdot d^2}{4} \right)} \quad p = 55.888 \text{ psi}$$

This pressure results in a maximum bending moment at center of the plate equal to

$$M_c := \frac{p \cdot d^2 \cdot (3 + \nu_c)}{16} \quad M_c = 5.272 \times 10^4 \frac{\text{lb} \cdot \text{in}}{\text{in}}$$

Therefore, the maximum bending stress in the lid bottom plate is

$$\sigma := \frac{E_s}{E_c} \cdot \frac{M_c \cdot y_c}{I_c} \quad \sigma = 5 \, 68 \times 10^3 \text{ psi}$$

and the corresponding safety factor is

$$\text{SF} := \frac{S_a}{\sigma} \quad \text{SF} = 10 \, 503$$

The maximum tensile stress in the concrete shielding is

$$\sigma_t := \frac{M_c (y_c - t_p)}{I_c} \quad \sigma_t = 429 \, 4 \text{ psi}$$

Per the ACI Code the maximum allowable tensile stress for normal weight concrete is

$$f_r := 7.5 \cdot \sqrt{\frac{f_c}{\text{psi}}} \cdot \text{psi} \quad f_r = 430.8 \text{ psi}$$

The safety factor against tensile cracking of the concrete is

$$\text{SF} := \frac{f_r}{\sigma_t} \quad \text{SF} = 1.003$$

This result validates the assumption that the concrete shielding and the lid bottom plate act together as a composite structure to resist the bending moment.

3.M.3.2 Lid Shell Weld to Lid Bottom Plate and to Lid Top Plate

3.M.3.2.1 Lid Bottom Plate-to Lid Shell Weld

As a minimum, the lid bottom plate and the lid shell are connected by a 1/8" fillet weld around the perimeter. The shear stress in this limiting weld configuration due to the total vertical load is computed as follows:

$$W := p \cdot \frac{\pi \cdot d^2}{4} \quad W = 2.09 \times 10^5 \text{ lbf}$$

$$t_w := \frac{1}{8} \cdot \text{in}$$

$$A_w := \pi \cdot d \cdot (0.7071 \cdot t_w)$$

$$\tau := \frac{W}{A_w} \quad \tau = 1.091 \times 10^4 \text{ psi}$$

Thus the safety factor is

$$\text{SF}_{\text{weld1}} := \frac{.42 \cdot S_u}{\tau} \quad \text{SF}_{\text{weld1}} = 2.695$$

3.M.3.2.2 Lid Top Plate-to Lid Shell Weld

This weld is an outside fillet weld attaching the lid shell to the top plate. The weld leg size is "tf" where

$$tf := \frac{5}{16} \cdot \text{in} \quad \text{Drawing 1561, sheet 2}$$

The total load applied to the weld from the postulated drop consists of the total weight of the shield material, the lid bottom plate, and the lid shell, all amplified by the design basis deceleration.

$$\text{Load} := G \cdot (W_{\text{shield}} + W_{\text{bot}} + W_{\text{shell}}) \quad \text{Load} = 2.375 \times 10^5 \text{ lbf}$$

This load is supported by the lid shell-bottom plate fillet weld acting in shear. The weld shear stress is computed as

$$\tau_{\text{weld_shear}} := \frac{\text{Load}}{\pi \cdot (d + .667 \cdot tf) \cdot (0.7071 \cdot tf)} \quad \tau_{\text{weld_shear}} = 4.944 \times 10^3 \text{ psi}$$

For the postulated Level D drop event, the allowable weld stress is based upon the ultimate strength of the base material. Therefore, the safety factor, SF, for this weld is

$$SF := 42 \cdot \frac{S_u}{\tau_{\text{weld_shear}}} \quad SF = 5.946$$

This weld does not provide the minimum safety factor under this condition.

3.M.3.3 Lid Shell (conservatively considered as a membrane shell and neglecting end effects)

The circumferential membrane stress away from supports is

$$R := \frac{d}{2} - \frac{t_s}{2}$$
$$\sigma_c := p \cdot \frac{R}{t_s} \quad \sigma_c = 1.9 \times 10^3 \text{ psi}$$

The axial membrane stress away from supports is

$$\sigma_a = 5 \cdot \sigma_c \quad \sigma_a = 950.09 \text{ psi}$$

The safety factor on primary stress intensity is

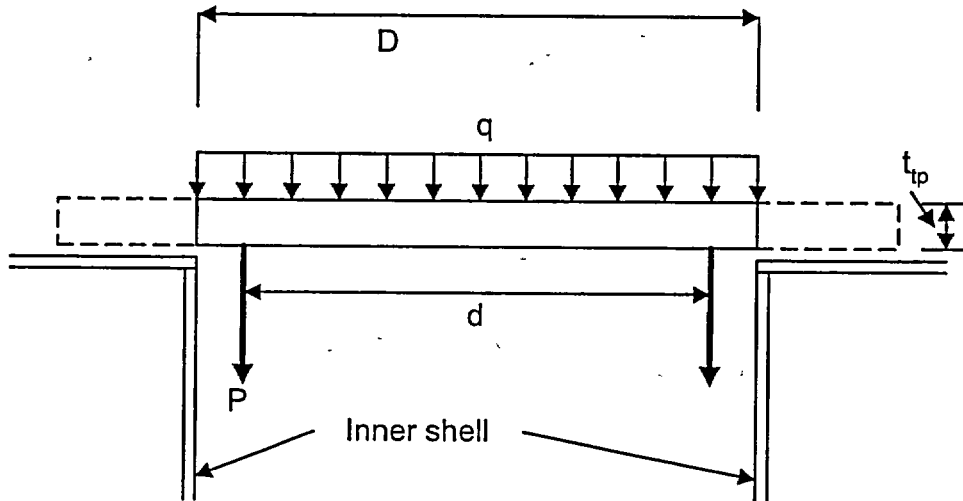
$$SF_{I_s} := \frac{S_{\text{apm}}}{\sigma_c} \quad SF_{I_s} = 20.919$$

3.M.3.4 Lid Top Plates

The lid top plates are two separate components each of thickness

$$t_{tp} := .5 \cdot T \quad t_{tp} = 2 \text{ in}$$

Under the postulated handling event, the lower of the two plates will deflect more than the upper plate because the total load is greater (the lid shield and surrounding steel weighs more than the shield block and its surrounding steel (see Appendix 3.K, subsections 3.K.4.2 and 3.K.4.3). Therefore, we focus the stress analysis on the lower of the two lid top plates. The configuration is analyzed as a simply supported plate with diameter equal to the outer diameter of the inner shell of the HI-STORM 100 storage overpack. The overhanging part of the top plate is conservatively neglected since the overhanging weight will give stresses that reduce the stress in the central section of the top plate. The configuration is shown below:



$$D := 73.5 \cdot \text{in} + 1.5 \cdot \text{in} \quad \text{DWG. 1495, sheet 2}$$

$$d = 69 \text{ in}$$

The weight of the lid shell (see appendix 3.K) is $W_{\text{lidshell}} := 634.8 \cdot \text{lbf}$

Therefore, the load P (per unit circumferential length) is

$$P := \frac{G \cdot (W_{\text{shield}} + W_{\text{bot}} + W_{\text{lidshell}})}{\pi \cdot d} \quad P = 1.096 \times 10^3 \frac{\text{lbf}}{\text{in}}$$

The amplified pressure due to the lid plate self weight is

$$q := G \cdot 283 \cdot \frac{\text{lb} \cdot \text{ft}}{\text{in}^3} \cdot t_{tp} \quad q = 25.47 \text{ psi} \quad (\text{density from Subsection 3.3.1.1})$$

The maximum stress in the top lid plate occurs at the center of the plate. Using Timoshenko and Woinowsky-Krieger, Theory of shells (second edition, p. 64), calculate

$$a := \frac{D}{2} \quad c := \frac{d}{2} \quad v := \nu_s \quad Q := 2 \cdot \pi \cdot c \cdot P$$

$$M_1 := (1 - v) \cdot Q \cdot \frac{(c^2 - a^2)}{8 \cdot \pi \cdot a^2} - \frac{(1 + v) \cdot Q \cdot \log\left(\frac{c}{a}\right)}{4 \cdot \pi} \quad M_1 = -126.353 \text{ lbf}$$

$$\sigma_1 := 6 \frac{M_1}{t_{tp}^2} \quad \sigma := \frac{3 \cdot (3 + v)}{8} \cdot q \cdot \left(\frac{D}{2 \cdot t_{tp}}\right)^2 - \sigma_1 \quad \sigma = 1.127 \times 10^4 \text{ psi}$$

The safety factor is

$$SF_{\text{lid_top_plate}} := \frac{S_a}{\sigma} \quad SF_{\text{lid_top_plate}} = 5.293$$

Note that the lid remains in the elastic range under this loading; therefore, there is no potential for an impact with the MPC and no effect on continued retrievability of the MPC.

3.M.3.5 Inner Shell

The inner shell is conservatively assumed to resist the reaction load from the top plate plus its own amplified weight (including the shield shell), plus a linearly varying pressure from radial expansion of the concrete due to a Poisson ratio effect. In the following, the potential for overstress and compression buckling under the load is examined.

Input data

Inner shell thickness $t_{is} := 1.25 \cdot \text{in}$ BM-1575

Inside diameter of inner shell $d_{\text{inner}} := 73.5 \text{ in}$ DWG 1495 sheet 2

Shield shell thickness $t_{ss} := 0.0 \cdot \text{in}$ BM-1575

Length of inner shell $L_{is} := 224.5 \cdot \text{in}$

The amplified load applied through the lid top plate is conservatively assumed as the bounding weight of the top lid as listed in Table 3.2.1 and it is conservatively assumed that the inner shell supports the entire load.

$$W_{\text{total}} := 23000 \cdot \text{lb} \cdot \text{G} \quad W_{\text{total}} = 1.035 \times 10^6 \text{ lbf}$$

The load per unit mean circumferential length at the top of the of the inner shell is

$$P_{\text{mean}} := \frac{W_{\text{total}}}{\pi \cdot (d_{\text{inner}} + t_{\text{is}})} \quad P_{\text{mean}} = 4.407 \times 10^3 \frac{\text{lbf}}{\text{in}}$$

This results in a constant compressive stress in the inner shell equal to

$$\sigma_{\text{mean}} := \frac{P_{\text{mean}}}{t_{\text{is}}} \quad \sigma_{\text{mean}} = 3.526 \times 10^3 \text{ psi}$$

An amplified bounding weight of the shells adds an additional stress to the above value at the bottom of the storage overpack inner shell as follows:

$$W_{\text{shells}} := 0.283 \cdot \frac{\text{lbf}}{\text{in}^3} \cdot \frac{\pi}{4} \cdot \left[(d_{\text{inner}} + 2 \cdot t_{\text{is}} + 2 \cdot t_{\text{ss}})^2 - d_{\text{inner}}^2 \right] \cdot L_{\text{is}} \quad W_{\text{shells}} = 1.865 \times 10^4 \text{ lbf}$$

$$\sigma_{\text{meanw}} := \frac{W_{\text{shells}} \cdot G}{\pi \cdot (d_{\text{inner}} + t_{\text{is}}) \cdot t_{\text{is}}} \quad \sigma_{\text{meanw}} = 2.859 \times 10^3 \text{ psi}$$

This stress component is zero at the top of the inner shell and varies linearly until it reaches the maximum value given above at the bottom of the inner shell.

Finally, there is an amplified pressure on the outer surface of the inner shell imposed by the Poisson ratio effect from the compression of the concrete in the radial shield. The maximum value of this radial stress is

$$P_{\text{radial}} := \frac{\nu_c}{1 - \nu_c} \cdot \sigma_c \quad \nu_c := 0.2$$

where σ_c is the compressive stress in the concrete at the baseplate. This stress is linearly varying from the top of the inner shell to the baseplate. The concrete compressive stress, at the base, is estimated as follows:

$$\text{The weight density of concrete is} \quad \gamma_c := 160.8 \cdot \frac{\text{lbf}}{\text{ft}^3}$$

Using the length of the inner shell as the height of the concrete column gives

$$\sigma_c := \gamma_c \cdot L_{\text{is}} \cdot G \quad \sigma_c = 940.092 \text{ psi}$$

Note that this is below the allowable compressive stress in the concrete (Table 3.3.5). Therefore, the maximum value of the radial(external) pressure imposed on the inner shell is

$$P_{\text{radial}} := \frac{\nu_c}{1 - \nu_c} \cdot \sigma_c \quad P_{\text{radial}} = 235\,023 \text{ psi}$$

Appendix 3.AK examines the structural integrity of the inner shell under this loading in accordance with ASME Code Case N-284, which has been used in the HI-STAR 100 FSAR and SAR to examine stability issues and is accepted by the NRC for these kind of evaluations. Both stability and yielding are examined and it is concluded that buckling of the inner shell is not credible

The safety factor is

$$SF := \frac{1.34}{.341} \quad SF = 3.93$$

The preceding analysis has computed vertical compressive stress acting on the inner shell above the inlet vents for the primary purpose of evaluating stability of the inner shell under the combination of external pressure plus compressive axial stress. On a cross section below the inlet vents, there will be an increase in the compressive stress level due to the reduction in metal area. Section 3.4.4.3.2.1 provides the reduced area calculation. The net metal area reduction for the inner and outer shells is

$$\text{Reduction_factor_inner_shell} := \frac{211.04}{293.54} \quad \text{Reduction_factor_outer_shell} := \frac{260.93}{310.43}$$

Therefore, the increased mean compressive primary stress on a section of the inner shell below the inlet duct is

$$\sigma_{\text{mcsi}} := \frac{\sigma_{\text{mean}} + \sigma_{\text{meanw}}}{\text{Reduction_factor_inner_shell}} \quad \sigma_{\text{mcsi}} = 8\,881 \times 10^3 \text{ psi}$$

Comparing the stress intensity with the allowable mean stress intensity for the inner shell under Level D conditions (Table 3.1.12) defines the safety factor

$$SF_{\text{mcs}} := \frac{S_{\text{apm}}}{\sigma_{\text{mcsi}}} \quad SF_{\text{mcs}} = 4.476$$

3.M.3.6 Outer Shell

The geometry of the outer shell is obtained from BM-1575.

$$d_{\text{outer}} := 132.5 \cdot \text{in} \quad t_{\text{outer}} := 0.75 \cdot \text{in} \quad L_{\text{outer}} := 224.5 \cdot \text{in}$$

The compressive stress developed at the base of the outer shell (just above the inlet vent) is

$$W_{\text{shells}} := 0.283 \cdot \frac{\text{lb} \cdot \text{ft}}{\text{in}^3} \cdot \frac{\pi}{4} \cdot \left[d_{\text{outer}}^2 - (d_{\text{outer}} - 2 \cdot t_{\text{outer}})^2 \right] \cdot L_{\text{outer}} \quad W_{\text{shells}} = 1.972 \times 10^4 \text{ lbf}$$

$$\sigma_{\text{meanw}} := \frac{W_{\text{shells}} \cdot G}{\pi \cdot (d_{\text{outer}} - t_{\text{outer}}) \cdot t_{\text{outer}}} \quad \sigma_{\text{meanw}} = 2.859 \times 10^3 \text{ psi}$$

Below the inlet duct, this mean stress is amplified to the value

$$\sigma_{\text{mcs}} := \frac{\sigma_{\text{meanw}}}{\text{Reduction_factor_outer_shell}} \quad \sigma_{\text{mcs}} = 3.401 \times 10^3 \text{ psi}$$

The safety factor for Level D mean stress in the outer shell is

$$\text{SF}_{\text{mcs}} := \frac{S_{\text{apm}}}{\sigma_{\text{mcs}}} \quad \text{SF}_{\text{mcs}} = 11.686$$

Instability of the outer shell is examined in Appendix 3.AK and is found to be not credible

3.M.3.7 Inlet Vent Horizontal Plates

The inlet vent horizontal plate is subject to the amplified weight of the concrete and is exposed to the pressure from the column of concrete above the plate. This pressure is

$$P_{\text{ip}} := \sigma_c \quad P_{\text{ip}} = 940.092 \text{ psi}$$

The dimensions of this plate are given in BM-1575. The length, width, and thickness, are

$$L_{\text{ip}} := 29.5 \cdot \text{in} \quad w_{\text{ip}} := 16.5 \cdot \text{in} \quad t_{\text{ip}} := 2 \cdot \text{in}$$

Under the vertical handling accident, the bending stress in this item is determined by treating the plate as simply supported on all four sides and using classical plate theory. From the text "Theory of Plates and Shells", Timoshenko and Woinowsky-Krieger, McGraw-Hill, 1959 (2nd Edition), the solution is found in Section 30, Table 8. Using the nomenclature of the referenced text,

$$b := L_{ip} \quad a := w_{ip} \quad \frac{b}{a} = 1.788$$

From the table, the maximum bending moment factor is

$$\beta := 0.0943$$

and

$$M_x := \beta \cdot p_{ip} \cdot a^2 \quad M_x = 2.414 \times 10^4 \text{ in} \cdot \frac{\text{lbf}}{\text{in}}$$

The maximum bending stress is

$$\sigma_{ip} := 6 \cdot \frac{M_x}{t_{ip}^2} \quad \sigma_{ip} = 3.62 \times 10^4 \text{ psi}$$

The safety factor is conservatively computed for this Level D condition as

$$SF_{ip} := \frac{S_a}{\sigma_{ip} + p_{ip}} \quad SF_{ip} = 1.606$$

The total vertical reaction load is conservatively assumed to be resisted only by the inlet vent vertical plates.

3 M.3.8 Inlet Vent Vertical Plates

Consistent with the assumptions used to qualify the inlet vent horizontal plate, the inlet vent vertical plate is analyzed for the mean compressive stress developed. From BM-1575, the inlet vent vertical plates have thickness, depth, and length given as

$$t_{ivp} := 0.75 \text{ in} \quad c := 10 \text{ in} \quad L_{ivp} := 29.5 \text{ in}$$

The compressive stress developed is conservatively calculated as

$$\sigma_{ivp} := \frac{p_{ip} \cdot L_{ip} \cdot w_{ip}}{2 \cdot t_{ivp} \cdot L_{ivp}} \quad \sigma_{ivp} = 1.034 \times 10^4 \text{ psi}$$

The safety factor is

$$SF := \frac{S_{apm}}{\sigma_{ivp}} \quad SF = 3.844$$

Because of the backing provided by the concrete, and the short span of this plate, an elastic instability is not credible

3.M.3.9 Pedestal Shield

The results obtained for this component in Appendix 3.D, specifically sub-section 3.D.8, are used here to establish safety factors under the postulated handling accident event. The following results are found in Appendix 3.D for the pedestal shield under 3 x 1.15 times the load from a loaded MPC.

$$SF_{\text{shield}} := 13.19 \quad \text{Concrete compression}$$

For the vertical handling accident condition of storage, the safety factors are reduced to

$$SF_{\text{pshield}} := SF_{\text{shield}} \cdot \frac{3 \cdot 1.15}{G} \quad SF_{\text{pshield}} = 1.011$$

3.M.3.10 Weld in the Load Path

The only structural weld that is subject to significant stress and needs evaluation under this accident event is the weld connecting the lid bottom plate to the lid shell. We have demonstrated earlier that this weld is adequately sized (see section 3.M.3.1). The remaining welds serve only to insure that lateral connections of the shells to adjoining flat sections are maintained. The load transfer is by metal-to-metal compression contact; the connection welds are not needed to maintain equilibrium. Nevertheless, weld capacities of other connecting welds are examined to demonstrate that confinement of the shielding is maintained.

3.M.3.10.1 Outer Shell-to-Baseplate Circumferential Weld

$$t_w := 0.375 \text{ in} \quad \text{weld size (fillet)} \quad (\text{Drawing 1495})$$

$$\text{Allowable weld stress} \quad \tau_{\text{allow}} := 0.42 \cdot S_u \quad \tau_{\text{allow}} = 2.94 \times 10^4 \text{ psi}$$

Under this load condition, the weld need only resist radial loading from the "hydrostatic" radial pressure from the concrete shielding.

$$d_{\text{outer}} = 132.5 \text{ in} \quad t_{\text{outer}} = 0.75 \text{ in}$$

The shear force per unit of periphery is computed by considering the shell to be subjected to uniform internal pressure, and completely restrained from radial displacement by the weld. The solution for the shear force is obtained by superposition of two classical shell solutions (internal pressure in a long shell, and end shear applied to an otherwise unloaded shell). Enforcing zero displacement at the end of the shell leads to the following expression for the shear force per unit of shell periphery.

$$E := E_s \quad \nu = 0.3$$

$$D := \frac{E \cdot t_{\text{outer}}^3}{12 \cdot (1 - \nu^2)} \quad \lambda := \left[\frac{3 \cdot (1 - \nu^2)}{(.5 \cdot d_{\text{outer}} \cdot t_{\text{outer}})^2} \right]^{25}$$

The shear force is

$$V_o := 2 \cdot D \cdot \lambda^3 \cdot p_{\text{radial}} \cdot \frac{(.5 \cdot d_{\text{outer}})^2}{E \cdot t_{\text{outer}}} \cdot (2 - \nu) \quad V_o = 1.096 \times 10^3 \frac{\text{lbf}}{\text{in}}$$

The weld capacity over the same 1" width is

$$\text{Weld_Capacity} := \tau_{\text{allow}} \cdot .7071 \cdot t_w \quad \text{Weld_Capacity} = 7.796 \times 10^3 \frac{\text{lbf}}{\text{in}}$$

Therefore the safety factor on the outer shell to baseplate weld is

$$\text{SF}_{\text{weldo}} := \frac{\text{Weld_Capacity}}{V_o} \quad \text{SF}_{\text{weldo}} = 7.116$$

3.M.3.10.2 Inner Shell-to-Baseplate Circumferential Weld

$$t_w := 0.375 \cdot \text{in} \quad \text{weld size (fillet)}$$

$$\text{Allowable weld stress} \quad \tau_{\text{allow}} := 0.42 \cdot S_u \quad \tau_{\text{allow}} = 2.94 \times 10^4 \text{ psi}$$

Under this load condition, the weld need only resist radial loading from the "hydrostatic" radial pressure from the concrete shielding. However, for added conservatism, we also assume that the weld supports a portion of the the mean compressive stress developed.

$$d_{\text{inner}} = 73.5 \text{ in} \quad t_{\text{is}} = 1.25 \text{ in}$$

The shear force per unit of periphery is computed by considering the shell to be subjected to uniform internal pressure, and completely restrained from radial displacement by the weld. The solution for the shear force is obtained by superposition of two classical shell solutions (internal pressure in a long shell, and end shear applied to an otherwise unloaded shell). Enforcing zero displacement at the end of the shell leads to the following expression for the shear force per unit of shell periphery.

$$E := E_s \quad \nu = 0.3$$

$$D := \frac{E \cdot t_{\text{is}}^3}{12 \cdot (1 - \nu^2)} \quad \lambda := \left[\frac{3 \cdot (1 - \nu^2)}{(.5 \cdot d_{\text{inner}} \cdot t_{\text{is}})^2} \right]^{25}$$

The shear force is

$$V_o := 2 \cdot D \cdot \lambda^3 \cdot p_{\text{radial}} \cdot \frac{(5 \cdot d_{\text{inner}})^2}{E \cdot t_{\text{is}}} \cdot (2 - \nu) \quad V_o = 1.053 \times 10^3 \frac{\text{lbf}}{\text{in}}$$

The weld shear stress to support V_o is

$$\tau_1 := \frac{V_o}{2 \cdot (.7071 \cdot t_w)} \quad \tau_1 = 1.986 \times 10^3 \text{ psi}$$

Assuming a portion of the compressive load (ratio of weld leg size to total contact length with baseplate) on the inner shell is transferred through the weld gives a weld shear stress component

$$\tau_2 := (\sigma_{\text{mcsi}} \cdot t_{\text{is}}) \cdot \left(\frac{1}{t_{\text{is}} + 2 \cdot t_w} \right) \quad \tau_2 = 5.551 \times 10^3 \text{ psi}$$

The weld safety factor is

$$SF_{\text{weld1}} := \frac{\tau_{\text{allow}}}{\sqrt{\tau_1^2 + \tau_2^2}} \quad SF_{\text{weld1}} = 4.987$$

3.M.3.10.3 Pedestal Shell-to-Baseplate Circumferential Weld

$$t_w := \frac{3}{16} \cdot \text{in} \quad \text{weld size (fillet)}$$

$$\text{Allowable weld stress} \quad \tau_{\text{allow}} := 0.42 \cdot S_u \quad \tau_{\text{allow}} = 2.94 \times 10^4 \text{ psi}$$

Under this load condition, the weld need only resist radial loading from the "hydrostatic" radial pressure from the concrete shielding. However, for added conservatism, we also assume that the weld supports a portion of the the mean compressive stress developed.

$$d_{\text{ps}} := 68.375 \cdot \text{in} \quad t_{\text{ps}} := 0.25 \cdot \text{in} \quad \text{BM-1575}$$

From Appendix 3.D, the lateral "hydrostatic" pressure from the compressed shield material is

$$p_{\text{shield}} := 23.99 \cdot \text{psi} \quad \text{under a load amplifier } 3 \times 1.15$$

Therefore, for the drop condition studied in this appendix, where 45 G is the amplifier, the pressure on the pedestal shell is

$$p_s := \frac{p_{\text{shield}} \cdot G}{3 \cdot 1.15} \quad p_s = 312.913 \text{ psi}$$

The shear force per unit of periphery is computed by considering the shell to be subjected to uniform internal pressure, and completely restrained from radial displacement by the weld. The solution for the shear force is obtained by superposition of two classical shell solutions (internal pressure in a long shell, and end shear applied to an otherwise unloaded shell). Enforcing zero displacement at the end of the shell leads to the following expression for the shear force per unit of shell periphery.

$$E = 2.8 \times 10^7 \text{ psi} \quad \nu = 0.3$$

$$D := \frac{E \cdot t_{ps}^3}{12 \cdot (1 - \nu^2)} \quad \lambda := \left[\frac{3 \cdot (1 - \nu^2)}{(.5 \cdot d_{ps} \cdot t_{ps})^2} \right]^{-2.5}$$

The shear force is

$$V_o := 2 \cdot D \cdot \lambda^3 \cdot p_s \cdot \frac{(.5 \cdot d_{ps})^2}{E \cdot t_{ps}} \cdot (2 - \nu) \quad V_o = 604.932 \frac{\text{lb}}{\text{in}}$$

The weld shear stress to support V_o is

$$\tau_1 := \frac{V_o}{7071 \cdot t_w} \quad \tau_1 = 4.563 \times 10^3 \text{ psi}$$

The weld capacity over the same unit width is

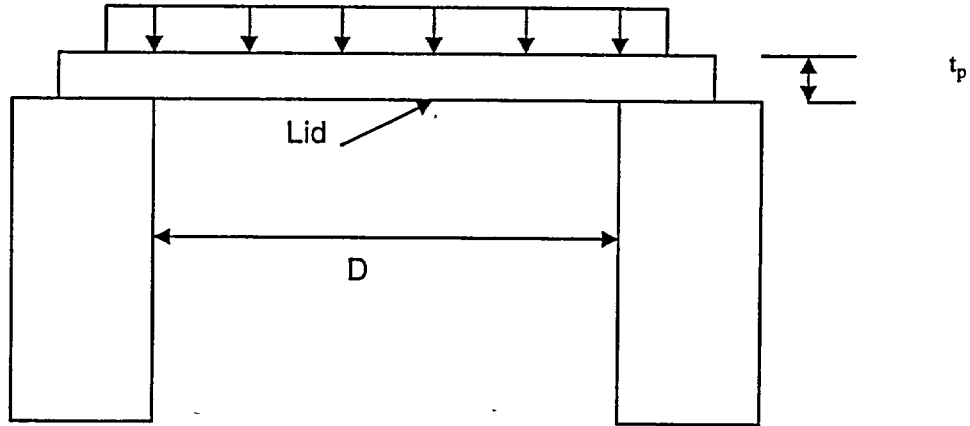
$$\text{Weld_Capacity} := \tau_{\text{allow}} \cdot 7071 \cdot t_w \quad \text{Weld_Capacity} = 3.898 \times 10^3 \frac{\text{lb}}{\text{in}}$$

Therefore the safety factor on the pedestal shell-to-baseplate weld is

$$\text{SF}_{\text{weld}} := \frac{\text{Weld_Capacity}}{V_o} \quad \text{SF}_{\text{weld}} = 6.444$$

3.M.4 Analysis of Bending of HI-STORM 100S Top Lid

Consider the following configuration for analysis (the upper of the two lid plates is most heavily loaded):



The thickness of the upper of two lids is

$$t_p = 2 \text{ in}$$

$$D := 73.5 \text{ in} \quad \text{Assume the pinned support is at the inner edge.}$$

The weight of the shield block concrete and the surrounding metal shell is obtained from the detailed weight analysis archived in the calculation package. The total weight of this component is

$$W := 5881 \text{ lbf}$$

The equivalent uniform pressure is

$$q_1 := \frac{W \cdot G}{\left(\frac{\pi \cdot D^2}{4} \right)} \quad q_1 = 62.373 \text{ psi}$$

The amplified pressure due to the lid plate self weight is

$$q_2 := G \cdot 283 \cdot \frac{\text{lbf}}{\text{in}^3} \cdot t_p \quad q_2 = 25.47 \text{ psi} \quad (\text{density from Subsection 3.3.1.1})$$

Therefore, the total amplified pressure on the upper of two top lids (conservatively assume it carries all of the load from the shield block and neglect any resisting interface pressure from the lower plate) is

$$q := q1 + q2$$

The bending stress in the center of the plate is

$$\sigma := \frac{3 \cdot (3 + \nu)}{8} \cdot q \cdot \left(\frac{D}{2 \cdot t_{\text{pl}}} \right)^2$$
$$\sigma = 3.67 \times 10^4 \text{ psi}$$

$$SF_{\text{lid_top_plate}} := \frac{S_a}{\sigma}$$
$$SF_{\text{lid_top_plate}} = 1.625$$

3.M.5 Conclusion

The HI-STORM 100 storage overpack meets Level D requirements for Load Case 02.a in Table 3.1.5. Even under the postulated accident condition loads, the calculated stress levels do not imply that any significant deformations occur that would preclude removal of a loaded MPC. Thus ready retrievability of fuel is maintained after such an event.